

**Functional studies**  
**of**  
**NMDA receptor concatemers**  
**in**  
*Xenopus laevis* oocytes

Doctoral thesis

by

Monika Jeromin

performed at the Department of Biochemistry I - Receptor Biochemistry,  
Graduate School of Chemistry and Biochemistry (GSCB),  
Faculty of Chemistry and Biochemistry,  
Ruhr-University Bochum

**Functional studies**  
**of**  
**NMDA receptor concatemers**  
**in**  
*Xenopus laevis* oocytes

by  
Monika Jeromin

performed at the Department of Biochemistry I - Receptor Biochemistry,  
Graduate School of Chemistry and Biochemistry (GSCB)

A thesis  
in fulfilment of the requirements  
for the Degree of the Doctor of Natural Sciences (Dr. rer. nat.)  
conferred by the Faculty of Chemistry and Biochemistry,  
Ruhr-University Bochum

2<sup>nd</sup> February 2004 until 13<sup>th</sup> January 2007

Advisor : Prof. Dr. M. Hollmann  
Co-advisor : PD Dr. I. Dietzel-Meyer

## **Declaration**

I hereby declare that this dissertation entitled "Functional studies of NMDA receptor concatemers in *Xenopus laevis* oocytes" is my own original work and effort and has been written with no other sources and aids than quoted.

Monika Jeromin

January 2007

# TABLE OF CONTENTS

1	INTRODUCTION .....	1
1.1	SYNAPTIC TRANSMISSION IN THE NERVOUS SYSTEM.....	1
1.2	FAMILY OF IONOTROPIC GLUTAMATE RECEPTORS .....	2
1.2.1	Background.....	2
1.2.2	Tertiary structure of GluR subunits.....	4
1.2.3	The Q/N/R site of ionotropic glutamate receptors.....	5
1.2.4	Quarternary structure of GluR subunits.....	6
1.3	THE NMDA RECEPTOR .....	8
1.3.1	NMDAR subunits and splice variants.....	8
1.3.2	Electrophysiological and pharmacological properties of the NMDA receptor .....	8
1.3.3	Expression pattern of NMDAR subunits.....	11
1.3.3.1	In the brain.....	11
1.3.3.2	Intracellular trafficking.....	12
1.3.4	Role of the NMDA receptor during synaptic transmission.....	13
1.4	THE CONCATEMER STRATEGY .....	14
1.4.1	The concatemer strategy applied to other ion channels .....	14
1.4.2	The concatemer strategy applied to glutamate receptors.....	15
1.4.2.1	Previous work by other groups .....	15
1.4.2.2	Previous work in the lab .....	17
1.4.2.2.1	Generation and analysis of homomeric GluR1 concatemers .....	17
1.4.2.2.2	Engineering strategy to generate concatemers from all 18 mammalian GluR cDNAs.....	19
1.5	AIMS OF THE PRESENT STUDY .....	21
2	MATERIALS AND METHODS.....	23
2.1	BACTERIAL GROWTH .....	23
2.2	MEDIUM SCALE ("MIDI") PREPARATION OF PLASMID DNA ( $\leq 100 \mu\text{g}$ PLASMID DNA).....	23
2.3	AMPLIFICATION OF DNA USING THE POLYMERASE CHAIN REACTION (PCR).....	24
2.4	CLONING OF DNA FRAGMENTS INTO PLASMID VECTORS .....	26
2.4.1	Phosphorylation of PCR products.....	28
2.4.2	Restriction digest of DNA.....	29
2.4.3	Purification of DNA from salts, impurities and agarose .....	29
2.4.4	Ligation of DNA fragments to plasmid vectors .....	29
2.4.5	Transformation of heat-shock competent <i>Escherichia coli</i> .....	30
2.4.6	Selection of recombinant transformants.....	30
2.4.7	Automated sequencing .....	31
2.5	IN VITRO-SYNTHESIS OF CRNA.....	31
2.5.1	Linearisation of the DNA template.....	31
2.5.2	Transcription reaction .....	32
2.6	PREPARATION OF <i>XENOPUS LAEVIS</i> OOCYTES .....	33
2.7	CRNA INJECTION IN OOCYTES .....	33
2.8	ELECTROPHYSIOLOGICAL RECORDINGS USING TWO-ELECTRODE VOLTAGE CLAMPING .....	34
3	RESULTS.....	36
3.1	CONSTRUCTION OF NMDA RECEPTOR CONCATEMERS .....	36
3.1.1	Overview of all newly generated constructs.....	36
3.1.2	Preparation of the NR2A subunit.....	44
3.1.2.1	Identification of a frame shift mutation in the available NR2A cDNA clone.....	44
3.1.2.2	Repair of the mutated NR2A head subunit and the NR2A cDNA.....	45

3.2	ANALYSIS OF NR1-1A + NR2A HETERODIMERS .....	46
3.2.1	<i>NR1-1a-TG4L2-NR2A is functional when expressed alone in Xenopus oocytes</i> .....	46
3.2.1.1	Electrophysiological properties .....	46
3.2.1.1.1	Pre-injection of EGTA .....	48
3.2.1.1.2	Mg <sup>2+</sup> block below - 20 mV .....	50
3.2.1.1.3	Ca <sup>2+</sup> permeability .....	53
3.2.1.2	Pharmacological properties.....	55
3.2.1.2.1	Inhibition by APV, MK-801, and insensitivity to ifenprodil .....	55
3.2.2	<i>Properties of the N598R mutation are preserved within the heterodimer</i> .....	60
3.2.2.1	Electrophysiological properties .....	63
3.2.2.1.1	Release of Mg <sup>2+</sup> block below - 20 mV .....	63
3.2.2.1.2	Ca <sup>2+</sup> impermeability .....	66
3.2.2.2	Pharmacological properties.....	67
3.2.2.2.1	Inhibition by APV and insensitivity to MK-801.....	67
3.3	ANALYSIS OF NR1-1A AND NR2A HOMODIMERS .....	70
3.3.1	<i>The homodimers NR1-1a-TG4L2-NR1-1a and NR2A-TG4L2-NR2A are not functional alone but give currents together with monomeric NR2A and NR1-1a, respectively</i> .....	70
3.3.2	<i>NR1-1a-TG4L2-NR1-1a(N598R) proves incorporation of the tail subunit in the receptor complex</i> .....	72
3.3.3	<i>Combining NR1-1a-TG4L2-NR1-1a with NR2A-TG4L2-NR2A generates functional channels as well</i> .....	74
3.4	TRAFFICKING OF NR1-1A + NR2A DIMERS .....	75
3.4.1	<i>NR2A facilitates the assembly of NR1-1a-TG4L2-NR2A and NR1-1a-TG4L2-NR1-1a</i> .....	75
3.4.2	<i>NR1-1a(N598R)-TG4L2-NR2A cannot be boosted by NR2A</i> .....	77
3.5	EFFECTS OF THE LINKAGE ON DIMER FUNCTION.....	79
3.5.1	<i>Glutamate affinity for NR1-1a-TG4L2-NR2A</i> .....	80
3.5.2	<i>Glycine affinity for NR1-1a-TG4L2-NR2A</i> .....	81
4	DISCUSSION.....	83
4.1	INTERPRETATION OF EXISTING DATA .....	83
4.1.1	<i>Comparison to concatemer studies in general</i> .....	83
4.1.2	<i>Comparison to Prybylowski et al.</i> .....	85
4.1.3	<i>Comparison to Schorge and Colquhoun</i> .....	86
4.1.3.1	Qualitative behaviour.....	86
4.1.3.2	Quantitative behaviour.....	90
4.1.3.3	Subunit arrangement within the NR1-1a + NR2A dimer .....	92
4.1.3.4	Trafficking of NR1-1a + NR2A dimers .....	101
4.2	OUTLOOK.....	102
4.2.1	<i>Protein biochemistry</i> .....	102
4.2.2	<i>Patch clamping</i> .....	107
4.2.3	<i>Construction of the 4<sup>th</sup> dimer to investigate the anticipated arbitrary subunit order within NMDAR dimers</i> .....	108
4.2.4	<i>Cloning of four tetramers to determine the stoichiometry of NMDA receptors</i> .....	111
4.2.5	<i>Role of the NR3 subunit for NMDAR stoichiometry</i> .....	112
5	SUMMARY.....	116
6	REFERENCES .....	118

## TABLE OF FIGURES

Fig. 1 : Subunits belonging to the superfamily of vertebrate glutamate receptors .....	3
Fig. 2 : Topology of a GluR subunit .....	4
Fig. 3 : Developmentally regulated expression of NR2A and NR2B in rat brain .....	11
Fig. 4 : Concatemer strategy using a C-terminally truncated head subunit.....	15
Fig. 5 : Concatemer strategy using an additional transmembrane domain as linker .....	16
Fig. 6 : Topology of the $\alpha_1$ -subunit of the GABA <sub>A</sub> receptor.....	17
Fig. 7 : Series of TG4 linkers .....	18
Fig. 8 : Concatemer strategy used in the present study.....	18
Fig. 9 : General cloning scheme to construct dimeric GluR concatemers .....	19
Fig. 10 : The transcription vector pXSGEM .....	27
Fig. 11 : Schematic structure of the mutated NR2A cDNA AF001423.....	45
Fig. 12 : NR1-1a-TG4L2-NR2A currents in normal frog Ringer.....	47
Fig. 13 : NR1-1a + NR2A (1:1) without EGTA pre-injection.....	49
Fig. 14 : NR1-1a-TG4L2-NR2A without EGTA pre-injection .....	49
Fig. 15 : NR1-1a-TG4L2-NR2A with EGTA pre-injection .....	50
Fig. 16 : NR1-1a-TG4L2-NR2A currents in Mg <sup>2+</sup> -Ringer .....	51
Fig. 17 : NR1-1a + NR2A (1:1) in Mg <sup>2+</sup> -Ringer .....	52
Fig. 18 : NR1-1a-TG4L2-NR2A in Mg <sup>2+</sup> -Ringer without EGTA pre-injection .....	52
Fig. 19 : NR1-1a-TG4L2-NR2A in Mg <sup>2+</sup> -Ringer with EGTA pre-injection .....	53
Fig. 20 : NR1-1a-TG4L2-NR2A currents in Ca <sup>2+</sup> -Ringer .....	54
Fig. 21 : Block of NR1-1a-TG4L2-NR2A currents by APV.....	55
Fig. 22 : Reversible block of NR1-1a-TG4L2-NR2A currents by MK-801 .....	57
Fig. 23 : Insensitivity of NR1-1a-TG4L2-NR2A currents to ifenprodil.....	59
Fig. 24 : NR1-1a(N598R)-TG4L2-NR2A in normal frog Ringer.....	61
Fig. 25 : NR1-1a(N598R) + NR2A (1:1) in normal frog Ringer.....	61
Fig. 26 : NR1-1a(N598R)-TG4L2-NR2A currents in normal frog Ringer .....	62
Fig. 27 : NR1-1a(N598R)-TG4L2-NR2A currents in Mg <sup>2+</sup> -Ringer .....	63
Fig. 28 : NR1-1a(N598R) + NR2A (1:1) in Mg <sup>2+</sup> -Ringer .....	65
Fig. 29 : NR1-1a(N598R)-TG4L2-NR2A in Mg <sup>2+</sup> -Ringer.....	65
Fig. 30 : NR1-1a(N598R)-TG4L2-NR2A currents in Ca <sup>2+</sup> -Ringer .....	66
Fig. 31 : Block of NR1-1a(N598R)-TG4L2-NR2A currents by APV .....	68
Fig. 32 : Insensitivity of NR1-1a(N598R)-TG4L2-NR2A currents to MK-801 .....	69
Fig. 33 : Homodimer currents in normal frog Ringer.....	71
Fig. 34 : NR1-1a-TG4L2-NR1-1a(N598R) + NR2A in Mg <sup>2+</sup> -Ringer .....	72
Fig. 35 : NR1-1a-TG4L2-NR1-1a + NR2A in Mg <sup>2+</sup> -Ringer .....	73
Fig. 36 : Co-expression of NR1-1a-TG4L2-NR1-1a and NR2A-TG4L2-NR2A.....	74
Fig. 37 : Trafficking of NR1-1a-TG4L2-NR2A.....	76
Fig. 38 : Retention of concatemers with mutated NR1-1a.....	78
Fig. 39 : Influence of the linker on dimer currents.....	79
Fig. 40 : EC <sub>50</sub> curves of glutamate .....	81
Fig. 41 : EC <sub>50</sub> curves of glycine .....	82
Fig. 42 : Subunit arrangement in NMDAR tetramers by Schorge and Colquhoun.....	93
Fig. 43 : Subunit arrangement in NMDAR dimers by Furukawa et al. ....	96
Fig. 44 : Possible subunit arrangement in NMDAR dimers based on the results of the present study.....	97
Fig. 45 : Failed attempt to detect oocyte protein from total homogenate .....	104
Fig. 46 : Difficulties in detecting NR1 protein in membranes prepared from oocytes.....	105
Fig. 47 : Combining NR1-1a-TG4L2-NR2A with NR2A-TG4L2-NR1-1a .....	109
Fig. 48 : Functional isolation of a receptor combined from NR1-1a-TG4L2-NR2A and NR2A(T690I)-TG4L2-NR1-1a(N598R) .....	110
Fig. 49 : Tetramers permitting to determine NMDAR stoichiometry.....	111

Fig. 50 : NMDA receptors incorporating the NR3A subunit may be tetramers.....	113
Fig. 51 : NMDA receptors incorporating the NR3A subunit may be pentamers .....	114

## TABLE OF ABBREVIATIONS

aa	amino acid(s)
AMPA	$\alpha$ -amino-3-hydroxymethyl-4-isoxazole-propionic acid
AMPAR	AMPA receptor
D-APV	D-(-)-2-amino-5-phosphonate pentanoic acid
bp	base pair(s)
CaR	Ca <sup>2+</sup> -Ringer
CNS	central nervous system
DEPC	diethylpyrocarbonate
EC <sub>50</sub>	efficient concentration at half maximal (50 %) response
EDTA	ethylenediamine tetraacetic acid
EGTA	ethylene glycol tetraacetic acid
EPSP	excitatory postsynaptic potential
ER	endoplasmic reticulum
F	phenylalanine
GABA	$\gamma$ -aminobutyric acid
GluR	glutamate receptor
HEK	human embryonic kidney
HEPES	4-(2-hydroxyethyl)-1-piperazine-ethanesulphonic acid
IC <sub>50</sub>	concentration producing half maximal (50 %) inhibition
I/V	current-voltage (relation)
KA	kainate
kbp	kilo base pair(s)
L	leucine
LTD	long-term depression
LTP	long-term potentiation
MgR	Mg <sup>2+</sup> -Ringer
mins	minutes
mRNA	messenger RNA
N	asparagine
NFR	normal frog Ringer

NMDA	<i>N</i> -methyl-D-aspartate
NMDAR	NMDA receptor
NMDG	<i>N</i> -methyl-D-gluconate
ORF	open reading frame
pBS	pBluescript
PBS	phosphate buffered saline
PCR	polymerase chain reaction
PEG	polyethylene glycol
Q	glutamine
R	arginine
SEM	standard error of the mean
sp	signal peptide
TG4	<u>t</u> ransmembrane linker consisting of the <u>4</u> <sup>th</sup> TMD of the $\alpha_1$ -subunit of the bovine <u>G</u> ABA <sub>A</sub> receptor
TG4L	TG4 plus adjacent hydrophilic residues
TG4L2	TG4L flanked by the restriction sites used for cloning
TMD	transmembrane domain
Tris	Tris(hydroxymethyl)-aminomethane
UTP	uridine 5'-triphosphate
UTR	untranslated region
Y	tyrosine

# 1 Introduction

## 1.1 Synaptic transmission in the nervous system

The human brain contains about  $10^{11}$  neurons. They mediate the majority of fast information processing transmitted at their synapses. A synapse is formed from the terminal branches of an axon of the presynaptic neuron and a dendrite or the cell body of the postsynaptic neuron (in the central nervous system; CNS), or between an axon terminal and an effector cell such as a muscle, termed neuromuscular junction (in the peripheral nervous system). Synapses are classed as being electrical or chemical. Electrical synapses are effectively gap junctions and result in the direct electrical coupling of both neurons. A chemical synapse is defined as the arrangement of a presynaptic release site of neurotransmitter separated from the opposing specialised postsynaptic membrane by a narrow cleft; it is the point at which action potentials are converted into a chemical signal which in turn induces an electrical response in the postsynaptic cell. Most intercellular, i.e. neural and neuromuscular, communication in nervous systems relies on the activity of chemical synapses.

The action potential arises in a distinct initial segment of the axon, the axon hillock. It is propagated by the subsequent opening of voltage-activated  $\text{Na}^+$  and  $\text{K}^+$  channels : When the resting membrane potential (around - 60 mV) is depolarised to a threshold level (ca. - 15 mV) by an incoming action potential in the postsynaptic cell,  $\text{Na}^+$  channels open. The entry of  $\text{Na}^+$  leads to further depolarisation (around + 20 mV ), also in surrounding membrane segments where adjacent  $\text{Na}^+$  channels are activated. This allows the activation to be spread along the axon membrane. Opposed to the original Hodgkin-Huxley theory, neighbouring  $\text{Na}^+$  channels are not independent, but may operate and be activated cooperatively (Naundorf et al., 2006).

When the action potential reaches the presynaptic terminal, voltage-activated  $\text{Ca}^{2+}$  channels can open. This  $\text{Ca}^{2+}$  influx triggers vesicles to undergo membrane fusion (called exocytosis) at the presynaptic terminal, thereby releasing neurotransmitter molecules into the synaptic cleft. Their subsequent binding to their postsynaptic receptors then changes the potential of the postsynaptic cell.

Depolarisation not only leads to the opening of  $\text{Na}^+$  channels but also to the opening of voltage-triggered  $\text{K}^+$  channels : The action potential is terminated by the closing of the  $\text{Na}^+$  channels and the outflow of  $\text{K}^+$  which repolarises the membrane to the resting potential.

## 1.2 Family of ionotropic glutamate receptors

### 1.2.1 Background

The amino acid L-glutamate is the most abundant excitatory neurotransmitter in the mammalian CNS. Ionotropic glutamate receptors (GluRs) are ligand-activated and ion-selective channels permeable for cations ( $\text{Na}^+$  und  $\text{K}^+$  ions but also  $\text{Mg}^{2+}$  and  $\text{Ca}^{2+}$  ions).

The cloning of cDNAs encoding ionotropic GluR subunits took place mainly between 1989 and 1992 with the first subunit GluR1(Q)flop<sup>1</sup> (from *Rattus norvegicus*) identified in 1989 by expression cloning (Hollmann et al., 1989). Earlier findings in this field had shown that the *N*-methyl-D-aspartate (NMDA) receptor antagonist D-APV had neuroprotective and anticonvulsant effects and that  $\text{Ca}^{2+}$  entry through glutamate (particularly NMDA) receptor channels might play a role in a variety of neurological diseases as well as development and synaptic plasticity, i.e. learning and memory processes [reviewed by Palmer et al. (2005) for AMPA receptors; Cull-Candy et al. (2001) and Wenthold et al. (2003) for NMDA receptors].

For GluRs, expression cloning had turned out to be the method of choice due to the lack of high affinity ligands and a very low sequence similarity to other ion channels that had been successfully cloned and whose sequence information was therefore already known.

For these proteins (such as acetylcholine, glycine and  $\text{GABA}_A$  receptors) sharing the availability of high affinity ligands, common biochemical isolation and purification strategies using affinity chromatography followed by sequencing of the identified protein and the isolation of the corresponding cDNA via degenerated primers had proven successful. However, for the reasons mentioned above, this strategy had turned out to be insufficient for GluRs and, accordingly, cDNA screening procedures based on already known receptor sequences had been unsuccessful as well.

Contrary to protein biochemistry, expression cloning identifies single clones of a cDNA library which are expressed in *Xenopus laevis* oocytes and tested for functionality in electrophysiological recordings. As an advantage, the full-length cDNA of a functional receptor subunit is already available at the time point of its identification.

The superfamily of vertebrate GluRs comprises 5 pharmacologically as well as molecularly defined subfamilies based on their ligands with the highest affinities and on

---

<sup>1</sup> The AMPA receptor subunit GluR1 was originally assigned to the kainate receptor subfamily (and thus named GluR-K1) due to kainate causing slower desensitisation than glutamate or AMPA and therefore producing larger currents. However, ligand binding data available later on showed that AMPA and glutamate had much higher affinities for this receptor than kainate.

sequence homology : AMPA ( $\alpha$ -amino-3-hydroxymethyl-4-isoxazole-propionic acid), kainate (KA) and NMDA receptors as well as kainate binding proteins (KBPs; not present in mammals) and the delta subunits (also termed orphan receptors) (Fig. 1).

After the identification of the AMPA receptor GluR1, the sequencing information now available was used to screen cDNA libraries by low-stringency hybridisation or through polymerase chain reaction (PCR) amplification. This allowed to rapidly isolate subfamilies of GluR subunit cDNAs encoding AMPA and kainate receptors [reviewed by Hollmann and Heinemann (1994) and Hollmann (1999)]. Since initial attempts to clone NMDAR subunits based on sequence similarity to AMPA and kainate receptors failed, the first NMDA receptor, NR1, was again isolated by functional expression in *Xenopus laevis* oocytes (Moriyoshi et al., 1991). Subsequently, all other subunits of the NMDAR subunit family could again be cloned based on the known (non-NMDA GluR and) NR1 sequences [Monyer et al., 1992, Ishii et al., 1993, Boulter, 1997 (for NR2A-NR2D); Sullivan et al., 1994 (for NR2B); Sucher et al., 1995, Ciabarra et al., 1995 (for NR3A); Chatterton et al., 2002 (for NR3B)]. Nine subunits of the AMPA/KA receptor subfamily and seven of the NMDAR subfamily (whereby eight splice variants for NR1 exist; see 1.3.1) have been described so far.

The first three subfamilies mentioned above are well-studied, while the function of kainate binding proteins as well as the function and ligands of the delta subunits are still unknown. These last two subfamilies share about 30% sequence homology with other members of the GluR family.

### Subunits belonging to the superfamily of vertebrate glutamate receptors

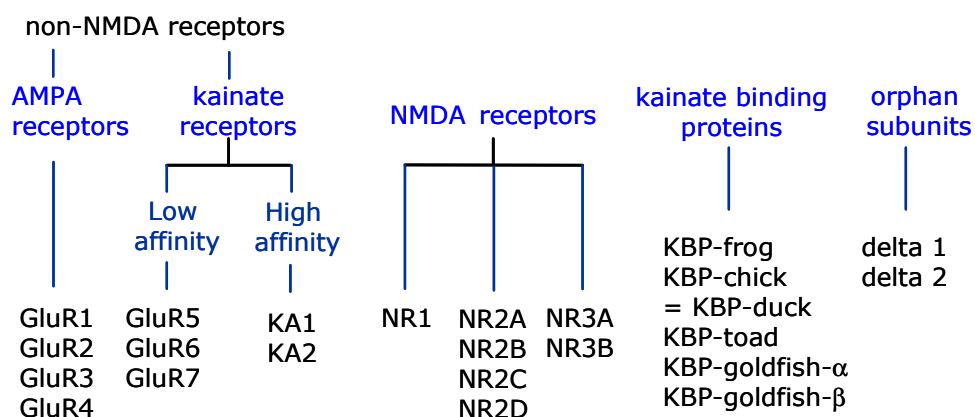


Fig. 1 : The superfamily of vertebrate glutamate receptors consists of five subfamilies harbouring 23 subunits. The five KBPs do not occur in mammals; frog: *Rana pipiens* (the leopard frog); chick: *Gallus domesticus* (domestic chick); duck: *Anas domesticus*; toad: *Xenopus laevis*; goldfish: *Carassius auratus*; KBP-toad = XenU1 (Ishimaru et al., 1996; Green et al., 2002).

### 1.2.2 Tertiary structure of GluR subunits

All GluR subunits possess a common transmembrane topology : The initially expected transmembrane topology, a four-transmembrane-domain model, was revised by the analysis of endogenous and introduced *N*-glycosylation sites [shown for GluR1 by Hollmann et al. (1994)].

#### Topology of a GluR subunit

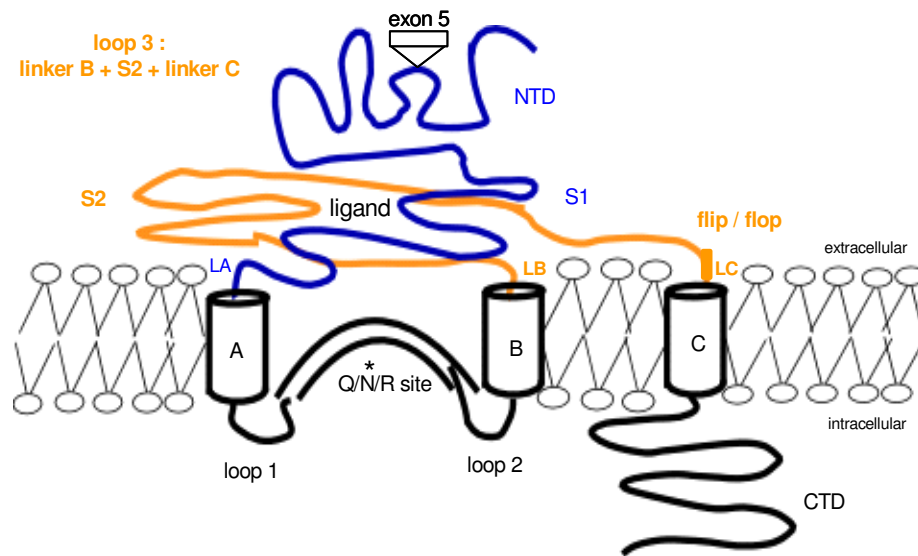


Fig. 2 : A GluR subunit owns three TMDs (termed A, B and C) and a cytoplasm-facing membrane domain constituting the ion pore.

NTD: N-terminal domain, CTD: C-terminal domain. S1 and S2 designate the two ligand binding domains.

LA, LB, LC: The linkers A, B and C connect the extracellular domains to the TMDs A, B and C, respectively.

Exon 5 is the exon insert characteristic for "b"-splice variants of the NR1 subunit.

The alternatively spliced flip/flop exon occurs in AMPA receptors.

The Q/N/R site in the ion pores of AMPA, kainate and NMDA receptors controls not only ion channel conductance but also receptor trafficking. It is used as an electrophysiological marker in the present study (cf. 1.2.3).

According to the current model, GluRs have only three transmembrane domains (TMDs) plus a cytoplasm-facing hairpin loop, which does not actually cross the membrane. Consequently, the N terminus is located extracellularly and the C terminus is intracellular (see Fig. 2). The three TMDs are separated by three loops, two of them located on the intracellular and one on the extracellular side.

The glutamate binding region is formed by two extracellular domains, S1 following the N terminus and S2 formed by loop 3. The S1 and S2 lobes form a hinge-like structure that undergoes a conformational change to enclose the ligand upon binding (Armstrong et al., 1998).

A hairpin loop entering the membrane from the cytoplasmic side constitutes the ion pore domain (Hollmann et al., 1994).

The N terminus forms a separate domain homologous to the bacterial periplasmic leucine-isoleucine-valine-binding protein (LIV-BP). As shown for AMPA receptors, it mediates subunit-specific assembly of receptor complexes (Leuschner and Hoch, 1999), while the C-terminal domain of NMDAR subunits constitutes a target for binding of PDZ<sup>2</sup> domain-containing postsynaptic density (PSD) proteins of the PSD-95<sup>3</sup> family expressed in neurons (Kornau et al., 1995; Kim et al., 1996).

### 1.2.3 The Q/N/R site of ionotropic glutamate receptors

The primary transcripts for the AMPA receptor GluR2 and the kainate receptors GluR5 and GluR6 are post-transcriptionally modified *in vivo* by RNA editing which causes a single-amino acid exchange of glutamine (Q) to arginine (R) (in GluR2 at position 586, for example). Functionally, the arginine in GluR2 leads to low single-channel conductance, low Ca<sup>2+</sup> and Mg<sup>2+</sup> permeability, and a change from an inwardly rectifying to a linear current-voltage relation due to a release of block by cytoplasmic polyamines (e.g. spermine), even in receptors containing only one GluR2(R) subunit. The R editing variant is therefore considered to be dominant in terms of the features mentioned above. While 99 % of the GluR2 mRNA population has arginine, only about 50 % of GluR5 and 80 % of GluR6 are edited at the Q/R site. In fish, however, the Q/R site arginine is genomically encoded [reviewed by Hollmann (1999)].

Arg586 is also the major trafficking determinant of GluR2 by controlling ER (endoplasmic reticulum) export : GluR2(R) is retained in an intracellular reserve pool in the ER where it is complexed with GluR3 but not with GluR1. Mutation to GluR2(Q) leads to rapid ER export and prominent surface expression as seen for GluR1 (Greger et al., 2002). In principal neurons, GluR2(R) is present in most channels (therefore being Ca<sup>2+</sup> impermeable), while interneurons only express low levels of GluR2 (and therefore Ca<sup>2+</sup>

---

<sup>2</sup> abbreviation for PSD-95, the *Drosophila* septate junction protein Discs-large, and the mammalian tight junction protein ZO-1

<sup>3</sup> postsynaptic density protein of 95 kDa / SAP 90 : synapse associated protein of 90 kDa

permeable AMPA receptors) (Jonas and Burnashev, 1995). Two functional implications have been hypothesised for Q/R-controlled ER export : On the one hand, concentration of GluR2(R) in the ER might increase the probability of its incorporation during AMPAR assembly and thus explain its presence in the majority of AMPA receptors in the brain. On the other hand, Liu and Cull-Candy reported in 2000 that repetitive synaptic stimulation resulted in a switch from GluR2-lacking to GluR2-containing AMPA receptors in the cerebellum which would protect neurons from excessive  $\text{Ca}^{2+}$  influx through AMPA receptors during increased synaptic activity. In a more detailed analysis of the assembly rules of GluR2, Greger et al. (2003) found out that GluR2 (R/Q) heterodimer formation is preferred over homodimerisation and that GluR2 (R) tetramerisation is energetically disfavoured. Occlusion of GluR2(R) homomers makes sense since such channels display a very low single-channel conductance and would decrease the activity of a synapse.

Other arginine-based retention motifs have been reported, e.g. RKR for ATP-sensitive  $\text{K}^+$  channels (Zerangue et al., 1999), NR1-1a, NR3A and NR2B (Perez-Otano et al., 2001). Contrary to the Q/R point mutation in GluR2, these motifs comprise more than one arginine and lie outside a transmembrane segment (Perez-Otano et al., 2001; Greger et al., 2002).

Where non-NMDA receptors contain a glutamine, NMDA receptors feature an asparagine (N). Correspondingly, site-directed mutagenesis substituting the asparagine at position 598 in NR1-1a with an arginine *in vitro*<sup>4</sup> affected single-channel conductance and  $\text{Ca}^{2+}$  permeability. In addition to this, the mutation N598R abolished voltage-dependent block by  $\text{Mg}^{2+}$  and inhibition by  $\text{Zn}^{2+}$  and the open channel blocker (+)MK-801 (Sakurada et al., 1993). Recent models for the trafficking of NMDA receptors to the plasma membrane are discussed in section 1.3.3.2.

#### 1.2.4 Quarternary structure of GluR subunits

The exact subunit composition of GluRs has been a matter of debate for a long time. While previous data were consistent with pentameric AMPA and NMDA receptors (Wenthold et al., 1992; Premkumar et al., 1997), recent crystallographic studies (e.g. for the ligand-binding domain of GluR2 complexed with kainate; Armstrong et al., 1998; Sun et al., 2002) and single-channel recordings (Rosenmund et al., 1998 in HEK cells) indicate that

---

<sup>4</sup> No RNA editing has been observed for NMDA receptors (Hollmann and Heinemann, 1994).

AMPA and kainate receptors (Mayer, 2005; Nanao et al., 2005; Naur et al., 2005) most likely consist of four subunits assembled as a dimer of dimers.

In the case of NMDA receptors, two studies using similar single-channel recording techniques came to different results regarding the number of NR1 subunits, with Behe et al. (1995) assuming two copies and Premkumar and Auerbach (1997) claiming three.

In 2003, Schorge and Colquhoun constructed homomeric and heteromeric NMDAR tandems containing head subunits truncated before the 3<sup>rd</sup> TMD and intracellular tail (see also 1.4.2.1) and expressed these in HEK cells. By patch clamp analysis, they postulated a tetrameric NMDAR structure arranged as a dimer of dimers with a pairwise (rather than an alternating) pattern of like subunits in the complex.

In 2005, Furukawa et al. presented the crystal structure of the NR1-NR2A ligand binding core in complex with glutamate and glycine. Complemented by biochemical, electrophysiological and sedimentation experiments, their data identified the NR1-NR2A heterodimer as the functional unit in NMDA receptors, thereby also assuming an overall pairwise arrangement of two NR1 and two NR2A subunits in a tetrameric receptor channel (as Schorge and Colquhoun did in 2003). The heteromeric substructure within a tetrameric NMDA receptor proposed by this group reflects a more precise insight in the subunit assembly of an entire channel than the results by Schorge and Colquhoun (Fig. 43). It is, however, opposed to AMPA and kainate receptor studies where an assembly of a homodimer of dimers was postulated.

Due to the existence of a third subunit type in the NMDAR subfamily, NR3, the stoichiometry of NMDAR channels still requires a more detailed analysis regarding the contribution of this subunit to the formation and structure of a functional NMDAR complex. In a recent report, Atlason and McIlhinney (Atlason and McIlhinney, FENS Abstr., 2006) used cross-linking studies and combined them with measurements of cell surface expression in transfected HEK cells to show that NR1 but not NR2 or NR3 can form dimers when expressed alone. Their data would be more consistent with the formation of NR1-NR2 and NR1-NR3 heterodimers (rather than homodimers) before their assembly into functional tetramers.

Despite its physiological relevance, determining the structure of a full-length vertebrate glutamate receptor in its native oligomeric state will probably remain difficult to achieve for some time. This is because successful techniques for the overexpression and purification of eukaryotic ion channel proteins are just at the beginning and the crystallisation of membrane proteins in their native conformation is intrinsically difficult.

### **1.3 The NMDA receptor**

#### **1.3.1 NMDAR subunits and splice variants**

Over the past decade, seven different NMDAR subunits have been identified : the ubiquitously expressed gene NR1 (Moriyoshi et al., 1991), a family of four distinct NR2 genes [A, B, C and D; Monyer et al., 1992, Ishii et al., 1993, Boulter, 1997 (for NR2A-NR2D); Sullivan et al., 1994 (for NR2B)], and two NR3 genes [Sucher et al., 1995, Ciabarra et al., 1995 (for NR3A); Chatterton et al., 2002 (for NR3B)].

The NR1 subunit gene consists of 22 exons and has eight different splice variants, which arise from different combinations of an N-terminal exon insertion (exon 5) and three different C-terminal exon deletions. This gives rise to NR1-1a, -1b, -2a, -2b, -3a, -3b, -4a and -4b (Hollmann et al., 1993). NR1-1 is the longest clone, while NR1-2 lacks exon 21. NR1-3 lacks the beginning of exon 22, leading to the use of a new, previously out-of-frame stop codon in the 3'-UTR (untranslated region) of NR1-1. NR1-4 combines the two deletions occurring in NR1-2 and NR1-3.

The lower case letters a and b indicate the absence (a) and presence (b) of exon 5. These splice variants differ in their electrophysiological and pharmacological properties, with current amplitudes larger for NR1-3 than for NR1-1, NR1-4, and NR1-2 (in this order). Currents for subunits with exon 5 (b) are ~ three fold larger compared to currents for those without (a). Most antagonists discriminate between the two types of splice variants, with "a"-splice variants being blocked to a smaller extent than "b"-splice variants (Hollmann et al., 1993). At physiological pH, splice variants that include exon 5 are fully active, whereas "a"-splice variants are partially blocked by protons (Cull-Candy et al., 2001).

Similarly, each of the NR2B-NR2D and NR3 subunits (but not NR2A) has several splice variants, although their functional relevance is unknown (Cull-Candy et al., 2001). For NR3A, the existence of the splice variant NR3A-2 has been reported. Here, splicing leads to a 20-amino acid insert in the C-terminal domain. However, the functional relevance of NR3A-2 could not be shown yet.

#### **1.3.2 Electrophysiological and pharmacological properties of the NMDA receptor**

Fast information transmission in the nervous system is mediated by ionotropic receptors and can be differentiated into a fast (milliseconds) and slow (tens or hundreds of milliseconds) component.

While AMPA and kainate receptors mediate this fast synaptic activity in the millisecond range, NMDA receptors are notorious for their slow kinetics, i.e. activation and deactivation times in a hundred-of-millisecond range.

NMDAR channels first open about 10 ms after glutamate has been released into the synaptic cleft, and continue to open and close repeatedly for several hundreds of milliseconds until glutamate unbinds from receptor (Behe et al., 1999). The decay times of NMDA receptor-mediated excitatory postsynaptic currents (EPSCs), and the concomitant affinity of the receptors for glutamate, are both dominated by the identity of the NR2 subunits involved (see below).

The NMDA receptor possesses several other unique features [reviewed by Dingledine et al. (1999)] : It not only allows an influx of  $\text{Na}^+$  and an efflux of  $\text{K}^+$ , but also an influx of  $\text{Ca}^{2+}$ . It requires the simultaneous binding of glutamate and the co-agonist glycine. Besides the glutamate binding and the glycine binding regulatory sites, it is thought to have several other pharmacologically distinct sites, i.e. a voltage-dependent (non-competitive)  $\text{Mg}^{2+}$  binding site, several different  $\text{Zn}^{2+}$  binding sites, and sites in the channel that bind various channel blockers.

$\text{Mg}^{2+}$  ions act as open channel blockers and bind to the narrow constriction deep within the NMDAR channel, at the tip of the pore loop, to occlude the flow of cations (Beck et al., 1999; cf. Fig. 2). Both the NR1 and NR2 subunits of a heteromeric NMDA receptor are thought to contribute to the binding site (Kuner et al., 1996).

At resting membrane potentials (about - 60 mV), NMDA receptors are blocked by external  $\text{Mg}^{2+}$ . This block is relieved only when the neuron is depolarised simultaneously (above - 20 mV; 1.3.4).

NMDAR antagonists comprise the competitive antagonist D-APV [D-(-)-2-amino-5-phosphonate pentanoic acid; a phosphono derivative of a short-chain (five carbons) amino acid], the non-competitive antagonist ifenprodil, and open channel blockers<sup>5</sup> such as (+)MK-801 and cytoplasmic polyamines.

D-APV is a competitor of the glutamate or NMDA binding site. Ifenprodil acts through the proton sensor of the NR1 subunit, which is the sequence encoded by exon 5 of NR1 (Traynelis et al., 1995; Masuko et al., 1999). Ifenprodil has an  $\text{IC}_{50}$  (concentration producing half maximal inhibition) that is about 400 fold lower for an NR2B-containing

---

<sup>5</sup> Open channel blockers only act on the activated receptor, not the receptor at rest, i.e. their binding site is available once the channel is in the open state. The bound blocker is trapped by channel closure and can be recovered (i.e. removed) by additional application of agonist.

NMDA receptor or NR1 alone than for NR2A-, NR2C- or NR2D-containing receptors (Cull-Candy et al., 2001; Williams, 1993). Consequently, ifenprodil has been applied as a suitable subunit-selective drug, being neuroprotective in animal models of cerebral ischemia (Gotti et al., 1988; Dingledine et al., 1999).

As mentioned above, many of the unique features of NMDA receptors are influenced by the subunit composition : In 1994, Monyer et al. investigated recombinant NR1-NR2 channels in HEK cells and found that all four receptor types showed a comparable high  $\text{Ca}^{2+}$  permeability but differed markedly in their  $\text{Mg}^{2+}$  block and decay times : NR1-NR2A and NR1-NR2B receptors exhibited a stronger voltage-sensitivity of the  $\text{Mg}^{2+}$  block than the NR1-NR2C and NR1-NR2D channels. The decay time of NR1-NR2A channels was 3-4 times faster than that of NR1-NR2B or NR1-NR2C and these latter two about 10 times faster than the decay of the NR1-NR2D combination. Thus, differences in EPSC decay could be used to infer the NR2 subunit composition of native NMDA receptors (Cull-Candy et al., 2001).

The NR3 subunits NR3A or NR3B do not form functional receptors alone, but can assemble with NR1 to form a glycine receptor (Chatterton et al., 2002). They can also co-assemble with NR1 and NR2 and seem to exert an inhibitory function on NR1/NR2 complexes by associating in a yet undefined fashion [Ciabarra et al., 1995, Sucher et al., 1995, Das et al., 1998, Perez-Otano et al., 2001 (for NR3A); Nishi et al., 2001 (for NR3B)] : Co-expression of recombinant NR3A or NR3B results in smaller whole-cell currents, single-channel conductances, and  $\text{Ca}^{2+}$  permeabilities compared to "conventional" (NR1/NR2) NMDA receptors. Consistent with this role for, e.g., NR3A found in heterologous expression systems, mice lacking NR3A have larger NMDAR currents and increased numbers of dendritic spines in cerebrocortical neurons (Das et al., 1998). Taken together, this suggests that NR3 subunits are involved in development and plasticity of the CNS by modulating the activity of "conventional" NMDA receptors.

As explained in (1.2.4), most likely two NR1 subunits partner with two NR2 subunits of at least one type to form a functional NMDAR channel. Regarding the subunit structure of NMDA receptors, it is still unclear how exactly the NR3A (and also NR3B) subunit is incorporated in the NMDAR complex (cf. 4.2.5).

### 1.3.3 Expression pattern of NMDAR subunits

#### 1.3.3.1 In the brain

While NR1 is ubiquitously and continuously expressed in the CNS, *in situ* hybridisation studies from rat and mouse brain have shown that expression patterns of the individual NR2 subunit mRNAs change strikingly, depending on the developmental stage as well as brain region (Monyer et al., 1994; McBain and Mayer, 1994). NR2B and NR2D subunits predominate in the embryonic brain where NR2A and NR2C are absent. In contrast, in the adult brain, NR2A predominates (and becomes ubiquitously expressed) while NR2B expression disappears from the cerebellum and becomes restricted to forebrain areas (hippocampus and neocortex). NR2C becomes highly enriched in the cerebellum. Over the course of development, NR2B expression is thus supplemented with or replaced by NR2A, and in some regions NR2C subunits (e.g. cerebellar granule cells) (Fig. 3).

#### Developmentally regulated expression of NR2A and NR2B in rat brain

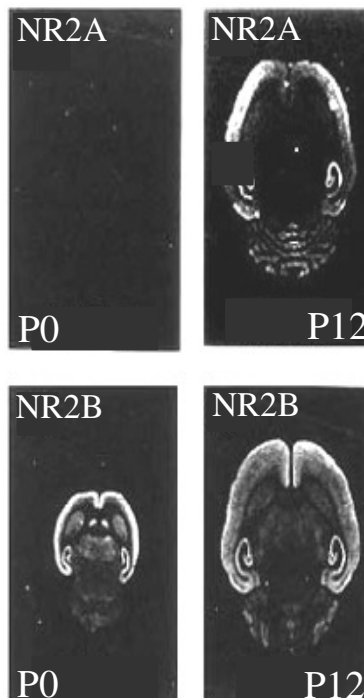


Fig. 3 : Expression of NR2A and NR2B subunits in the neonatal (P0) and postnatal (P12) rat brain was shown by *in situ* hybridisation (autoradiograms taken, with written permission, from Monyer et al., 1994, (c) 1994 by Elsevier, "[www.neuron.org](http://www.neuron.org)"). The NR2A and NR2B subunits are the most widespread NR2 subunits. NR2A mRNA is expressed only in the adult brain. By contrast, NR2B mRNA predominates prenatally and becomes mainly forebrain specific after birth (hippocampus and neocortex).

From *in situ* and immunocytochemical analyses of adult rats, NR3B expression appears limited to motor neurons where it might take part in transmission in the spinal cord, a region in which glycine has long been known to have synaptic actions (Chatterton et al., 2002).

In contrast to NR3B, NR3A is more widely distributed, and primarily expressed during brain development : From the embryonic period until the first postnatal week, it can be found in many regions of the developing rat brain. In the following, however, transcript levels decline drastically and remain at very low levels into adulthood. The developmental and regional expression pattern of NR3A suggests that it could influence NMDAR effects on axonal outgrowth and synaptogenesis during brain development (Sucher et al., 1995; Ciabarra et al., 1995).

### **1.3.3.2 Intracellular trafficking**

The process by which an NMDA receptor assembles from its individual subunits and is trafficked to synaptic and extrasynaptic sites remains poorly understood [reviewed by Prybylowski and Wenthold (2004)]. Neurons have a large excess of the NR1 subunits relative to NR2 subunits, and the pool of unassembled NR1 does not reach the cell surface. Overexpression of NR2A or NR2B by transfection increases the number of surface NMDA receptors in primary cultures of cerebellar granule cells, demonstrating that the formation of functional NMDA receptors is limited, at least in part, by the availability of NR2 subunits (Prybylowski et al., 2002).

In heterologous cells, the NR1 splice variant NR1-1 and the NR2 subunits are retained in the ER when expressed alone, but when expressed together, they assemble to form functional receptors that exit the ER and reach the cell surface (McIlhinney et al., 1996 and 1998). ER retention of the (unassembled) NR1-1 and NR2B subunits is likely to depend on a di-arginine RXR-motif in the C terminus (for NR1-1 it is located in exon 21; cf. 1.2.3). The C termini of other NR2 subunits (including NR2A) contain a di-lysine motif (KKXX) [reviewed by Wenthold et al. (2003)].

As a mechanism underlying the ER retention of unassembled NMDAR subunits, it has been hypothesised that the ER retention signals mentioned above are unmasked in individual, unassembled subunits. Export from the ER would then require that the C termini of the two subunits (of a dimeric subcomplex) interact and mutually mask their retention signals. Such a mechanism allows for release of only those complexes that are properly folded and assembled with the correct stoichiometry of subunits.

Additional sites are candidates to mediate the retention and the synaptic localisation of the NMDA receptor. Independent groups found that a second, conformationally-dependent motif involving the amino acid sequence HLFY<sup>6</sup> in NR2A and NR2B (through interaction with a protein) is necessary for a functional NMDA receptor to leave the ER (Vissel et al., 2001; Zheng et al., 1999; Hawkins et al., 2004).

In neurons, the PDZ domain binding sites in the C termini of the NR2A and NR2B subunits have also been shown to be critical for localisation of the NMDA receptor to the synapse (Prybylowski et al., 2002; Perez-Otano et al., 2001; cf. 1.2.2).

Finally, it must be further considered that, for non-NMDA receptors, control of ER export is exerted by a single arginine at the Q/R editing site within the ion pore (1.2.3).

The role of the equivalent site in NMDA receptors (N598R in NR1-1a) has not been addressed yet.

#### **1.3.4 Role of the NMDA receptor during synaptic transmission**

Owing to their fast kinetics, non-NMDA receptors play a major role in mediating excitatory moment-to-moment communication in the CNS.

NMDA receptors are also present at excitatory synapses in the CNS but have specialised characteristics, including high  $\text{Ca}^{2+}$  permeability,  $\text{Mg}^{2+}$  block at resting membrane potentials, and slow kinetics [reviewed by Cull-Candy et al. (2001)]. These properties have led to the major implication of these receptors in long-lasting changes of structure and function of neurons and their synapses, generally termed synaptic plasticity. Synaptic plasticity is classified in long-term potentiation (LTP, increase in EPSPs) and long-term depression (LTD, decrease in EPSPs) and thought to underlie learning and memory processes induced by  $\text{Ca}^{2+}$  and protein kinase C-mediated alterations in gene expression [initially hypothesised by Bliss and Lomo (1973); Bliss and Collingridge, 1993]. However, there is controversy about this coincidence because Zamanillo and colleagues (Zamanillo et al., 1999) noticed that learning was unimpaired in GluR1 knock-out mice although LTP was undetectable.

A recent study has found that the "type" of plasticity (i.e. LTP or LTD) is controlled only by the number and subunit composition of NMDA receptors available on the postsynaptic membrane (Barria and Malinow, 2005).

---

<sup>6</sup> The four amino acids of the HLFY motif are located behind the last TMD, immediately at the beginning of the C terminus.

Apart from the positive effects of  $\text{Ca}^{2+}$  mediating plasticity after frequent activation of NMDA receptors, excess  $\text{Ca}^{2+}$  influx through NMDA receptors (beside other ion channels : Aarts et al., 2003; Xiong et al., 2004) can lead to excitotoxic effects and neuronal cell death in brain damage and stroke.

Since NMDA receptors are subject to an extracellular  $\text{Mg}^{2+}$  block at resting membrane potentials, their activation always requires a simultaneous depolarisation of the postsynaptic membrane, presumably through activation of the fast non-NMDA component. The necessity for co-activation is likely to represent a control for  $\text{Ca}^{2+}$  influx and synaptic activity through NMDA receptors. In fact, there are functionally inactive or "silent" postsynaptic membranes that contain NMDA receptors but no AMPA receptors. AMPA receptors can be recruited to these synapses within minutes (probably from extrasynaptic regions) after either spontaneous or stimulated NMDAR activation. The "unsilencing" of such synapses by the rapid insertion of functional AMPA receptors is likely to be a key determinant for NMDAR-dependent synaptic plasticity [reviewed by Wenthold et al. (2003) and Palmer et al. (2005)].

## **1.4 The concatemer strategy**

### **1.4.1 The concatemer strategy applied to other ion channels**

The concatemer strategy entails the covalent linkage of two or more subunits of a multimeric protein complex. This allows to constrain a defined ratio and order of subunits in the protein complex assembled from the concatemers. Exploiting this advantage, the concatemer strategy has been employed to study the stoichiometry of voltage-gated  $\text{K}^+$  channels (Liman et al., 1992) followed by other neurotransmitter receptors and membrane proteins such as the  $\text{GABA}_A$  receptor, the nicotinic acetylcholine receptor (Groot-Kormelink et al., 2004), cyclic nucleotide-gated channels, P2X (ATP-gated) channels (Nicke et al., 2003), and also the NMDAR subfamily of GluRs (Prybylowski et al., Soc. Neurosci. Abstr., 1999; Schorge and Colquhoun, 2003). However, a potential pitfall of the concatemer approach has become evident recently : In addition to a disruption of normal receptor association, steric constraints of the covalent linker and independent behaviour of subunits, two groups reported the problem of lower order byproducts that contributed to receptor assembly to a great degree (or even much more than) the concatemers themselves (Nicke et al., 2003 and Groot-Kormelink et al., 2004).

As explanations for these unwanted byproducts, the usage of internal methionines as translation start sites, a proteolytic cleavage of full-length concatemers and a premature termination of translation (most likely) have been proposed in the case of P2X receptors (Nicke et al., 2003).

In all these reports, except for the NMDAR study, both termini of each subunit were on the same side of the membrane, providing the opportunity to join both subunits via a short covalent linker.

## 1.4.2 The concatemer strategy applied to glutamate receptors

### 1.4.2.1 Previous work by other groups

Concatemeric constructs have previously been employed to study NMDAR stoichiometry and subunit arrangement (Schorge and Colquhoun, 2003).

Owing to the revised membrane topology of glutamate receptors (see 1.2.2), N and C termini lie on opposite sides of the membrane. Thus, it is not possible to directly link them together. This challenge was tackled in two different ways :

1) Schorge and Colquhoun (2003) used C-terminally truncated monomers (similar to the bacterial glutamate-activated  $K^+$  channel GluR0 with only two TMDs) to form receptors which became functional when the missing final TMD and intracellular tail was expressed as a separate polypeptide (Fig. 4). By joining these truncated monomers to full-length subunits, functional "tandems" were obtained suggesting that NMDA receptors are tetramers arranged as dimers of dimers in a pairwise orientation of two NR1 and two NR2 subunits.

#### Concatemer strategy using a C-terminally truncated head subunit

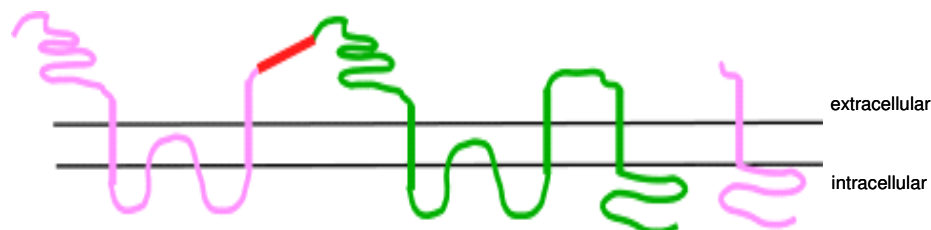


Fig. 4 : 1<sup>st</sup> approach : C-terminal truncation of the 1<sup>st</sup> (head) subunit and co-expression of the missing C tail as separate polypeptide (schematic structure according to Schorge and Colquhoun, 2003).

The 2<sup>nd</sup> (tail) subunit is full-length. The red line represents the newly generated linkage which joins the truncated head to the tail subunit.

The fact that the tandems required the missing final TMD for function suggested that the truncated subunits within the tandems contributed to the channels. Additionally, it was possible to distinguish electrophysiologically between a functional contribution from truncated and full-length subunits since the former were "tagged" with a loss of desensitisation due to their truncation.

Qualitatively, the tandems behaved like wild type channels and showed blockage by APV,  $Mg^{2+}$  and kynurenic acid. Quantitatively, however, potencies of glutamate and glycine were dramatically shifted compared to controls. A possible reason for this given by the authors was a (partial) disruption of the S2 domain in the head subunit caused by the linkage of the truncated head to the wild type tail subunit. This would in turn affect the ligand binding sites formed in part by the S2 domain.

As an additional point of criticism, it should be considered that a membrane insertion of the missing C tails in close proximity to the tandems has not been shown.

2) Prybylowski et al. (Soc. Neurosci. Abstr., 1999) introduced a long transmembrane linker, the 4<sup>th</sup> TMD of the  $\alpha_1$ -subunit of the bovine GABA<sub>A</sub> receptor, between the C terminus of the head and N terminus of the tail subunit of the tandem (Fig. 5) and proposed a pentameric stoichiometry for NMDA receptors. This project was abandoned because the two tandems generated showed breakdown in Western blotting before the tail subunit.

### Concatemer strategy using an additional transmembrane domain as linker

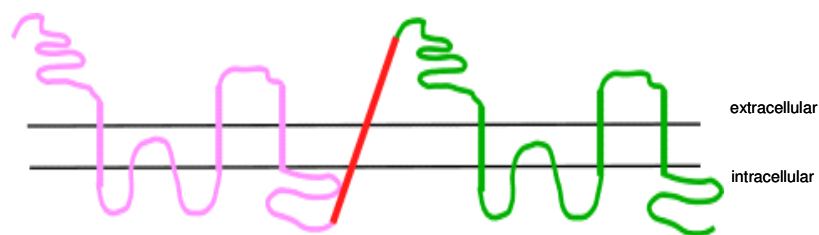


Fig. 5 : 2<sup>nd</sup> approach : Insertion of a long membrane-spanning linker between two full-length NMDAR subunits [schematic structure according to Prybylowski et al., Soc. Neurosci. Abstr. (1999)].

The **head subunit** of the dimer is shown in **pink**, the **tail subunit** in **green** and the **linker** in **red** (colour code as in Fig. 4).

## 1.4.2.2 Previous work in the lab

### 1.4.2.2.1 Generation and analysis of homomeric GluR1 concatemers

Previous work in the lab focussed on the generation and analysis of homomeric GluR1 dimers and trimers. Among different long transmembrane linkers [e.g. the GluR1 signal peptide, the 3<sup>rd</sup> TMD of GluR1, and the 4<sup>th</sup> TMD of the  $\alpha_1$ -subunit of the bovine GABA<sub>A</sub> receptor (= TG4)], TG4L was identified as the most suitable domain (Figs. 6, 7). TG4L consists of TG4 plus neighbouring hydrophilic amino acids. Concatemers incorporating TG4L yielded the largest current amplitudes.

The incorporation of both subunits of the GluR1 concatemers could be shown electrophysiologically for dimers (M. Hollmann, personal communication).

### Topology of the $\alpha_1$ -subunit of the GABA<sub>A</sub> receptor

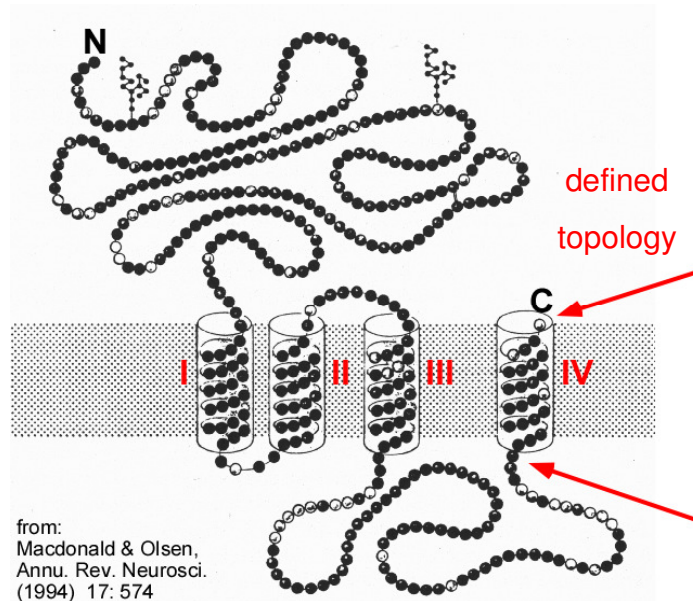


Fig. 6 : The  $\alpha_1$ -subunit of the GABA<sub>A</sub> receptor, whose topology is known, comprises four transmembrane domains (I, II, III and IV). TMD IV forms the core of the "TG4 linker series" (Fig. 7) which was chosen to construct GluR concatemers.

Figure reprinted, with written permission, from the Annual Review of Neuroscience, Volume 17 (c) 1994 by Annual Reviews, "[www.annualreviews.org](http://www.annualreviews.org)".

### Series of TG4 linkers

TG4 (34 aa):

TMD IV  
GSKIDRLSRIAFPLLFGIFNLVYWATYLNREKLG

TG4L (56 aa):

TMD IV  
GKKTFFNSVSKIDRLSRIAFPLLFGIFNLVYWATYLNREPQLKAPTPHQYVLSTKLG

TG4L2 (56 aa):

TMD IV  
KSFKQKKTFFNSVSKIDRLSRIAFPLLFGIFNLVYWATYLNREPQLKAPTPHQYVLSTKLG

TG4L : TG4 + adjacent hydrophilic residues

TG4L2 : TG4L + 8-cutter restriction sites (*Swa* I, *Pme* I + *Asc* I)

(black: native; blue: artificial; orange: introduced for cloning purpose)

Fig. 7 : Sequence of linker domains used to construct GluR concatemers. All linkers are based on the 4<sup>th</sup> TMD of the  $\alpha_1$ -subunit of the bovine GABA<sub>A</sub> receptor (Fig. 6). TG4L and TG4L2 turned out to be the most suitable TMDs. TG4L2 was used in the present study. TG4L is TG4 flanked by hydrophilic amino acids intended to reduce a putative steric hindrance by the covalent linkage. TG4L2 differs from TG4L by the presence of restriction sites required for cloning.

Thus, we are using the same core unit as a linker as Prybylowski et al. did in 1999. However, TG4L and TG4L2 contain additional hydrophilic amino acids adjacent to the core linker which were introduced to reduce a suspected steric hindrance owing to the presence of an additional long membrane-spanning domain in the concatemer (Fig. 8).

### Concatemer strategy used in the present study

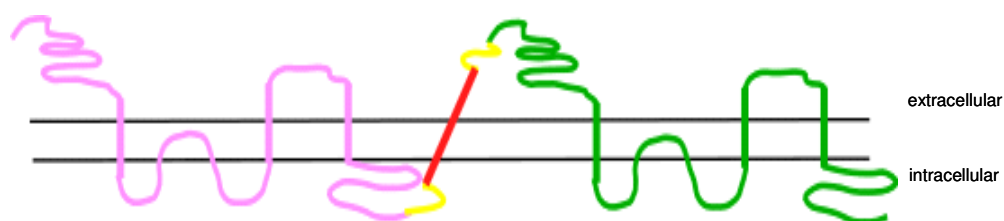


Fig. 8 : Similar to Prybylowski et al. (Soc. Neurosci. Abstr., 1999) in Fig. 5, an **additional membrane-spanning domain** was inserted between a full-length **head** and **tail** GluR subunit in the present study. However, the **linker (TG4L2)** used in this study is flanked by **additional hydrophilic amino acids**. Colour code as in Figs. 4, 5.

### 1.4.2.2.2 Engineering strategy to generate concatemers from all 18 mammalian GluR cDNAs

A strategy had previously been developed in the lab allowing the construction of dimeric concatemers of all 18 mammalian GluR cDNAs using a set of four restriction endonucleases, all of them 8-cutters (Fig. 9).

#### General cloning scheme to construct dimeric GluR concatemers

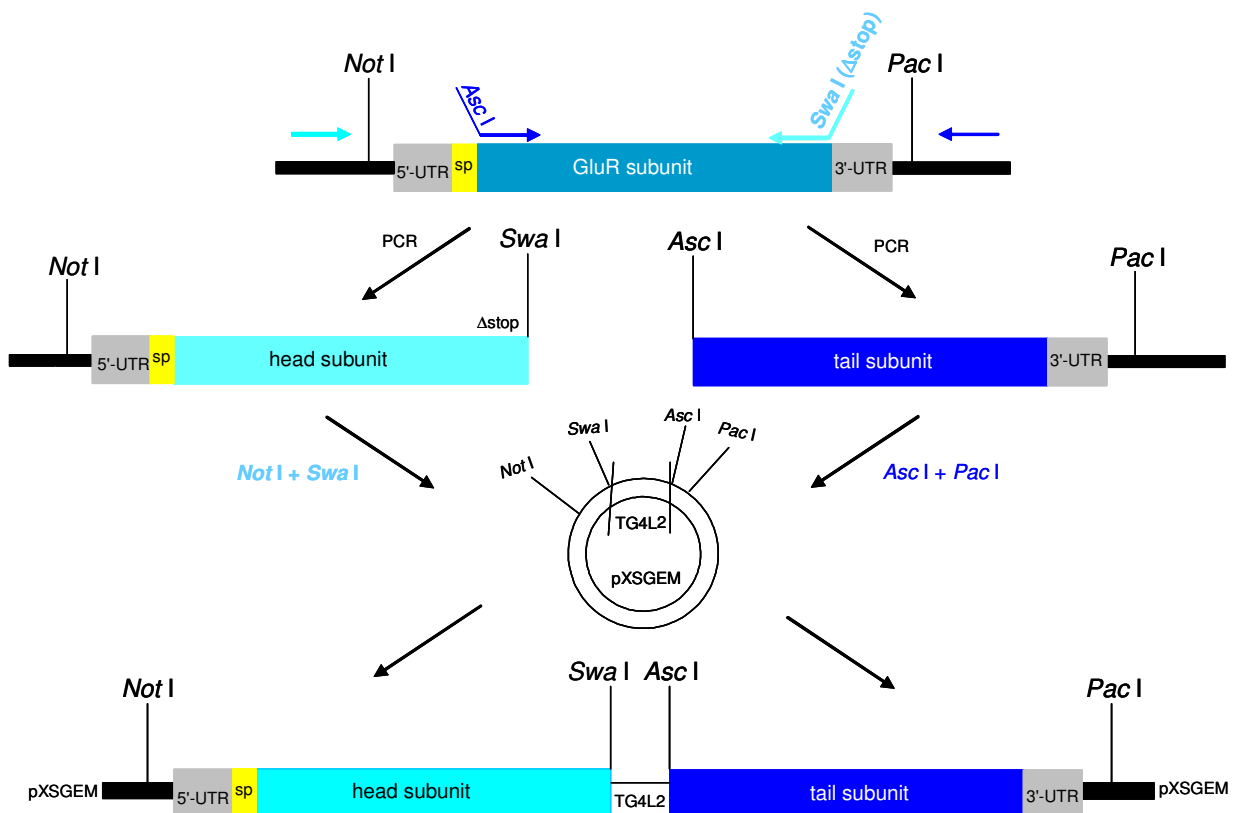


Fig. 9 : Cloning strategy applicable to generate dimers of all 18 mammalian GluR subunits; UTR: untranslated region; sp: signal peptide.

Head and tail subunits are amplified by PCR and appropriate restriction sites are introduced. For a head subunit the stop codon is omitted in the primer. The tail subunit lacks its signal peptide.

The fragments are then ligated in the vector pXSGEM in which the linker TG4L2 was cloned before. TG4L2 is flanked by the restriction sites used for cloning.

pXSGEM is a derivative of pGEM-HE which allows efficient expression in *Xenopus* oocytes due to the presence of the 5'- and 3'-UTRs of a *Xenopus* β-globin gene. The restriction enzymes used are *Not*I, *Swa*I, *Asc*I and *Pac*I.

Using this cloning strategy, five monomeric precursor constructs and the heterodimer GluR1(Q)flop(L479F)-TG4L2-GluR2(R)flop-pXSGEM had been constructed (Diplomarbeit by D. Schmaltz; cf. 2.4). The head subunit was tagged with a desensitisation-inhibiting mutation (L479F<sup>7</sup>). The tail part of the dimer was marked with an "R" at the editing site that conveys Ca<sup>2+</sup> impermeability to the subunit and the channel in a dominant manner and leads to a linear current-voltage relation (I/V). A "Q" at the editing site would lead to an inwardly rectifying I/V (see 1.2.3). Both mutations were chosen to electrophysiologically prove the integration of both head and tail subunits in the resulting channel.

The concatemer was functional but did not generate a current large enough to record a reliable I/V. To increase the amplitude, the dimer was co-expressed with the protein stargazin which is known to be involved in targeting AMPA receptor subunits to (and in) the plasma membrane via its PDZ binding domain (Chen et al., 2000). This led to a larger current but, unexpectedly and inexplicably, to a change of the I/V curve from linear to rectifying two days after RNA injection. These alterations of I/Vs were not observed for wild type AMPA receptors in combination with stargazin. Thus, heterodimeric AMPAR concatemers make further investigation necessary in the future.

---

<sup>7</sup> This was supposed to be L479Y; the wrong amino acid exchange was due to a false primer.

## 1.5 Aims of the present study

The concatemer approach, i.e. the covalent linkage of two or more subunits of a glutamate receptor, allows to constrain a defined ratio and order of subunits in the receptor complex. Thus, a contamination with monomers and resulting heterogenous population of receptors can be avoided which necessarily occurs when - as is usually done - independent single subunits are co-expressed in heterologous cell systems. Unlike in these common approaches, the properties of the obtained homogenous receptor populations can thus be analysed electrophysiologically in the light of a known subunit composition and arrangement within the concatemer. The challenge of the concatemer strategy lies in the introduction of an additional transmembrane domain between two receptor subunits which allows to preserve integrity and functionality of the concatemer.

The specific objectives of this thesis were to :

- 1) continue previous work in the lab based on the construction and analysis of GluR1 homomers. The next step was to construct and functionally test GluR1-GluR2 dimers for a "proof of principle", i.e. to prove that functional concatemers in the AMPAR subfamily could be obtained also for AMPAR heterodimers.
- 2) To detect weak and still unknown interactions between subunits belonging to different GluR subfamilies (e.g. between GluR1-NR1, GluR1-GluR6 and GluR6-NR1) by studying the corresponding "hybrid" dimers.  
Potentially occurring weak interactions between different subunits will normally be undetectable in a heterogenous receptor population dominated by strongly interacting identical subunits when performing biochemical assays or functional (e.g. electrophysiological) tests. The concatemer approach that covalently links two or more GluR subunits to each other offers the opportunity to avoid the problem of homomeric contamination and possibly the proof of low-affinity "promiscuous" interactions.
- 3) To find a transmembrane domain suitable to construct NR1 + NR2 dimers functional in *Xenopus laevis* oocytes. First, the transmembrane linker TG4L2 (consisting of the 4<sup>th</sup> TMD of the  $\alpha_1$ -subunit of the bovine GABA<sub>A</sub> receptor flanked by hydrophilic

amino acids) already available in the lab was to be tested in this regard. The utility of TG4L2 in the NMDAR subfamily was in doubt since another lab had reported breakdown of their dimers in HEK cells using the same core linker and therefore given up the project (Prybylowski et al., Soc. Neurosci. Abstr., 1999). The NMDAR subunits NR1-1a and NR2A were chosen to allow comparison to a previously published study (Schorge and Colquhoun, 2003).

- 4) After the identification of an appropriate linker the integrity of the dimers was to be proven electrophysiologically to verify that both head and in particular tail subunits of the dimers are integrated in the receptor channel. The electrophysiological experiments were envisioned to be complemented by protein biochemistry and confocal microscopy.
- 5) To analyse the electrophysiological and pharmacological properties of functional dimeric NMDAR concatemers and to compare these to co-expressed monomeric wild type NR1-1a and NR2A subunits. In particular, effects of the linkage of the two subunits on dimer function were to be studied. This was to be done qualitatively and quantitatively.
- 6) Data obtained from all four NR1-1a + NR2A dimers would allow to find out whether a distinct subunit arrangement is required within the dimer to convey functionality to the entire tetrameric NMDAR complex. This is a recent matter of debate (Schorge and Colquhoun, 2003; Furukawa et al., 2005). It must here be emphasised that - using the approach presented in the current study - two complete wild type GluR subunits are covalently connected to each other.
- 7) To determine the stoichiometry of the NR3 subunit in the NMDAR complex, i.e. whether the NR3 subunit interacts with one or more NR1 and / or NR2 subunits to form a tetrameric complex, or whether the pre-formed tetrameric channel complex is actually enlarged by an additional NR3 subunit to become a pentamer.

## 2 Materials and Methods

### 2.1 Bacterial growth

For the growth of *Escherichia coli* (*E. coli*) cells, 2.5 - 10 mL (for a "mini" culture) or 100 mL (for a "midi" culture) of LB (Luria-Bertani) broth supplemented with 200 µg/mL ampicillin were inoculated with a single colony of transformed bacteria toothpicked from a fresh selective LB agar plate, with bacterial cells picked from a selective "replica plate" or by using 10 - 1000 µL of a liquid overnight culture. The bacteria were grown at 37 °C for (at least) 12 - 18 hrs ("over night") with vigorous shaking ( $\approx$  200 - 300 rpm) until late logarithmic phase or until the cell density of the culture seemed to be high enough.

It became apparent that several constructs grew very poorly (sometimes an incubation time of up to 48 hrs was necessary) and were replicated very slowly in the bacterial cells (probably due to the size of the constructs), making it difficult to achieve a sufficient number of recombinant transformants during the first cloning attempt.

Alternatively, to achieve a higher cell density, the richer growth medium 2 x YT (2 x yeast extract + tryptone) was used and the incubation time reduced to (at least) 8 hrs (but occasionally up to 36 hrs).

### 2.2 Medium scale ("midi") preparation of plasmid DNA ( $\leq$ 100 µg plasmid DNA)

This was done using the JETSTAR Plasmid Purification Kit (Genomed) according to the manufacturer's manual. Plasmid DNA is extracted from the bacterial cells using the alkaline lysis method (Birnboim and Doly, 1979). The centrifugation step applied to clear the lysate was replaced by a shorter filtration step.

Contrary to the "mini" plasmid DNA extraction kit using a silica matrix (Vogelstein and Gillespie 1979; Birnboim and Doly, 1979), the "midi" kit involves anion-exchange chromatography to purify the bacterial DNA. Plasmid DNA is eluted in a high salt (and high pH) buffer and then concentrated and desalted by isopropanol precipitation.

Agarose gels [in 1 x TBE (Tris-Cl, boric acid, EDTA) buffer] were used to detect, quality-check and quantitate characteristic fragments of digested or amplified plasmid DNA. They also served to isolate plasmid DNA fragments to be used in cloning procedures. The DNA fragment was excised from the gel and purified.

### 2.3 Amplification of DNA using the polymerase chain reaction (PCR)

The constructs GluR2(R)flop / pSGEM and NR2A repaired / pSGEM (for explanations see 3.1.2) served as templates to amplify PCR products for head and tail subunits of GluR dimers.

The following oligonucleotides were used for the PCRs (sequences 5' => 3'; expected fragment sizes in parentheses) :

GluR2(R)flop head subunit (3090 bp) :

sense primer : CCCAGCTTGCTTGTTCTTT

anti-sense primer : AAGTATTT**AAA**TATTTTAACTCTCGATGCCAT

*Swa* I

NR2A head subunit :

sense primer : CCCAGCTTGCTTGTTCTTT

anti-sense primer : TCTCATTT**AAA**TACATCAGATTCGATACTAGG (4495 bp; *Not* I and *Swa* I)

anti-sense primer : GGCGCCGA**ATT**CACATCAGATTCGATAC (alternative cloning scheme) (4495 bp; *Eag* I and *EcoR* I)

NR2A tail subunit (5478 bp) :

sense primer : AAAAGGCGCGCCCGCGATCCGGCACAGAACGC

*Asc* I

anti-sense primer : GATTACGCCAAGCTATTTAGGTGACTATA

The length of the signal peptide (18 aa) determined by the sense primer corresponds to that assigned by Monyer et al. (1992).

Primers were ordered from biomers.net (Germany).

The recognition sites of restriction endonucleases are underlined. In the anti-sense primer for the GluR2(R)flop head subunit, the stop codon TAG is abolished by mutating it to TTT (Phe) (**in bold**). Similarly, in the NR2A head subunit, TAA was changed to TTT (Phe). Since repeated cloning attempts remained unsuccessful, an alternative cloning scheme had to be applied (using *Eag* I and *EcoR* I instead of *Not* I and *Swa* I) for the NR2A head subunit. In the new anti-sense primer, TAA was changed to AAT (Asn).

PCR conditions :

~ 1 fmol or 1 - 10 ng of plasmid DNA as template were used for the PCR.

The PCR was performed in a 50  $\mu$ L volume consisting of :

35.5  $\mu$ L dH<sub>2</sub>O

10  $\mu$ L of 5 x reaction (HF or GC) buffer (Finnzymes; corresponding to a final concentration of 1.5 mM MgCl<sub>2</sub> in the reaction mixture)

1  $\mu$ L of each primer sense and anti-sense (100 pmol/ $\mu$ L each)

2  $\mu$ L of deoxynucleotide mix (10 mM of each dNTP; Fermentas)

1  $\mu$ L template DNA

0.5  $\mu$ L (corresponding to 2.5 units) of Phusion Polymerase (5 u/ $\mu$ L; Finnzymes)

The MgCl<sub>2</sub> concentration was optimised by performing a series of trial PCRs at concentrations ranging from 1.5 mM to 4.5 mM (50 mM MgCl<sub>2</sub> stock; Finnzymes). The lowest MgCl<sub>2</sub> concentration possible was chosen to decrease the presence of non-specific products.

The PCR reagents were mixed on ice as mastermixes, the DNA template and the enzyme being added as the last components. Amplification was performed in a MJ Research thermocycler using the following profile :

30 s at 98 °C initial denaturation to melt template DNA sufficiently,

30 s at the same hybridisation temperature as below,

X mins at 72 °C for extension (15 - 45 s per kbp) **for 1 cycle**,

followed by

10 s at 98 °C to melt template,

30 s at a distinct hybridisation temperature to anneal the primers to the template  
(50 - 64 °C),

X mins at 72 °C for extension (15 - 45 s per kbp) **for 29 cycles**,

terminated by

10 s at 98 °C,

30 s at the hybridisation temperature,

10 mins at 72 °C as final elongation **for 1 cycle**.

5 µL of the PCR mixes were examined by electrophoresis in agarose gels.

For each individual transcript, the choice of buffer, the extension time, the amount of polymerase and the MgCl<sub>2</sub> concentration needed to be optimised.

## 2.4 Cloning of DNA fragments into plasmid vectors

The following constructs were used as templates to clone GluR dimers :

Construct	Accession no. in GenBank (rat)	Length of ORF [bp]	Length of signal peptide [aa]	Reference / Origin of construct
GluR2(R)flop / pSGEM <sup>8</sup>	M85035	2652	21	Boulter et al., 1990
GluR2(R)flop(L483F) / pcDNA3 <sup>9</sup>	---	2652	21	T. Morth, 1999
TG4L2- GluR1(Q)flop(L479F) / pXSGEM	X17184.1	2889		M. Hollmann, 1989 and M. Hartley, 1998 (GluR1(Q)flop); D. Schmaltz, 2002
GluR1(Q)flop(L479F)- TG4L2-GluR2(R)flop / pXSGEM	---	5541	18	D. Schmaltz, 2002
NR1-1a-TG4L2 / pXSGEM	U08261	2982	18	J. Boulter, 1994; D. Schmaltz, 2002
TG4L2-NR1-1a / pXSGEM	U08261	2982	---	J. Boulter, 1994; D. Schmaltz, 2002

<sup>8</sup> AMPA receptors were not analysed in the present study (cf. 3.1).

<sup>9</sup> This was thought to be L483Y; the wrong amino acid exchange was introduced by a wrong primer.

NR2A mutated / pSGEM	AF001423 (later repaired with D13211 cassette; see 3.1.2)	4394	19	J. Boulter, 1997; I. Paarmann, 1996
NR2A / pBluescript-SK-	D13211	4395	22	Ishii et al., 1993
s(hort)NR1-1a(N598R) / pGEM-HE	---	2817	18	S. Traynelis (5'-UTR shortened compared to NR1-1a)

The vector used for the expression of GluR subunits in *Xenopus laevis* oocytes was the plasmid pXSGEM (by D. Schmaltz), a derivative of pSGEM, that contains additional 8-cutter restriction sites in the polylinker (Fig. 10).

pSGEM itself was made from the vector pGEM-HE but contains the multiple cloning site of pBluescript-SK (M. Hollmann, personal communication).

### The transcription vector pXSGEM

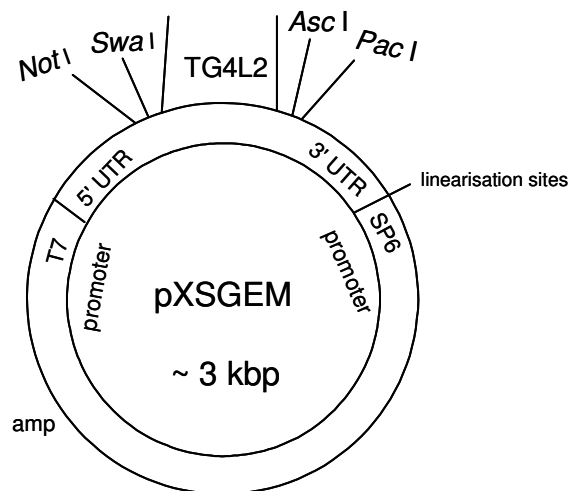


Fig. 10 : Schematic map of the vector pXSGEM intended for the *in vitro* synthesis of RNA and the efficient translation of transcripts in *Xenopus laevis* oocytes. Amp: gene encoding  $\beta$ -lactamase (conveying resistance to ampicillin); 5'-UTR: 5'-UTR of a *Xenopus*  $\beta$ -globin gene; 3'-UTR: 3'-UTR of a *Xenopus*  $\beta$ -globin gene; T7 and SP6: RNA polymerase promoters; TG4L2: linker introduced between two full-length subunits of the concatemer (cf. Fig. 7); the linearisation sites downstream of the 3'-UTR of the *Xenopus*  $\beta$ -globin gene served to obtain a higher transcript yield by forcing run-off transcripts.

pGEM-HE was developed by Liman et al. (1992) who inserted the 5'- and 3'-UTRs (untranslated regions) of a *Xenopus*  $\beta$ -globin gene up- and downstream of the respective cDNA insert. These 5'- and 3'-UTRs (the latter one in particular) had been shown to increase the translation efficiency of transcripts in *Xenopus* oocytes (Krieg and Melton, 1984). The pGEM-HE construct is derived from the pGEM-3Z vector (Promega) which contains T7 and SP6 RNA polymerase promoter regions and is therefore usable for the synthesis of RNA *in vitro*.

The vector usable for the expression of GluR subunits in mammalian cell lines (e.g. HEK cells) was the plasmid pcDNA3.1(+), equipped with the cytomegalovirus (CMV) promoter 5' of the multiple cloning site (gift from Dr. A. Jeromin).

pBS-KS+ was provided by Dr. R. Trippe.

The cloning of DNA fragments into plasmid vectors can be divided into 4 stages : isolation of the properly restricted DNA fragments, ligation of fragment to vector, transformation of host *E. coli*, and selection of transformants.

The isolation of DNA involves the restriction digestion of both vector and insert (either a purified PCR fragment or an insert cloned into another vector) with the appropriate restriction enzyme(s) and then the purification of these from the enzymes and other impurities (a digested PCR product, however, was also directly used in the subsequent ligation).

At the beginning of this work, a PCR product was subcloned into pBS-KS+ before cloning into the target plasmid. This was the case for the GluR2 and NR2A head subunits. Since the oligonucleotides used were not phosphorylated at their 5' ends, the PCR product had to be phosphorylated prior to ligation into the blunt end (*EcoR* V) site of pBS-KS+.

Later, we found out that a PCR product (although large in size) could be successfully digested and the resulting fragment directly ligated into the target construct. The time-consuming subcloning step could therefore be overcome. This was the case for the NR2A tail subunit and the NR2A head subunit carrying *Eag* I and *EcoR* I restriction sites (alternative cloning scheme; cf. 2.3).

#### **2.4.1 Phosphorylation of PCR products**

To increase phosphorylation efficiency, approximately 1  $\mu$ g of a gel purified PCR product was heated to 70 °C for 5 mins and chilled on ice. The following components were then

added to start the kinase reaction : 2  $\mu\text{L}$  10 x ligase buffer (NE Biolabs; this is compatible with the kinase buffer), 1 - 1.5  $\mu\text{L}$  T4 polynucleotide kinase (NE Biolabs; 10 u /  $\mu\text{L}$ ) and 2  $\mu\text{L}$  5 % PEG (polyethylene glycol) 8000. Phosphorylation was carried out in a 20  $\mu\text{L}$  volume for 1 hr at 37 °C. Subsequently, T4 polynucleotide kinase was heat-inactivated (otherwise it would phosphorylate the probably dephosphorylated vector in the subsequent ligation) at 65 °C for 20 mins.

The phosphorylated PCR product was now ready for ligation into the *EcoR* V site of pBS-KS+ according to 2.4.4.

#### **2.4.2 Restriction digest of DNA**

This was done using buffers supplied by the manufacturer (various companies such as NE Biolabs, Fermentas, Roche, Boehringer Mannheim). The total reaction volume was 20 - 50  $\mu\text{L}$ , with the enzyme(s) maximally at 1/10 of the total volume since a glycerol concentration above 5 % (originating from the enzyme's storage buffer) was likely to either inhibit the restriction endonuclease's activity or promote star activity.

From 100 ng to 1  $\mu\text{g}$  of the desired end product were used in each reaction and incubated with 5 - 20 units of restriction enzyme for 2 ½ hours up to over night.

The digests were run in 0.8 - 2.0 % agarose gels. Fragments of the expected size separated by gel electrophoresis were cut from the gel and purified.

#### **2.4.3 Purification of DNA from salts, impurities and agarose**

This was done by agarose gel electrophoresis followed by purification of the desired DNA fragment using the QIAquick or Jetquick Gel Extraction Kits (Qiagen or Genomed, respectively) according to the supplier's recommendations. This typically produced a recovery of 30 - 50 %.

The DNA concentration of the eluate was estimated by running 5  $\mu\text{L}$  of extracted DNA in a 0.8 - 2.0 % agarose gel next to a DNA ladder (with bands of known concentration).

#### **2.4.4 Ligation of DNA fragments to plasmid vectors**

In the standard reaction 30 - 100 ng of vector were used which had been digested with the appropriate restriction endonuclease(s) and gel purified. In some cases, the DNA was also treated with calf intestinal alkaline phosphatase (CIAP) following the digest and preceding the gel purification to prevent religation of the vector. Typically, 1  $\mu\text{L}$  of CIAP (10 u /  $\mu\text{L}$ ; Fermentas) was added to the restriction digest and incubated for 30 - 45 mins.

Purified vector fragment was then combined with insert DNA (also gel purified; a phosphorylated or digested PCR product, however, was directly used in the ligation, cf. 2.4) at varying molar ratios and the volume made up to 17  $\mu\text{L}$  with  $\text{dH}_2\text{O}$ . To this 2  $\mu\text{L}$  of 10 x ligase buffer was added along with 1  $\mu\text{L}$  of T4 DNA ligase (1000 Weiss units /  $\mu\text{L}$ ; Fermentas). The reaction was incubated at 14 - 16  $^\circ\text{C}$  over night (12 - 18 hrs) and subsequently chilled at 4  $^\circ\text{C}$  or frozen at - 20  $^\circ\text{C}$ .

#### **2.4.5 Transformation of heat-shock competent *Escherichia coli***

DNA transformations were made into heat-shock competent *E. coli* XL1 Blue MRF' (lab stock) and XL10 Gold cells (gift from A. Koop). Both strains were chosen for their recombinase deficiency [genotype information available from Stratagene (<http://www.stratagene.com>)].

Heat-shock competent bacteria were prepared according to a  $\text{CaCl}_2$ -based lab protocol.

The ligated DNA (8 - 20  $\mu\text{L}$  of the total reaction volume) was added to a 50 - 200  $\mu\text{L}$  - aliquot of heat-shock competent cells thawed on ice. The suspension was mixed by gently tapping the reaction tube and left on ice for a further 30 minutes. The remaining ligation reaction was chilled at 4  $^\circ\text{C}$  or frozen at - 20  $^\circ\text{C}$ .

The bacteria were then heat-shocked in a water bath for about 45 seconds and then placed on ice for a further 2 minutes. Following this, 950 - 800  $\mu\text{L}$  of pre (to 42  $^\circ\text{C}$ ) -warmed non-selective nutrient medium (e.g. SOB, 2 x YT) was added to the reaction and the bacterial cells incubated in a shaking incubator for 1 hr at 37  $^\circ\text{C}$  to allow antibiotic resistance to be conferred to the bacteria by the plasmid which can then be used as a selectable marker for plasmid-containing cells. The bacteria were concentrated by centrifugation (5 mins at 6,000 rpm) in a table-top centrifuge and resuspended in approximately 200  $\mu\text{L}$  of the supernatant. This was plated onto an antibiotic-containing LB agar plate and incubated at least over night at 37  $^\circ\text{C}$  (or later at room temperature) in an inverted position.

#### **2.4.6 Selection of recombinant transformants**

To distinguish bacteria transformed by recombinant plasmids from those carrying empty "wild type" plasmids (i.e. empty vectors) the following strategy was pursued :

Single colonies were toothpicked from the selective agar plate and grown in an appropriate growth medium for an appropriate time (2.1). The plasmid DNA was then harvested using an alkaline lysis protocol (Sambrook and Russell, 2001; Birnboim and Doly, 1979).

Recombinant plasmids were identified by restriction analysis and further processed according to 2.2 and 2.4.7.

#### **2.4.7 Automated sequencing**

Lab clones, inserts generated by PCR and exchanged cloning cassettes were confirmed by sequencing (single strand) (see also 3.1.1).

Typically 1 - 7.5 µg (depending on the construct size and the sequencing facility) of template for plasmid DNA were used.

For each reaction, 100 pmol primer in 10 µL dH<sub>2</sub>O (i.e. 10 pmol / µL) were prepared. Standard sequencing primers were provided by the sequencing facility.

Automated sequencing was carried out by MWG Biotech according to the companies' guidelines or by the sequencing facility of the Lehrstuhl für Molekulare Neurobiochemie, Ruhr-University Bochum.

Restriction maps were generated using the programme SeqBuilder, version 6.1.3 (DNASTAR). Alignments to interpret sequencing data were performed using the programme ClustalW (available online at <http://www.ebi.ac.uk/clustalw/>).

### **2.5 *In vitro*-synthesis of cRNA**

#### **2.5.1 Linearisation of the DNA template**

To achieve a higher yield of the desired transcript, template DNA was prepared from circular plasmid cDNA by linearising each clone over night with a suitable restriction enzyme [either *Nhe* I (Fermentas) or *Pac* I (NE Biolabs) were used]. If the starting DNA is incompletely linearised, the yield of desired transcript decreases due to lack of a termination signal and, consequently, accumulation of longer transcripts of variable length. 10 µg of DNA were linearised with 50 units of restriction enzyme in a 50 µL volume. The enzyme was removed by phenol / chloroform extraction, the DNA ethanol-precipitated and dissolved in DEPC (diethylpyrocarbonate)-treated water : For this, 350 µL TE buffer (10 mM Tris·Cl with 1 mM EDTA, pH 7.9) were added to the digest. The DNA was extracted by adding 200 µL phenol (suitable for DNA extraction, i.e. equilibrated with TE buffer to a pH of 7.5 - 8.0<sup>10</sup>) and 200 µL chloroform, followed by vortexing and centrifugation for 5

---

<sup>10</sup> Phenol with a pH > 7 had to be used because DNA undergoes hydrolysis under acidic conditions.

mins at maximum speed and room temperature in a bench-top centrifuge. Residual phenol was extracted by adding 400  $\mu\text{L}$  chloroform to the aqueous phase, followed by mixing and spinning for 2 mins under the same conditions as before. The purified DNA was precipitated with 100  $\mu\text{L}$  10 M ammonium acetate ( $\frac{1}{3}$  to  $\frac{1}{4}$  of the starting volume) and 100 % ethanol (2.5 times of the starting volume). The solution was stored at - 80 °C for 1 - 2 hrs or at - 20 °C over night and centrifuged for 30 mins (as above but at 4 °C). After washing with 75 % ethanol, the vacuum-dried pellet was resuspended in 20  $\mu\text{L}$  DEPC-treated  $\text{dH}_2\text{O}$ .

The digest quality was checked in an agarose gel.

### 2.5.2 Transcription reaction

The transcription reaction was performed under conditions that minimise contamination with RNases. All solutions were prepared in DEPC-treated  $\text{dH}_2\text{O}$ .

Capped cRNA was synthesised from 1  $\mu\text{g}$  of linearised template using an *in vitro* transcription kit (reagents from different suppliers such as Fermentas, Stratagene, Amersham) with a modified standard protocol that employs each of the nucleotides at 800  $\mu\text{M}$  (except for GTP, 200  $\mu\text{M}$ ), 400  $\mu\text{M}$  cap analogue [ $\text{m}^7\text{G}(5')\text{ppp}(5')\text{G}$ ] for capping, and an extended reaction time of 2  $\frac{1}{2}$  hrs with T7 RNA polymerase (Fermentas; 20 u /  $\mu\text{L}$ ). The transcription reaction was followed by removal of template by treatment with RNase free DNase I (Fermentas; 1 u /  $\mu\text{L}$ ). The RNA was then purified by phenol / chloroform extraction and ethanol-precipitated : Firstly, the transcription reaction was stopped by adding 300  $\mu\text{L}$  of a phenol / chloroform / isoamylalcohol mixture (25 : 24 : 1) (if only phenol was used, the RNA would get dissolved in the organic phase and thus get lost). This phenol was suitable for RNA extraction and saturated with water to a pH of 4.5 - 5<sup>11</sup>. This was followed by vortexing and centrifugation for 5 mins at maximum speed and 4 °C in a table-top centrifuge. The extraction step of components of the reaction was repeated once with the aqueous phase. Residual phenol was removed by adding 300  $\mu\text{L}$  of a chloroform / isoamylalcohol mixture (24 : 1) to the aqueous phase, followed by vortexing and centrifugation as described above.

---

<sup>11</sup> In this case, phenol with a pH < 7 had to be used because RNA undergoes hydrolysis under alkaline conditions due to the 2'-hydroxyl group of the ribose.

Secondly, the purified RNA was pelleted with 75  $\mu$ L 10 M ammonium acetate ( $\frac{1}{4}$  of the starting volume) and 100 % ethanol (2.5 times of the starting volume) by spinning for 40 mins (under the same conditions as above). Ammonium acetate was used instead of sodium acetate because ammonium acetate does not precipitate nucleotides or oligonucleotides ( $\leq 100$  bases) which might have remained in the reaction mixture after the phenol / chloroform extraction.

The supernatant was discarded taking care not to remove the loose RNA pellet which was then washed with 75 % ethanol (as carefully as before). Finally, the vacuum-dried pellet was resuspended in DEPC-treated dH<sub>2</sub>O to a concentration of 200 ng /  $\mu$ L.

Trace labelling of all cRNAs was performed during RNA synthesis through the addition of [ $\alpha$ -<sup>32</sup>P]-UTP, to permit calculation of yields by scintillation counting and control of transcript quality by formaldehyde-agarose gel electrophoresis.

## 2.6 Preparation of *Xenopus laevis* oocytes

*Xenopus laevis* oocytes of stages V-VI were obtained from parts of the ovaries of anaesthetised frogs [supplied in the lab as described by Stuehmer (1992)]. Follicular cells were removed with collagenase (type I) in Ca<sup>2+</sup> free Barth's medium (see below) at 20°C for ca. 2 hrs with slow agitation. Then, oocytes were washed with (Ca<sup>2+</sup>-containing) Barth's medium (88 mM NaCl, 1.1 mM KCl, 2.4 mM NaHCO<sub>3</sub>, 0.3 mM Ca(NO<sub>3</sub>)<sub>2</sub>, 0.4 mM CaCl<sub>2</sub>, 0.8 mM MgSO<sub>4</sub>, 15 mM HEPES, pH 7.6 with NaOH; supplemented with 40  $\mu$ g/mL gentamycin, 40  $\mu$ g/mL streptomycin and 63  $\mu$ g/mL penicillin). After selection, oocytes were maintained in Barth's medium at 17 °C.

## 2.7 cRNA injection in oocytes

Prior to injection, RNA preparations were centrifuged for ca. 20 mins at 13,000 rpm and 4 °C. Centrifugation served to precipitate particles suspended in solution which could clog the injection capillaries.

Injection capillaries (World Precision Instruments, WPI) had a diameter of 10 - 15  $\mu$ m. cRNA was injected with a total amount of 20 ng 4 to 24 h after collagenase treatment using an electrical nL-injector (WPI). For co-injections, approximate molar ratios for the injected cRNAs were calculated beforehand. In these cases, the two RNAs were mixed thoroughly prior to loading into the capillary.

The cRNA-injected oocytes were incubated in Barth's medium at 17 °C for 5 - 12  $\frac{1}{2}$  days.

## 2.8 Electrophysiological recordings using two-electrode voltage clamping

All chemicals and reagents used were standard lab material of the highest purity grade available and are not specifically acknowledged in this thesis.

Since the absolute current response depends on the batch of oocytes (i.e. the individual frog), all electrophysiological experiments were carried out by comparing concatemer-expressing oocytes to oocytes from the same batch injected at the same time with control wild type (NR1-1a + NR2A) cRNA : Steady-state current amplitudes were normalised to the response of wild type (% NR1-1a + NR2A current).

Also, to avoid variability between transcriptions, cRNA preparations to be used in comparative recordings were made in the same batch.

Oocytes typically had a resting potential in the range of - 10 to - 50 mV. For reliable estimation of current amplitudes, holding currents needed to maintain a potential of - 70 mV. The "leakage currents" were supposed to be not larger than - 1  $\mu$ A. Larger leakage currents were specifically acknowledged.

Steady-state currents after application of 100  $\mu$ M L-glutamate plus 10  $\mu$ M glycine were recorded in normal frog Ringer (NFR; in mM, 115 NaCl, **1.8** CaCl<sub>2</sub>, 2.5 KCl, and 10 HEPES, pH 7.2<sup>12</sup> with NaOH) by clamping the voltage at - 70 mV. Voltage electrodes had resistances of approximately 0.2 to 5 M $\Omega$ , and current electrodes of 0.1 to 1.5 M $\Omega$ . Electrodes were filled with 3 M KCl.

Recordings lasted 1 - 2 mins with 20 s agonist applications.

Electrophysiological recordings were performed with a Turbo Tec-10CD/CX amplifier (npi electronic) in voltage clamp mode. The optical and mechanical components of the electrophysiological setup were mounted to a vibration-isolation table (Technical Manufacturing Corporation, TMC) and surrounded by a Faraday cage.

Leakage current in the absence of agonists was subtracted from the agonist-induced current with the programme Pulse, versions 8.53-8.61 (HEKA electronics). In general, data were acquired and analysed using this software and the programmes Excel (Microsoft) and GraphPad Prism, version 4.03 (GraphPad Software).

Agonists were dissolved as follows : L-glutamate was prepared as 100 mM aliquots in dH<sub>2</sub>O and pHed to 8.1<sup>13</sup> with NMDG (*N*-methyl-D-gluconate). Glutamate, and not NMDA,

---

<sup>12</sup> The pH of the Ringer solutions is in the range of the cytosolic pH of the oocyte (~ 7.2 - 7.4) (Stocker et al., 1999).

<sup>13</sup> The buffer capacity of the Ringer solution (pH 7.2) should be high enough to maintain an overall pH of 7.2.

was chosen as the agonist throughout the present study because it is the endogenous agonist at NMDA receptors.

Glycine was prepared as 100 mM aliquots in 10 mM HEPES, and the pH was adjusted to 7.2 with NMDG.

The antagonists D-APV (applied at 100  $\mu$ M), (+)MK-801 (applied at 1  $\mu$ M) and ifenprodil (applied at 3  $\mu$ M) were prepared in dH<sub>2</sub>O at 10 mM.

All agonist and antagonist aliquots were stored at - 20 °C.

Current-voltage relationships (*I/V*s) were recorded in Mg<sup>2+</sup>-Ringer (MgR; in mM, 115 NaCl, 1.8 MgCl<sub>2</sub>, 2.5 KCl, and 10 HEPES, pH 7.2 with NaOH) by ramping voltage slowly (100 mV/s) with 2 s ramps from - 150 mV to + 50 mV. The initial, fast peak current representing Ca<sup>2+</sup>-activated Cl<sup>-</sup> channels endogenous to *Xenopus* oocytes was disregarded. Leakage currents were recorded before and after agonist application, averaged and subtracted from the agonist-induced steady-state current traces with the programme Pulse (see above).

Calcium permeability was analysed in Ca<sup>2+</sup>-Ringer (CaR; in mM, 80 CaCl<sub>2</sub>, and 10 HEPES, pH 7.2 with NMDG).

All experiments were performed at room temperature.

All pooled data were expressed as mean  $\pm$  SEM (standard error of the mean). The number *n* of oocytes recorded for each clone is shown in each table in the results section (3).

To suppress endogenous Cl<sup>-</sup> channels in the oocyte which are activated by an intracellular rise in Ca<sup>2+</sup> entering through NMDA receptors, 50 nL of 200 mM EGTA, pH 8.0 (with NaOH), were pre-injected 30 mins prior to recording in some experiments.

## 3 Results

### 3.1 Construction of NMDA receptor concatemers

Originally, it had been planned to analyse GluR1-GluR2 dimers and "hybrid" dimers (containing two GluR subunits belonging to different subfamilies), as well as NMDAR dimers (cf. 1.5). Later on, the concatemer project was divided into two parts (AMPA and hybrid dimers on one side, and NMDAR dimers on the other side). AMPAR concatemers elicit only small responses in oocytes (10 - 20 nA) and require the co-expression of the protein stargazin to generate currents that are large enough to record a distinct current amplitude and current-voltage relation. Probably related to the stargazin co-expression, the AMPAR heterodimer GluR1(Q)flop(L479F)-TG4L2-GluR2(R)flop-pXSGEM (1.4.2.2.2) showed experimental problems due to an inexplicable alteration of the current-voltage relation a few days after oocyte injection.

NMDA receptors and their concatemers, by contrast, generate much larger currents than AMPA receptors and AMPAR concatemers. Consequently, NMDA receptors offer the advantage of a "stable" I/V curve. Therefore, it was decided to concentrate on NMDAR dimers in this thesis. The AMPAR and intersubfamily dimers constructed at the beginning of the present study were not analysed and are not functionally described in this thesis.

#### 3.1.1 Overview of all newly generated constructs

All constructs were generated based on the cloning strategy outlined in Fig. 9. In summary, head and tail subunits of a dimer were amplified from full-length lab clones by PCR. Primers were designed such that appropriate restriction sites were introduced (s. below) and changes to the full-length cDNAs were made : A head subunit lacks the 5'-UTR of the full-length cDNA and its stop codon. In a tail subunit, the signal peptide and the 3'-UTR of the cDNA are missing.

To allow cloning in pXSGEM-derived constructs, *Not* I and *Swa* I were introduced in a head subunit. As cloning attempts with these enzymes failed for the NR2A head subunit, *Eag* I and *EcoR* I were used instead of *Not* I and *Swa* I in this case. In a tail subunit, *Asc* I and *Pac* I were introduced (cf. 2.3).

An overview of all lab clones and precursor constructs used as parent clones is shown in 2.4.

At the beginning, PCR products were gel extracted, phosphorylated and subcloned into a blunt end site (here *EcoR* V) of pBS-KS+ (done for GluR2(R)flop-head / pBS-KS+ and NR2A-head-mutated / pBS-KS+). Next, the insert was cut out off the subclone using *Not* I and *Swa* I and ligated into the target construct.

Later in the present study, it became evident that it was also possible to directly digest and ligate the purified PCR product (despite its length of several kbp) in the target construct without a time-consuming subcloning step. This was done for NR1-1a(N598R)-TG4L2-NR2A / pXSGEM (introducing the NR2A tail subunit with *Asc* I and *Pac* I) and NR2A-TG4L2-GluR1(Q)flop(L479F) / pXSGEM (introducing the repaired NR2A head subunit with *Eag* I and *EcoR* I).

Important information about each dimer and the cloning procedure can be gathered from the following tables.

**AMPA dimers and intersubfamily dimers for expression in *Xenopus laevis* oocytes :**

Construct	Size in bp	No. of cloning attempts (several $\leq 5$ ; multiple $\leq 10$ )	Parent clones [digested with]	Cloning procedure	linearised with
1) GluR2(R)flop-head / pBS-KS+ (subclone)	6051	several	GluR2(R)flop / pSGEM and pBS-KS (+) [ <i>EcoR</i> V]	GluR2(R)flop-head was amplified by PCR, phosphorylated and ligated into pBS-KS+	---
2) GluR2(R)flop-TG4L2-GluR1(Q)flop (L479F) / pXSGEM	8995	multiple	GluR2(R)flop-head / pBS-KS+ [ <i>Not</i> I + <i>Swa</i> I] and TG4L2-GluR1(Q)flop(L479F) / pXSGEM [ <i>Not</i> I + <i>Swa</i> I]	GluR2(R)flop-head was ligated into TG4L2-GluR1(Q)flop(L479F) / pXSGEM	<i>Nhe</i> I

Construct	Size in bp	No. of cloning attempts	Parent clones [digested with]	Cloning procedure	linearised with
3) GluR2(R)flop (L483F)-TG4L2-GluR1(Q)flop (L479F) / pXSGEM	8995	1	GluR2(R)flop(L483F) / pcDNA3 [ <i>Mfe</i> I + <i>Hpa</i> I] and GluR2(R)flop-TG4L2-GluR1(Q)flop(L479F) / pXSGEM [ <i>Mfe</i> I + <i>Hpa</i> I]	the "L483F"-cassette of GluR2(R)flop(L483F) / pcDNA3 was ligated into the head subunit of GluR2(R)flop-TG4L2-GluR1(Q)flop(L479F) / pXSGEM	<i>Nhe</i> I
4) GluR1(Q)flop (L479F)-TG4L2-GluR2(R)flop (L483F) / pXSGEM	9316	1	GluR2(R)flop(L483F) / pcDNA3 [ <i>Mfe</i> I + <i>Hpa</i> I] and GluR1(Q)flop(L479F)-TG4L2-GluR2(R)flop / pXSGEM [ <i>Mfe</i> I + <i>Hpa</i> I]	the "L483F"-cassette of GluR2(R)flop(L483F) / pcDNA3 was ligated into the tail subunit of GluR1(Q)flop(L479F)-TG4L2-GluR2(R)flop / pXSGEM	<i>Nhe</i> I
5) GluR1(Q)flop (L479F)-TG4L2-GluR1(Q)flop (L479F) / pXSGEM	8950	1	GluR1(Q)flop(L479F)-TG4L2-GluR2(R)flop / pXSGEM [ <i>Not</i> I + <i>Swa</i> I] and GluR2(R)flop-TG4L2-GluR1(Q)flop(L479F) / pXSGEM [ <i>Not</i> I + <i>Swa</i> I]	GluR1(Q)flopL479F was ligated into GluR2(R)flop-TG4L2-GluR1(Q)flop(L479F) / pXSGEM to replace the head subunit	<i>Nhe</i> I
6) GluR2(R)flop-TG4L2-NR1-1a / pXSGEM	10121	multiple	GluR2(R)flop-head / pBS-KS+ [ <i>Not</i> I + <i>Swa</i> I] and TG4L2-NR1-1a / pXSGEM [ <i>Not</i> I + <i>Swa</i> I]	GluR2(R)flop-head was ligated into TG4L2-NR1-1a / pXSGEM	<i>Pac</i> I
7) NR1-1a-TG4L2-GluR2(R)flop / pXSGEM	9464	1	GluR1(Q)flop(L479F)-TG4L2-GluR2(R)flop / pXSGEM [ <i>Asc</i> I + <i>Pac</i> I] and NR1-1a-TG4L2 / pXSGEM [ <i>Asc</i> I + <i>Pac</i> I]	GluR2(R)flop-tail was ligated into NR1-1a-TG4L2 / pXSGEM	<i>Nhe</i> I

Construct	Size in bp	No. of cloning attempts	Parent clones [digested with]	Cloning procedure	linearised with
8) NR2A-TG4L2-GluR1(Q)flop(L479F) / pXSGEM	10471	1	NR2A repaired / pSGEM [Eag I + EcoR I] and TG4L2-GluR1(Q)flop(L479F) / pXSGEM [Eag I + EcoR I]	NR2A-head-repaired was amplified by PCR, digested and directly ligated into TG4L2-GluR1(Q)flop(L479F) / pXSGEM	<i>Nhe</i> I

Note : The constructs 6) and 7) were cloned as examples for intersubfamily dimers because precursor constructs were already available, and not for particular functional reasons.

The construct NR2A-TG4L2-GluR1(Q)flop(L479F) / pXSGEM (8) was cloned because this subunit combination allowed to use the restriction enzymes *Eag* I and *EcoR* I to excise NR2A head subunit fragments required for the construction of certain NMDAR dimers. Prior to this, multiple attempts to clone NR2A-TG4L2-NR1-1a / pXSGEM, NR2A-TG4L2-NR1-1a(N598R) / pXSGEM and NR2A-TG4L2-NR2A / pXSGEM by combining NR2A-head-repaired / pBS-KS+ and various target constructs had failed using *Not* I and *Swa* I.

#### NMDAR dimers and controls for expression in *Xenopus laevis* oocytes :

Construct	Size in bp	No. of cloning attempts	Template clones [digested with]	Cloning procedure	linearised with
9) NR2A-head-mutated / pBS-KS+ (subclone)	7520	several	NR2A mutated / pSGEM and pBS-KS+ [ <i>EcoR</i> V]	NR2A-head-mutated was amplified by PCR, phosphorylated and ligated into pBS-KS+	---

Construct	Size in bp	No. of cloning attempts	Template clones [digested with]	Cloning procedure	linearised with
10) NR2A-head-repaired / pBS-KS+ (subclone)	7521	1	NR2A-D13211 / pBluescript-SK- [ <i>Bln</i> I + <i>Bgl</i> II] and NR2A-head-mutated / pBS-KS+ [ <i>Bln</i> I + <i>Bgl</i> II]	a non-mutated cassette of NR2A-D13211 / pBluescript-SK- was ligated into NR2A-head-mutated / pBS-KS+ to replace its mutated region	---
11) NR2A repaired / pSGEM	8343; see 3.1.2	1	NR2A-D13211 / pBluescript-SK- [ <i>Avr</i> II + <i>Eco</i> R V] and NR2A mutated / pSGEM [ <i>Avr</i> II + <i>Eco</i> R V]	a non-mutated cassette of NR2A-D13211 / pBluescript-SK- was ligated into NR2A mutated / pSGEM to replace its mutated region	<i>Nhe</i> I
12) NR1-1a-TG4L2-NR1-1a / pXSGEM	10223	several	TG4L2-NR1-1a / pXSGEM [ <i>Asc</i> I + <i>Pac</i> I] and NR1-1a-TG4L2 / pXSGEM [ <i>Asc</i> I + <i>Pac</i> I]	NR1-1a-tail was ligated into NR1-1a-TG4L2 / pXSGEM	<i>Pac</i> I
13) NR1-1a (N598R)-TG4L2 / pXSGEM	6362	1	sNR1-1a(N598R) / pGEM-HE [ <i>Eco</i> 47 III + <i>Bln</i> I] and NR1-1a-TG4L2 / pXSGEM [ <i>Eco</i> 47 III + <i>Bln</i> I]	the "N598R"-cassette of sNR1-1a(N598R) / pGEM-HE was ligated into the head subunit of NR1-1a-TG4L2 / pXSGEM	---
14) TG4L2-NR1-1a (N598R) / pXSGEM	7164	1	sNR1-1a(N598R) / pGEM-HE [ <i>Eco</i> 47 III + <i>Bln</i> I] and TG4L2-NR1-1a / pXSGEM [ <i>Eco</i> 47 III + <i>Bln</i> I]	the "N598R"-cassette of sNR1-1a(N598R) / pGEM-HE was ligated into the tail subunit of TG4L2-NR1-1a / pXSGEM	---
15) NR1-1a (N598R)-TG4L2-NR1-1a / pXSGEM	10223	several	NR1-1a-TG4L2-NR1-1a / pXSGEM [ <i>Asc</i> I + <i>Pac</i> I] and NR1-1a(N598R)-TG4L2 / pXSGEM [ <i>Asc</i> I + <i>Pac</i> I]	NR1-1a-tail was ligated into NR1-1a(N598R)-TG4L2 / pXSGEM	<i>Pac</i> I

Construct	Size in bp	No. of cloning attempts	Template clones [digested with]	Cloning procedure	linearised with
16) <u>NR1-1a-TG4L2-NR1-1a(N598R)</u> / <u>pXSGEM</u>	10223	1	NR1-1a(N598R)-TG4L2-NR1-1a(N598R) / pXSGEM [Asc I + Pac I] and NR1-1a-TG4L2-NR1-1a / pXSGEM [Asc I + Pac I]	NR1-1a(N598R)-tail was ligated into NR1-1a-TG4L2-NR1-1a / pXSGEM to replace the tail subunit	<i>Pac I</i>
17) NR1-1a(N598R)-TG4L2-NR1-1a(N598R) / pXSGEM	10223	1	TG4L2-NR1-1a(N598R) / pXSGEM [Asc I + Pac I] and NR1-1a(N598R)-TG4L2 / pXSGEM [Asc I + Pac I]	NR1-1a(N598R)-tail was ligated into NR1-1a(N598R)-TG4L2 / pXSGEM	<i>Pac I</i>
18) <u>NR1-1a(N598R)-TG4L2-NR2A</u> / <u>pXSGEM</u>	11496	multiple	NR2A-repaired-pSGEM [Asc I + Pac I] and NR1-1a(N598R)-TG4L2-NR1-1a(N598R) / pXSGEM [Asc I + Pac I]	NR2A-tail-repaired was amplified by PCR, digested and directly ligated into NR1-1a(N598R)-TG4L2-NR1-1a(N598R) / pXSGEM to replace the tail subunit	<i>Nhe I</i>
19) <u>NR1-1a-TG4L2-NR2A</u> / <u>pXSGEM</u>	11496	1	NR1-1a(N598R)-TG4L2-NR2A / pXSGEM [Asc I + Pac I] and NR1-1a-TG4L2 / pXSGEM [Asc I + Pac I]	NR2A-tail was ligated into NR1-1a-TG4L2 / pXSGEM	<i>Nhe I</i>
20) <u>NR2A-TG4L2-NR2A</u> / <u>pXSGEM</u>	12870	1	NR1-1a(N598R)-TG4L2-NR2A / pXSGEM [Asc I + Pac I] and NR2A-TG4L2-GluR1(Q)flop(L479F) / pXSGEM [Asc I + Pac I]	NR2A-tail was ligated into NR2A-TG4L2-GluR1(Q)flop(L479F) / pXSGEM to replace the tail subunit	<i>Nhe I</i>

Construct	Size in bp	No. of cloning attempts	Template clones [digested with]	Cloning procedure	linearised with
NR2A-TG4L2-NR1-1a / pXSGEM	11591	multiple	constructs containing the NR1-1a tail subunit [i.e. 12) and 15)] [ <i>Asc</i> I + <i>Pac</i> I] <u>and</u> NR2A-TG4L2-GluR1(Q)flop(L479F) / pXSGEM (8) and NR2A-TG4L2-NR2A / pXSGEM (20) [ <i>Asc</i> I + <i>Pac</i> I]	NR1-1a-tail was ligated into 8) and 20) to replace the tail subunit	construct still not available
NR2A-TG4L2-NR1-1a (N598R) / pXSGEM	11591	multiple	constructs containing the NR1-1a(N598R) tail subunit [i.e. 14) and 16)] [ <i>Asc</i> I + <i>Pac</i> I] <u>and</u> NR2A-TG4L2-GluR1(Q)flop(L479F) / pXSGEM (8) and NR2A-TG4L2-NR2A / pXSGEM (20) [ <i>Asc</i> I + <i>Pac</i> I]	NR1-1a(N598R)-tail was ligated into 8) and 20) to replace the tail subunit	construct still not available

Underlined constructs were electrophysiologically characterised in the present study.

The reasons why these constructs were made and studied can be deduced from the results section below and the discussion section (4). In general, NMDAR concatemers were constructed and studied to show first, that they were functional in *Xenopus* oocytes and second, to investigate the subunit arrangement in the receptor (cf. 1.5). This was to be done in reference to an already existing study (Schorge and Colquhoun, 2003).

During the course of the present work, a crystal structure study appeared reporting the NR1-NR2A heterodimer to be the functional unit in NMDAR tetramers (Furukawa et al., 2005). This is why the heterodimer NR1-1a-TG4L2-NR2A gained special interest and was electrophysiologically analysed (4.1.3.1). The temporal order of cloning of the constructs was sometimes arbitrary, i.e. depended on the cloning success, or depended on the electrophysiological results that lay the ground for further constructs to be made.

**NMDAR dimers and controls for expression in HEK cells :**

HEK cell expression constructs were made because it was planned to use this mammalian expression system as an alternative and as a complement for *Xenopus* oocytes. HEK cells could be used for protein biochemistry (4.2.1) and patch clamping (4.2.2).

<b>Construct</b>	<b>Size in bp</b>	<b>No. of cloning attempts</b>	<b>Template clones [digested with]</b>	<b>Cloning procedure</b>	<b>linearised with</b>
21) NR1-1a-TG4L2-NR2A / pcDNA3.1(+)	13863	1	NR1-1a-TG4L2-NR2A / pXSGEM [Not I + Sal I] and pcDNA3.1 (+) [Not I + Xho I]	NR1-1a-TG4L2-NR2A was ligated into pcDNA3.1(+)	---
22) NR1-1a (N598R)-TG4L2-NR2A / pcDNA3.1(+)	13863	1	NR1-1a(N598R)-TG4L2-NR2A / pXSGEM [Not I + Sal I] and pcDNA3.1 (+) [Not I + Xho I]	NR1-1a(N598R)-TG4L2-NR2A was ligated into pcDNA3.1(+)	---
23) NR2A / pcDNAI/Amp	10092	1	NR2A repaired / pSGEM [Eag I + Xho I] and pcDNAI/Amp [Not I + Xho I]	NR2A repaired was ligated into pcDNAI/Amp	---
24) NR1-1a / pcDNAI/Amp	8098	1	NR1-1a / pSGEM [BamH I + EcoR V] and pcDNAI/Amp [BamH I + EcoR V]	NR1-1a was ligated into pcDNAI/Amp	---
25) sNR1-1a (N598R) / pcDNAI/Amp	7768	1	sNR1-1a(N598R) / pGEM-HE [BamH I + EcoR V] and pcDNAI/Amp [BamH I + EcoR V]	sNR1-1a(N598R) was ligated into pcDNAI/Amp	---

Construct	Size in bp	No. of cloning attempts	Template clones [digested with]	Cloning procedure	linearised with
26) NR1-1a-TG4L2-NR1-1a / pcDNA3.1(+)	11673	3	NR1-1a-TG4L2-NR1-1a-pXSGEM [ <i>Bam</i> H I + <i>Eco</i> R V] and pcDNA3.1 (+) [ <i>Bam</i> H I + <i>Eco</i> R V]	NR1-1a-TG4L2-NR1-1a was ligated into pcDNA3.1(+)	---

The integrity of the entire insert sequence of the subclones, and monomeric and dimeric precursor constructs was verified by sequencing and checked for mutations occurring during the PCR amplification. The identity of dimers was confirmed by restriction analysis and (in part) by sequencing : All constructs were restriction analysed, tested for the presence and correct length of head and tail subunits and, importantly, the linker TG4L2. Whenever possible, marker mutations were checked by restriction digests. Furthermore, all constructs were sequenced at their 5' and 3' ends. Short exchanged cloning cassettes were sequenced as well.

Sequencing was carried out on a single strand and completed before starting further experiments.

The constructs NR2Amutated / pSGEM, NR1-1a(U08261) / pSGEM, sNR1-1a(N598R) / pGEM-HE and NR2B(U11419) / pSGEM were available in the lab. NR1-1a(U08261) / pSGEM, NR1-1a(U08261) / pcDNAI/Amp and NR2B(U11419) / pSGEM, however, had not been full-length sequenced.

### 3.1.2 Preparation of the NR2A subunit

#### 3.1.2.1 Identification of a frame shift mutation in the available NR2A cDNA clone

To clone the NR2A cDNA [AF001423 or pNR2A251; J. Boulter (1997); available in the lab in the vector pSGEM] as head subunit in dimer constructs, the respective fragment was amplified by PCR, the PCR product (4495 bp) phosphorylated and subcloned in the *Eco*R V site of pBluescript (pBS). As the first attempt to exchange the cassette with the template clone failed, the construct was sent for sequencing.

Surprisingly, the PCR product differed in two positions from the GenBank sequence. Moreover, there was a "g" missing about 1800 bases downstream of the 3<sup>rd</sup> TMD leading to a premature stop 22 amino acids after the deletion (Fig. 11).

### Schematic structure of the mutated NR2A cDNA AF001423

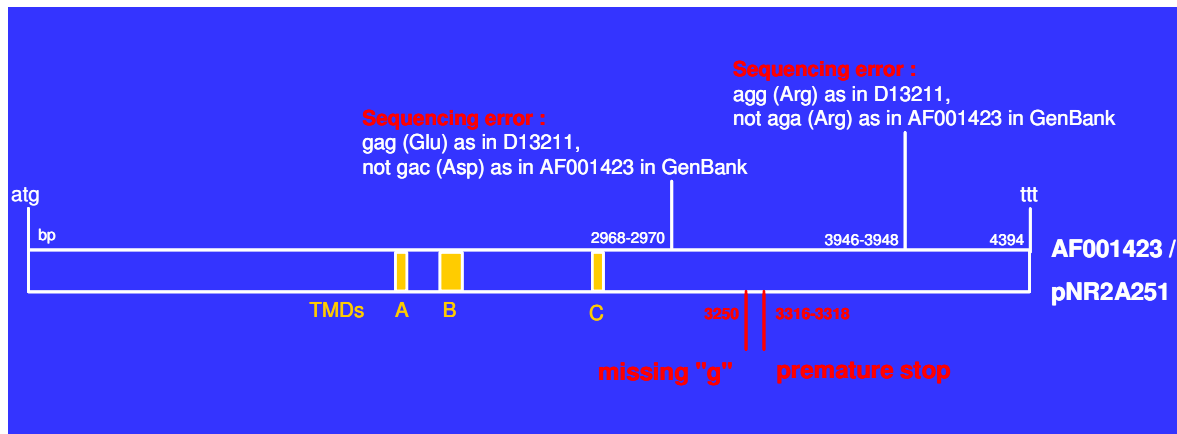


Fig. 11 : Sequencing of NR2A-head-AF001423 / pBS-KS+ showed that the cDNA differed in two positions from the GenBank entry (most probably sequencing errors). Secondly, a base was missing leading to a premature stop of translation. This mutation also occurred in the original cDNA AF001423 which therefore produces a truncated subunit.

All nucleotide positions are numbered starting from the first nucleotide of the first codon of the protein including the signal peptide.

Thus, all concatemers containing the NR2A subunit would have been truncated. Later on, it was found that the mutation was also present in the template clone used for the PCR and the original cDNA (pNR2A251 / pBS-SK-; J. Boulter, 1997).

Thus, the differences between the actual cDNA and its GenBank entry were most likely unrecognised sequencing errors submitted to GenBank.

#### 3.1.2.2 Repair of the mutated NR2A head subunit and the NR2A cDNA

To repair the NR2A head subclone and also the template construct used for the PCR, another NR2A cDNA which was available in the lab (D13211; Ishii et al., 1993) was sequenced at the site of interest and found to have no frame shift mutation. Using appropriate restriction enzymes, a cassette exchange was performed between NR2A-D13211 and both frame shifted clones. The repaired clones were confirmed by sequencing and used in all future experiments. Thus, a frame shift mutation in an essential cDNA

clone was discovered and repaired before starting further cloning attempts and electrophysiological analyses.

### 3.2 Analysis of NR1-1a + NR2A heterodimers

#### 3.2.1 NR1-1a-TG4L2-NR2A is functional when expressed alone in *Xenopus* oocytes

##### 3.2.1.1 Electrophysiological properties

The heterodimer NR1-1a-TG4L2-NR2A was *in vitro*-transcribed and the cRNA injected in oocytes. Currents were seen with 100  $\mu$ M glutamate and 10  $\mu$ M glycine in normal frog Ringer (NFR) that were distinctly larger (5 - 10 times) than the ones recorded for monomeric NR1-1a (injected as control) (Fig. 12). NR1-1a is known to give small responses to agonist in *Xenopus laevis* oocytes (Moriyoshi et al., 1991; Monyer et al., 1992; Hollmann et al., 1993; Soloviev, et al., 1996; Green et al., 2002).

These are greatly enhanced when NR1 is co-expressed with NR2 subunits (Monyer et al., 1992). Indeed, 27 oocytes injected with single NR1-1a yielded, at most, responses of 140 nA (on average between 10 - 50 nA) under voltage clamp at a holding potential of - 70 mV. For wild type NR1-1a + NR2A, the average value of the steady-state amplitude was about 6  $\mu$ A while dimer currents reached up to 2  $\mu$ A (on average, the steady-state current was about 600 nA). Consequently, the current amplitude measured for this dimer permitted to conclude that the dimer protein was synthesised full-length and remained intact in the oocyte (discussed in 4.1.1). Even larger currents were seen when monomeric NR2A was co-expressed with dimers (see 3.4.1).

Expression of NR2A alone in oocytes as control did not give rise to functional channels, in line with data reported before (Monyer et al., 1992). The very small responses observed for NR2A ( $0.1 \pm 0.3$  % of NR1-1a + NR2A current), which could also be "elicited" from uninjected oocytes ( $0.4 \pm 0.7$  %), are either artefacts or, more probably, due to the presence of yet unidentified endogenous agonist-responsive channels in the oocyte (Fig. 12). In the literature, uninjected oocytes did not give glutamate/glycine-evoked responses (e.g. Ishii et al., 1993; Monaghan and Larsen, 1997). However, it is not known what these authors considered to be a real response, and what they might have disregarded as a "flow artefact".

**NR1-1a-TG4L2-NR2A currents in normal frog Ringer**

	% NR1-1a + NR2A current (-70 mV)	SEM	n
NR1-1a + NR2A (1:1)	100	---	
NR1-1a-TG4L2-NR2A	12.1	3.7	9
NR1-1a	1.5	1.2	27
NR2A	0.1	0.3	6
uninjected oocytes	0.4	0.7	6

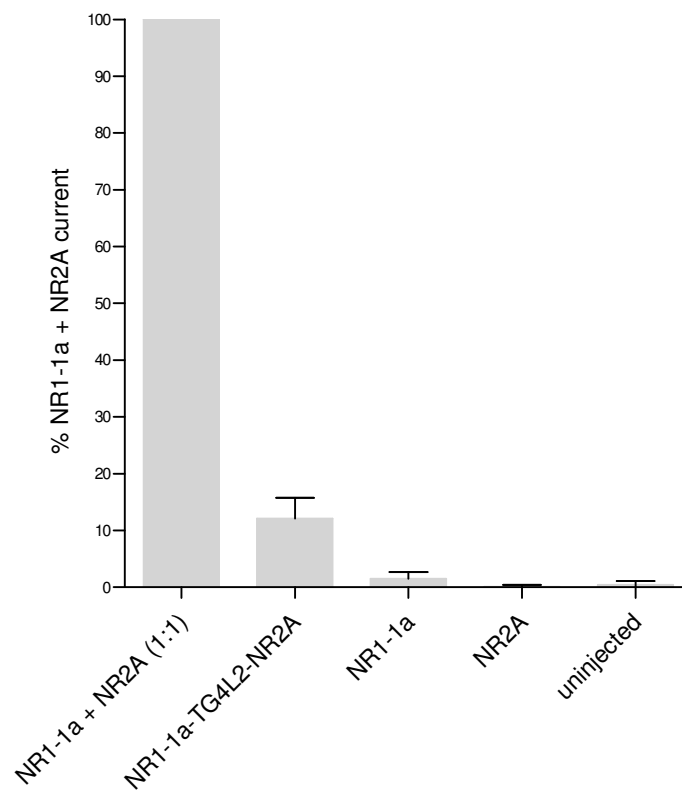


Fig. 12 : Currents were seen for NR1-1a-TG4L2-NR2A ( $n = 9$ ) when superfused with  $100 \mu\text{M}$  glutamate and  $10 \mu\text{M}$  glycine in normal frog Ringer (NFR) at a clamped voltage of  $-70 \text{ mV}$ . These were clearly larger (on average  $600 \text{ nA}$ ) than the NR1-1a control ( $n = 27$ ; on average  $10\text{-}50 \text{ nA}$ ), however, distinctly smaller than wild type NR1-1a + NR2A (11 independent measurements; on average  $6 \mu\text{A}$ ). Error bars indicate the standard error of the mean (SEM).

These experiments gave the first hint that tetrameric complexes assembled from NR1-1a-TG4L2-NR2A obviously contained not only the 1<sup>st</sup> but also the 2<sup>nd</sup> subunit of the dimer.

On the other hand, the currents elicited from the dimer were substantially smaller (70-95 % smaller) than those from monomeric wild type NR1-1a + NR2A co-injections. The drastic decrease in current amplitude compared to wild type is likely due to the covalent linkage of the two subunits by an additional transmembrane domain. A summary of the observations leading to this assumption is given further below (3.5).

To verify that the currents evoked indeed originated from an NMDAR-type channel, the following control experiments were carried out :

#### **3.2.1.1.1 Pre-injection of EGTA**

Currents for NR1-1a-TG4L2-NR2A as well as wild type NR1-1a + NR2A were very often preceded by a fast inward current spike (Figs. 13, 14). This spike most probably came from  $\text{Ca}^{2+}$ -activated  $\text{Cl}^-$  channels which are activated if  $\text{Ca}^{2+}$  enters the oocyte, probably through the opening of the NMDAR channel. The  $\text{Ca}^{2+}$ -induced  $\text{Cl}^-$  channel has in the past even been used to prove and quantify the amount of  $\text{Ca}^{2+}$  entering the egg (Barish, 1983; Leonard and Kelso, 1990; Chatterton et al., 2002). To rule out that the currents observed originated from these  $\text{Cl}^-$  channels triggered by  $\text{Ca}^{2+}$  entry, oocytes expressing NR1-1a-TG4L2-NR2A were pre-injected with 50 nL of 200 mM EGTA 30 mins before the measurement. The initial fast component disappeared, and an inward current with the shape typical of that of a glutamate receptor remained (Fig. 15). Neither the steady-state current amplitude nor the shape of the current-voltage relationship in  $\text{Mg}^{2+}$ -Ringer (MgR) (see 3.2.1.1.2) were altered.

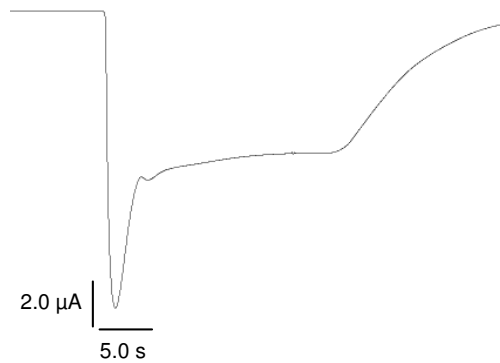
**NR1-1a + NR2A (1:1) without EGTA pre-injection**

Fig. 13 : Current amplitude in NFR with 100  $\mu\text{M}$  glutamate and 10  $\mu\text{M}$  glycine for wild type (NR1-1a + NR2A). Currents for channels with wild type NR1-1a were very often preceded by a fast inward current peak, most likely caused by the opening of endogenous  $\text{Cl}^-$  channels which are activated by an intracellular rise in  $\text{Ca}^{2+}$  entering through NMDA receptors (see also Fig. 14).

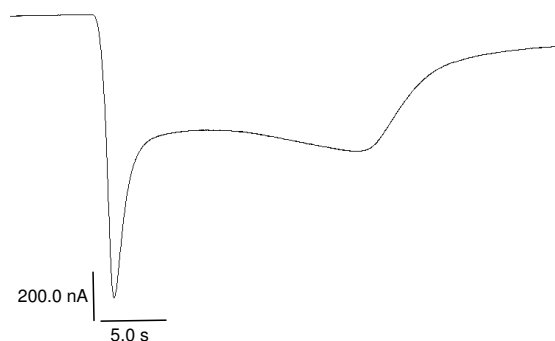
**NR1-1a-TG4L2-NR2A without EGTA pre-injection**

Fig. 14 : Current amplitude in NFR with 100  $\mu\text{M}$  glutamate and 10  $\mu\text{M}$  glycine for NR1-1a-TG4L2-NR2A. The initial fast spike points to  $\text{Ca}^{2+}$  influx through the NMDA receptor formed by the dimer.

### NR1-1a-TG4L2-NR2A with EGTA pre-injection

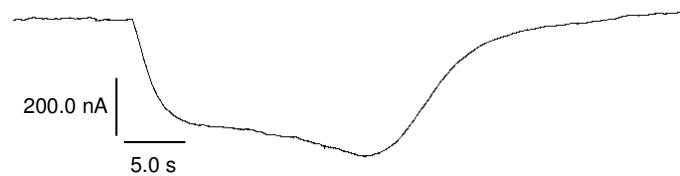


Fig. 15 : Current amplitude in NFR for NR1-1a-TG4L2-NR2A. The recording was done 30 mins after injection of 50 nL of 200 mM EGTA in the oocyte. This pre-injection of EGTA abolishes the contribution of the endogenous  $\text{Ca}^{2+}$ -activated  $\text{Cl}^-$  conductance to the observed current.

The  $\text{Cl}^-$  channel peak visible in Fig. 13 and Fig. 14 indeed vanished. Thus, the remaining current must stem from the dimer NR1-1a-TG4L2-NR2A.

#### 3.2.1.1.2 $\text{Mg}^{2+}$ block below - 20 mV

Consistent with the pharmacological profile of an NMDA receptor, NR1-1a-TG4L2-NR2A was substantially blocked by 1.8 mM extracellular  $\text{Mg}^{2+}$  (> 90 %). The same was seen for wild type (NR1-1a + NR2A; Fig. 16) as reported before (Ishii et al., 1993; Sakurada et al., 1993). Confirming previous studies, monomeric NR1-1a was able to form a functional receptor and - qualitatively - showed many of the basic properties characteristic of native NMDA (NR1 + NR2) receptors, such as voltage-dependent  $\text{Mg}^{2+}$  block, high  $\text{Ca}^{2+}$  permeability (3.2.1.1.3), and antagonism by APV and MK-801 (3.2.1.2.1) (Moriyoshi et al., 1991; Hollmann et al., 1993; Rodriguez-Paz et al., 1995; Kutsuwada et al., 1992; Meguro et al., 1992; Monyer et al., 1992). Quantitatively, however, heteromeric NMDA receptors and homomeric NR1 differ in their sensitivity to APV and MK-801 (cf. 3.2.1.2.1). These properties will be discussed in 4.1.3.1.

### NR1-1a-TG4L2-NR2A currents in Mg<sup>2+</sup>-Ringer

	% NR1-1a + NR2A current (- 70 mV)	SEM	n
NR1-1a + NR2A (1:1) in NFR	100	---	
NR1-1a + NR2A in MgR	9.8	3.3	12
NR1-1a-TG4L2-NR2A in NFR	29.2	5.9	6
NR1-1a-TG4L2-NR2A in MgR	0.8	0.9	6
NR1-1a in NFR	2.4	1.7	5
NR1-1a in MgR	0.2	0.4	5

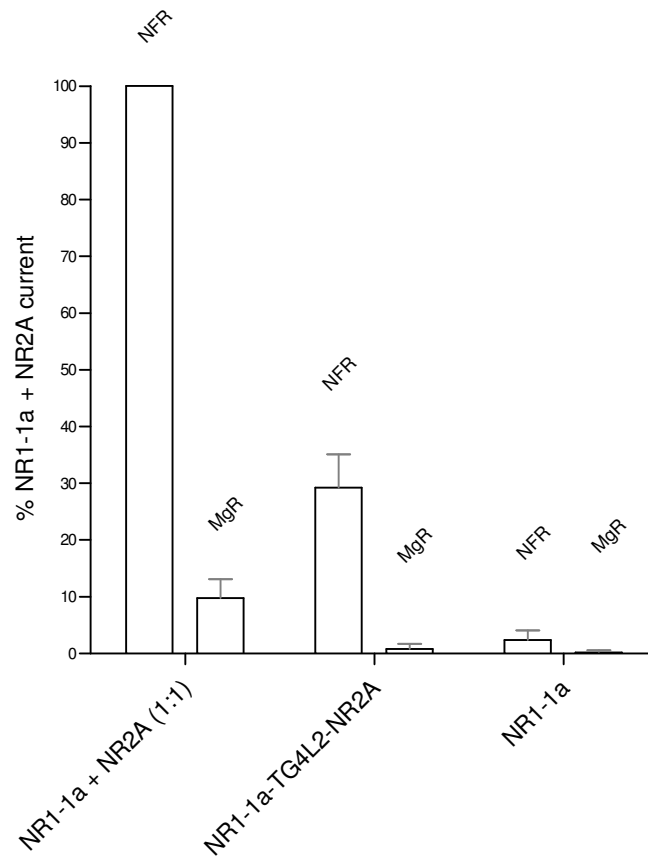


Fig. 16 : As wild type NR1-1a + NR2A and monomeric NR1-1a, NR1-1a-TG4L2-NR2A is blocked by Mg<sup>2+</sup> at a clamped voltage of - 70 mV. Currents were recorded in the indicated Ringer with 100  $\mu$ M glutamate and 10  $\mu$ M glycine.

Mg<sup>2+</sup>-Ringer (MgR) is NFR but with 1.8 mM MgCl<sub>2</sub> instead of CaCl<sub>2</sub>.

In addition to the maximal amplitudes, current-voltage relationships (I/V curves) were recorded in MgR (Figs. 17, 18). As expected, I/V curves showed a block below ca. -20 mV and were, apart from this, linear.

### NR1-1a + NR2A (1:1) in Mg<sup>2+</sup>-Ringer

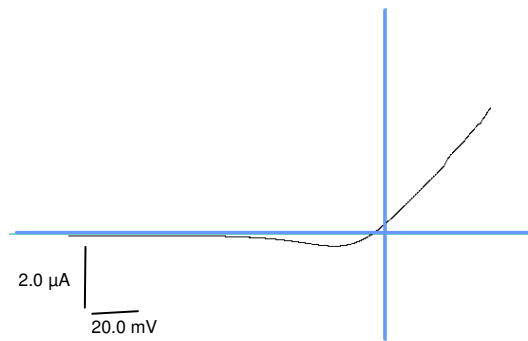


Fig. 17 : I/V for wild type (NR1-1a + NR2A) with receptor block below ca. -20 mV.

Current-voltage relations (I/V curves) were recorded in 1.8 mM-Mg<sup>2+</sup>-Ringer (MgR) during application of agonists (100 μM glutamate and 10 μM glycine). Voltage was ramped with 2 s - ramps from -150 mV to +50 mV.

### NR1-1a-TG4L2-NR2A in Mg<sup>2+</sup>-Ringer without EGTA pre-injection

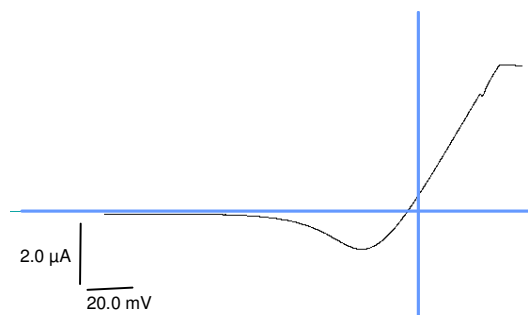


Fig. 18 : I/V for NR1-1a-TG4L2-NR2A in MgR with 100 μM glutamate and 10 μM glycine. Current block occurred below ca. -20 mV.

After injection of EGTA, the shape of the current-voltage relation in MgR remained unaltered (Fig. 19). For the particular oocyte shown here, the reversal potential was shifted to more positive values, possibly due to the absence of the  $\text{Cl}^-$  conductance.

### NR1-1a-TG4L2-NR2A in $\text{Mg}^{2+}$ -Ringer with EGTA pre-injection

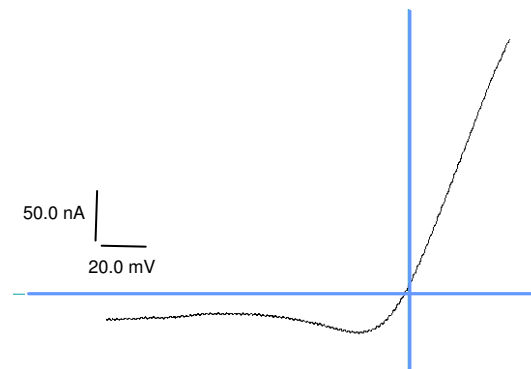


Fig. 19 : Unaltered I/V (in MgR with 100  $\mu\text{M}$  glutamate and 10  $\mu\text{M}$  glycine) for NR1-1a-TG4L2-NR2A after injection of EGTA. For unknown reasons, block for this particular oocyte was quite weak.

For all I/V curves, the reversal potential lay around - 5 to - 15 mV depending on the oocyte batch, near the oocyte  $\text{Cl}^-$  equilibrium potential (Sakurada et al., 1993; Weber, 1999).

#### 3.2.1.1.3 $\text{Ca}^{2+}$ permeability

The  $\text{Ca}^{2+}$  permeability was analysed in  $\text{Ca}^{2+}$ -Ringer (CaR) which contains 80 mM  $\text{Ca}^{2+}$  as the only permeable cation. Like wild type (NR1-1a + NR2A) (Ishii et al., 1993; Sakurada et al., 1993) and single NR1-1a, NR1-1a-TG4L2-NR2A is highly permeable to  $\text{Ca}^{2+}$ . Both the endogenous  $\text{Cl}^-$  channel spike (caused by  $\text{Ca}^{2+}$  entry through the NMDA receptor) and the steady-state current were enhanced in the nominated  $\text{Na}^+$  and  $\text{K}^+$  free CaR compared to NFR which contains 115 mM NaCl, 1.8 mM  $\text{CaCl}_2$  and 2.5 mM KCl.

First, the NMDA receptor is more efficiently permeable to  $\text{Ca}^{2+}$  than to  $\text{Na}^+$  and  $\text{K}^+$  (MacDonald and Nowak, 1990). Furthermore, while the intracellular concentration of  $\text{Ca}^{2+}$  is about 100 nM (Weber, 1999), the extracellular Ringer contains a million fold excess of  $\text{Ca}^{2+}$  ions. These two facts probably explain the observed large current amplitude with CaR, which exceeds the one measured with NFR (Fig. 20).

### NR1-1a-TG4L2-NR2A currents in Ca<sup>2+</sup>-Ringer

	% NR1-1a + NR2A current (- 70 mV)	SEM	n
NR1-1a + NR2A (1:1) in NFR	100	---	
NR1-1a + NR2A in CaR	119.6	11.5	11
NR1-1a-TG4L2-NR2A in NFR	29.2	5.9	6
NR1-1a-TG4L2-NR2A in CaR	190.2	15.1	6
NR1-1a in NFR	2.4	1.7	5
NR1-1a in CaR	5.2	2.5	5

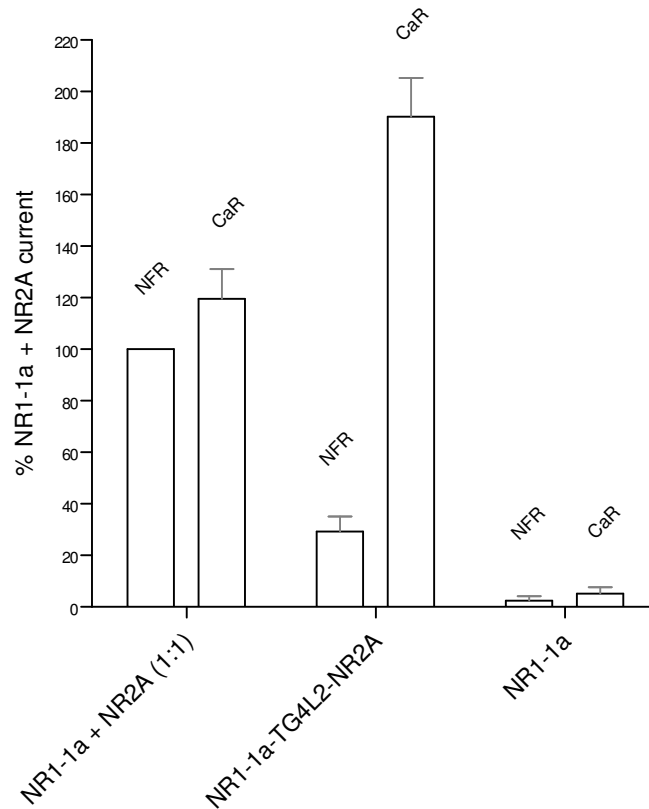


Fig. 20 : As wild type (NR1-1a + NR2A) and single NR1-1a, NR1-1a-TG4L2-NR2A is highly permeable to Ca<sup>2+</sup>. Currents were evoked in the indicated Ringer with 100  $\mu$ M glutamate and 10  $\mu$ M glycine. Ca<sup>2+</sup>-Ringer (CaR) contains 80 mM CaCl<sub>2</sub>.

### 3.2.1.2 Pharmacological properties

#### 3.2.1.2.1 Inhibition by APV, MK-801, and insensitivity to ifenprodil

a) APV

#### Block of NR1-1a-TG4L2-NR2A currents by APV

	% NR1-1a + NR2A current (- 70 mV)	SEM	n
NR1-1a + NR2A (1:1)	100	---	
NR1-1a + NR2A + APV	21.7	4.8	11
NR1-1a-TG4L2-NR2A	27.8	5.8	6
NR1-1a-TG4L2-NR2A + APV	6.4	2.8	6
NR1-1a	1.9	1.6	4
NR1-1a + APV	0.6	0.9	4

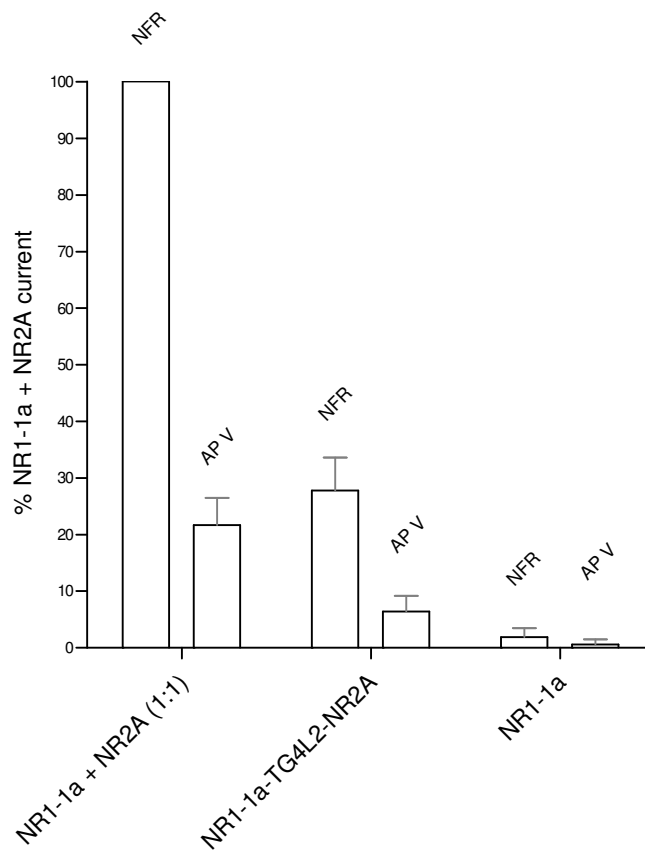


Fig. 21 : Like wild type (NR1-1a + NR2A) and monomeric NR1-1a, NR1-1a-TG4L2-NR2A is blocked by 100  $\mu$ M APV. Co-application of antagonist with 100  $\mu$ M glutamate and 10  $\mu$ M glycine in NFR was for 20 s.

APV is a competitive antagonist for the NMDA receptor, acting at the glutamate binding site. Altogether, NR1-1a + NR2A (wild type), single NR1-1a and NR1-1a-TG4L2-NR2A were inhibited by 100  $\mu$ M APV, with residual current of about 20 % (Fig. 21). The efficiency of antagonising the agonist-induced currents confirms results by Anson et al. (1998) and Verdoorn et al. (1989). The  $IC_{50}$  of APV for the NR1/NR2A combination had been determined to be 2.5  $\mu$ M by Ishii et al. (1993).

At this point, one has to remark that there is controversy in the literature about the effect of APV on NR1-1a : Whereas Moriyoshi et al. (1991) and Hollmann et al. (1993) saw a clear current reduction comparable to the one seen here, APV at concentrations up to 100  $\mu$ M (together with 100  $\mu$ M glutamate and 10  $\mu$ M glycine) had no effect for Green et al. (2002). Together with the other data for monomeric NR1-1a, this will be discussed in 4.1.3.1.

#### b) MK-801

MK-801 is a non-competitive antagonist that acts as an open channel blocker of the NMDA receptor (1.3.2). For NR1-1a-TG4L2-NR2A, wild type (NR1-1a + NR2A) and monomeric NR1-1a, application of agonists in the presence of 1  $\mu$ M MK-801 elicited a rapid initial spike representing the  $Ca^{2+}$ -triggered oocyte  $Cl^-$  channel.

However, once the NMDA receptor had opened, the blocker was trapped inside the channel and the response was rapidly inactivated, down to about 10 % at -70 mV for NR1-1-TG4L2-NR2A and wild type (Fig. 22). For Laurie and Seeburg (1994), MK-801 exhibited the affinity ranking of NR1-NR2A  $\gg$  NR1, and for NR1-1a Hollmann et al. (1993) reported block down to  $18.4 \pm 4.7$  % ( $n = 3$ ). The literature data confirm the data in Fig. 22 for NR-1a (block down to 21.1 %).

For the wild type control and NR1-1a, the responses could be partially recovered after washing with NFR for 2 mins followed by application of the agonists without MK-801 (see current amplitudes for washout in Fig. 22). Thus, for these two receptors, block by MK-801 was partially reversible, i.e. the antagonist could slowly be removed from its binding site within the ion pore by a subsequent application of agonists (Rodriguez-Paz et al., 1995; Ishii et al., 1993; Sakurada et al., 1993).

### Reversible block of NR1-1a-TG4L2-NR2A currents by MK-801

	% NR1-1a + NR2A current (- 70 mV)	SEM	n
NR1-1a + NR2A (1:1)	100	---	
NR1-1a + NR2A + (+)MK-801	13.2	3.8	11
NR1-1a + NR2A washout	67.6	8.7	10
NR1-1a-TG4L2-NR2A	27.8	5.8	6
NR1-1a-TG4L2-NR2A + (+)MK-801	2.3	1.7	6
NR1-1a-TG4L2-NR2A washout	22.8	5.2	6
NR1-1a	1.9	1.6	4
NR1-1a + (+)MK-801	0.4	0.8	4
NR1-1a washout	0.6	0.9	4

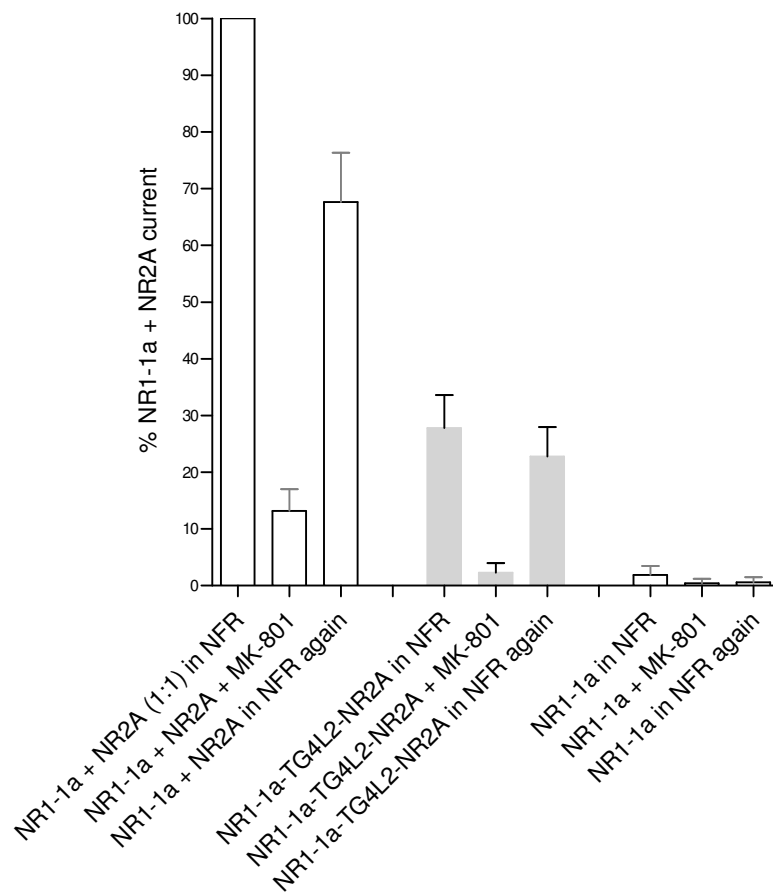


Fig. 22 : Like wild type (NR1-1a + NR2A), NR1-1a-TG4L2-NR2A is blocked by 1  $\mu$ M MK-801 at - 70 mV. Application of antagonist lasted 20 s. Block by MK-801 was reversible only for the concatemer.

By contrast, for the dimer NR1-1a-TG4L2-NR2A block by MK-801 was readily and fully reversible (% of NR1-1a + NR2A current in Fig. 22 :  $27.8 \pm 5.8$  % before block and  $22.8 \pm 5.2$  % after washout of MK-801). This reversible block is probably caused by the fact that the ion pore formed by two assembled dimers differs in structure from the wild type ion pore formed by four monomeric subunits. In the concatemer-derived pore, two of the four subunits of the channel complex cannot move freely because they are covalently tied to each other. Evidently, MK-801 is not able to bind to the concatemer-derived pore as tightly as to the native pore, leading to enhanced washout of the blocker when the closed receptor opens again.

Alterations of the ion pore structure in the concatemeric receptor would be in line with the observed drastic reduction in ion conductance of dimers (3.5 and 4.1.3.2).

### c) Ifenprodil

#### **Insensitivity of NR1-1a-TG4L2-NR2A currents to ifenprodil**

	% NR1-1a + NR2A current (- 70 mV)	SEM	n
NR1-1a + NR2A (1:1)	100	---	
NR1-1a + NR2A + ifenprodil	74.6	10.0	4
NR1-1a + NR2A washout	104.5	11.8	4
NR1-1a-TG4L2-NR2A	34.5	6.6	5
NR1-1a-TG4L2-NR2A + ifenprodil	25.8	5.7	5
NR1-1a-TG4L2-NR2A washout	35.5	6.7	5
NR1-1a + NR2B (1:1)	163.2	14.3	5
NR1-1a + NR2B + ifenprodil	79.1	9.9	5
NR1-1a + NR2B washout	235.1	17.1	5
NR1-1a	7.1	3.0	5
NR1-1a + ifenprodil	5.7	2.7	5
NR1-1a washout	11.5	3.8	5

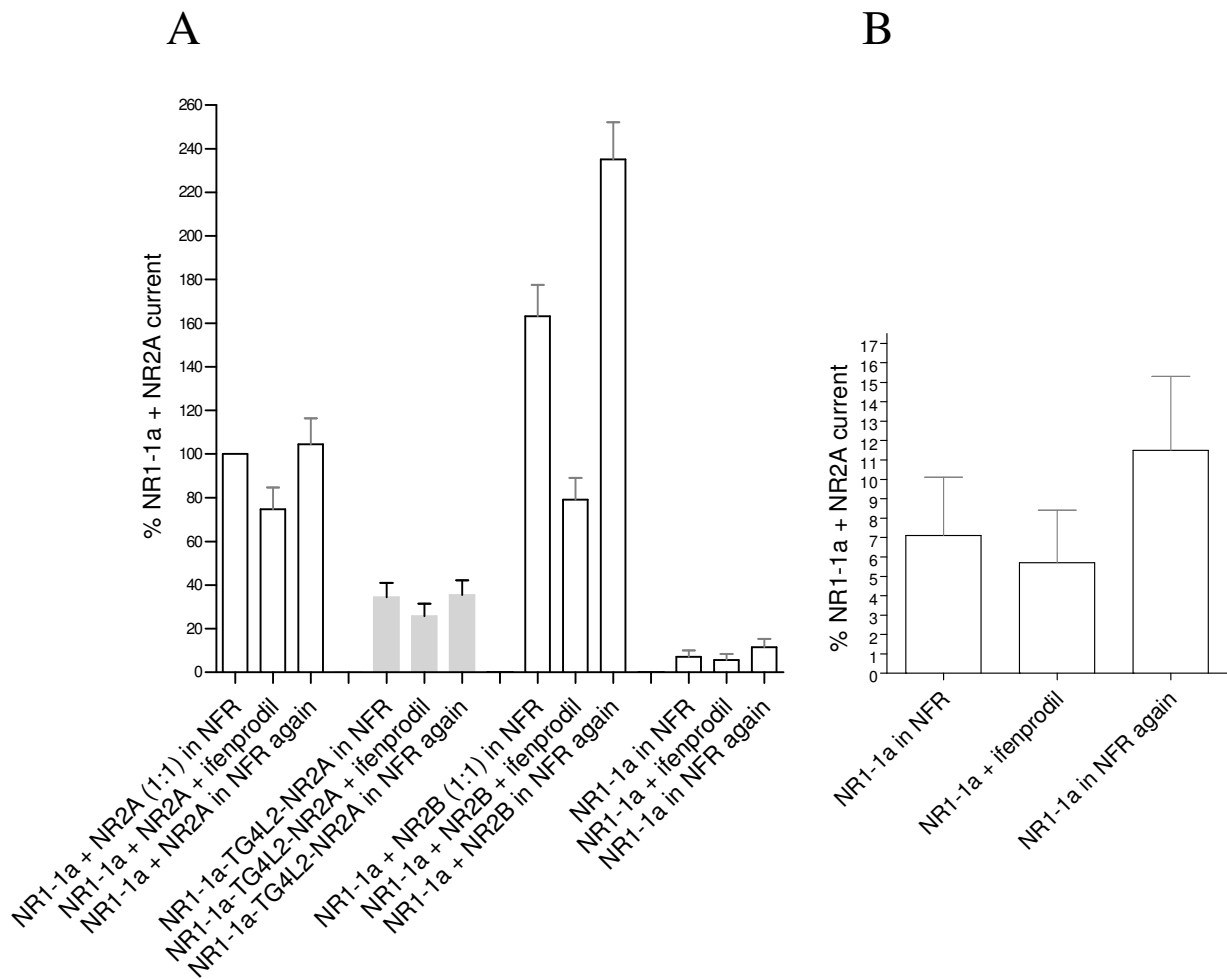


Fig. 23 :

A : Unlike monomeric NR1-1a, and NR2B in co-expression with NR1-1a - that are highly sensitive to ifenprodil - NR2A in co-expression with NR1-1a was significantly less blockable by ifenprodil (3  $\mu$ M). The same was seen for NR1-1a-TG4L2-NR2A which proves the formation of an NR1-NR2A channel by the entire dimer, thus incorporating not only the head (NR1-1a) subunit but also the tail (NR2A) subunit of the dimer.

B : Enlargement of the triplet of columns on the right-hand side of A, to allow better appreciation of small current sizes.

Ifenprodil belongs to the class of non-competitive antagonists that block NMDA receptors without reducing agonist potency. It was proposed to increase the potency of protons to block the NMDA receptor. Ifenprodil has become known as a suitable subunit-selective drug with an  $IC_{50}$  that is about 400 fold lower for NR2B-containing NMDA receptors (0.34  $\mu$ M) or NR1 alone (0.28  $\mu$ M) than for NR2A-containing receptors (146  $\mu$ M) (1.3.2). For the present study, it is important to note that ifenprodil can thus be used to discriminate

between a current arising from a combination of NR1-1a and NR2A, and one mediated by NR1-1a alone.

Indeed, NR1-1a + NR2B as well as NR1-1a alone were distinctly inhibited by 3  $\mu$ M ifenprodil (about 30 - 50 % of the response after washout) (Fig. 23). It is a general phenomenon with the oocyte expression system that very often the 2<sup>nd</sup> current response to agonist (i.e. the washout here) is larger than the 1<sup>st</sup>. This "warming up" of the oocyte is not yet understood. As a consequence, for NR1-1a + NR2B and NR1-1a alone the amount of ifenprodil block should be estimated in comparison to the response after washout ( $235.1 \pm 17.1$  % of wild type for NR1-1a + NR2B and  $11.5 \pm 3.8$  % of wild type for NR1-1a).

In contrast, NR1-1a + NR2A as well as the dimer NR1-1a-TG4L2-NR2A were significantly less blockable by ifenprodil (70 - 75 % of starting currents), and the block could be easily and fully washed out by NFR (Fig. 23). These data fit nicely with the cell culture results by Prybylowski et al. (2002) : NR2A-transfected cerebellar neurons showed significantly less reduction in current amplitude in the presence of 10  $\mu$ M ifenprodil ( $27.5 \pm 5.0$  %) than NR2B-transfected neurons ( $68.9 \pm 3.3$  %).

Importantly, the insensitivity of NR1-1a-TG4L2-NR2A to ifenprodil not only proves wild type-like (NR1-1a + NR2A-like) behaviour of NR1-1a-TG4L2-NR2A but also that the dimer currents originate from a receptor formed from NR1-1a and NR2A and not from NR1-1a alone, i.e. both the head (NR1-1a) and tail (NR2A) subunits of the dimer get incorporated into the receptor.

### **3.2.2 Properties of the N598R mutation are preserved within the heterodimer**

When the cRNA for the mutant heterodimer NR1-1a(N598R)-TG4L2-NR2A was injected and oocytes superfused with 100  $\mu$ M glutamate and 10  $\mu$ M glycine in NFR, inward currents arose similar to those seen for NR1-1a-TG4L2-NR2A. However, contrary to the latter dimer - which harbours a wild type NR1-1a subunit with an asparagine (N) at position 598 as opposed to the arginine (R) of this mutant dimer - NR1-1a(N598R)-TG4L2-NR2A never generated a fast, inward  $\text{Cl}^-$  peak, indicating the absence of  $\text{Ca}^{2+}$  influx into the cell (Fig 24). The same behaviour was observed for the monomeric control NR1-1a(N598R) + NR2A (Fig. 25). This finding already gave a hint that the N598R mutation conveying  $\text{Ca}^{2+}$  impermeability was indeed present in the dimer which was further investigated in 3.2.2.1.2.

### NR1-1a(N598R)-TG4L2-NR2A in normal frog Ringer

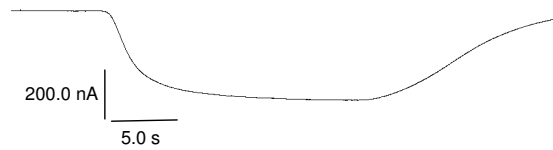


Fig. 24 : Currents for NR1-1a(N598R)-TG4L2-NR2A were characterised by the absence of a fast, inward  $\text{Cl}^-$  peak indicating the absence of  $\text{Ca}^{2+}$  influx into the cell. Agonists were 100  $\mu\text{M}$  glutamate + 10  $\mu\text{M}$  glycine in NFR.

### NR1-1a(N598R) + NR2A (1:1) in normal frog Ringer

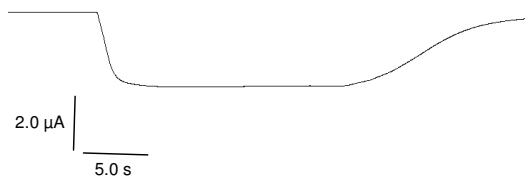


Fig. 25 : Currents for monomeric NR1-1a(N598R) + NR2A were also characterised by a lack of  $\text{Ca}^{2+}$  influx. Agonists were 100  $\mu\text{M}$  glutamate + 10  $\mu\text{M}$  glycine in NFR.

The amplitude for the monomeric control NR1-1a(N598R) + NR2A in NFR was more than 50 % reduced compared to the heteromeric wild type NR1-1a + NR2A (Fig. 26), confirming previous data (Sakurada et al., 1993). The monomeric mutant NR1-1a(N598R) yielded only  $0.4 \pm 0.6$  % of the heteromeric wild type current (this is, however, in the range of background responses also observed for uninjected oocytes; see Fig. 12), while NR1-1a had shown  $1.5 \pm 1.2$  % of wild type (cf. Fig. 12).

From this data it was expected that NR1-1a(N598R)-TG4L2-NR2A should show a similar reduction in current amplitude when compared to the wild type heterodimer. There is, in fact, such a difference between the current amplitude of NR1-1a-TG4L2-NR2A ( $12.1 \pm 3.7$  % of wild type NR1-1a + NR2A; Fig. 12) and NR1-1a(N598R)-TG4L2-NR2A ( $5.2 \pm 2.3$  % of wild type; Fig. 26). This difference can also be seen for co-expressions of

NR1-1a(N598R)-TG4L2-NR2A with monomers, such as NR2A and NR1-1a. For a more detailed discussion of the role of monomers in co-expressions with dimers see 3.4.1 and 3.4.2.

### NR1-1a(N598R)-TG4L2-NR2A currents in normal frog Ringer

	% NR1-1a + NR2A current (- 70 mV)	SEM	n
sNR1-1a(N598R) + NR2A (1:1)	45.7	7.0	15
NR1-1a(N598R)-TG4L2-NR2A	5.2	2.3	16
NR1-1a-TG4L2-NR2A	12.1	3.7	9
sNR1-1a(N598R)	0.4	0.6	7

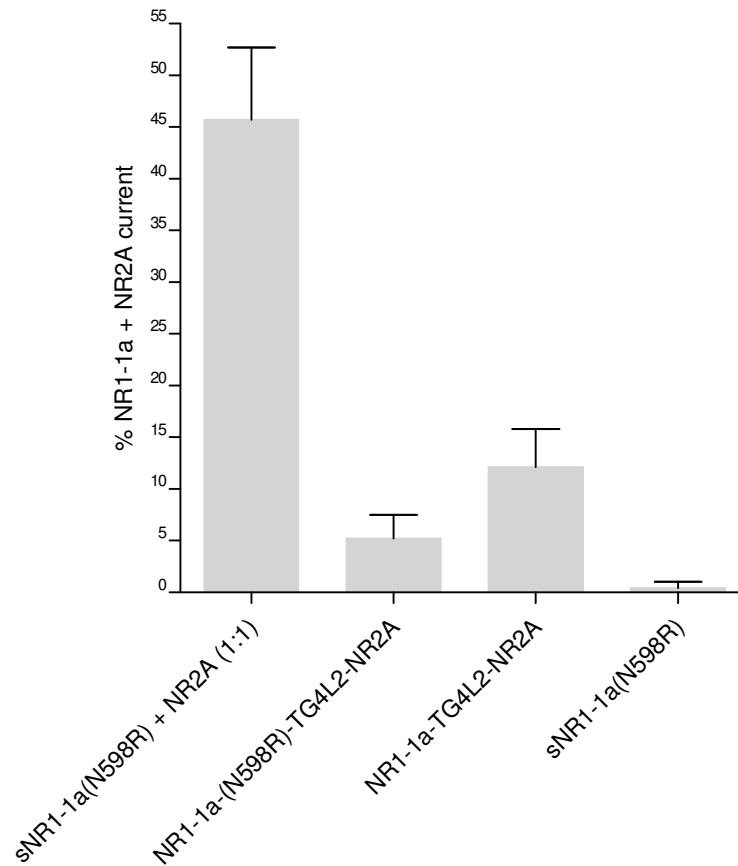


Fig. 26 : Currents were also seen for NR1-1a(N598R)-TG4L2-NR2A with 100  $\mu$ M glutamate and 10  $\mu$ M glycine in NFR. These were reduced in comparison to the wild type heterodimer NR1-1a-TG4L2-NR2A similar to the extent that NR1-1a(N598R) + NR2A was reduced compared to wild type (NR1-1a + NR2A).

### 3.2.2.1 Electrophysiological properties

#### 3.2.2.1.1 Release of $Mg^{2+}$ block below - 20 mV

	% NR1-1a + NR2A current (- 70 mV)	SEM	n
sNR1-1a(N598R) + NR2A (1:1) in NFR	38.5	6.7	7
sNR1-1a(N598R) + NR2A in MgR	42.5	7.0	7
NR1-1a(N598R)-TG4L2-NR2A in NFR	4.1	2.5	3
NR1-1a(N598R)-TG4L2-NR2A in MgR	3.8	2.4	3
sNR1-1a(N598R) in NFR	0.1	0.3	3
sNR1-1a(N598R) in MgR	0.0	0.0	3

#### NR1-1a(N598R)-TG4L2-NR2A currents in $Mg^{2+}$ -Ringer

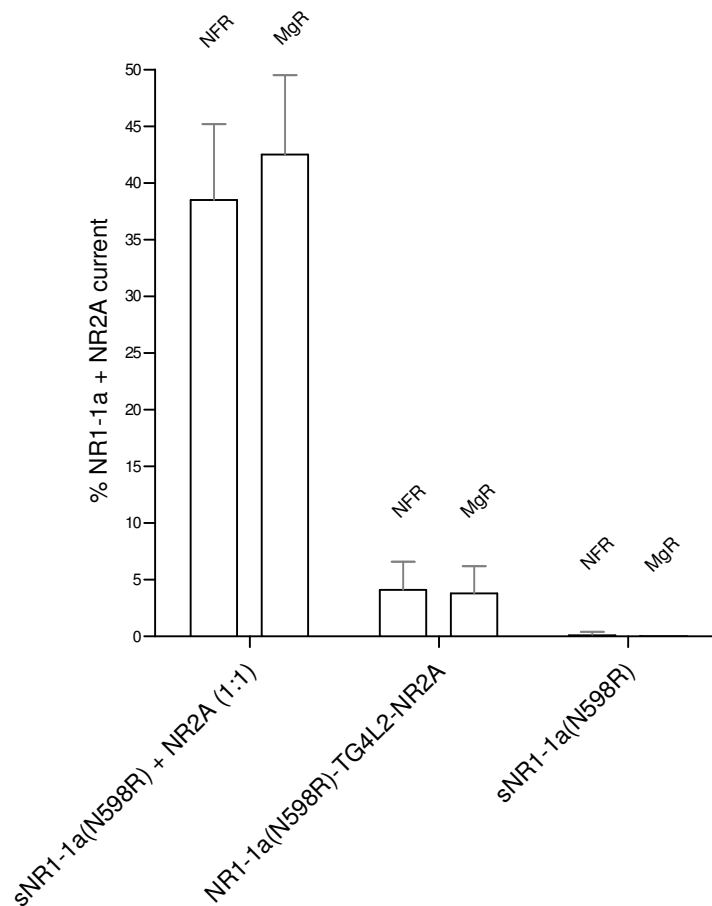


Fig. 27 : Like NR1-1a(N598R) together with NR2A, and unlike receptors with wild type NR1-1a, NR1-1a(N598R)-TG4L2-NR2A shows release of  $Mg^{2+}$  block at - 70 mV.

Currents were activated in the indicated Ringer by application of 100  $\mu$ M glutamate and 10  $\mu$ M glycine.

$Mg^{2+}$ -Ringer (MgR) is NFR but with 1.8 mM  $MgCl_2$  instead of 1.8 mM  $CaCl_2$ .

Investigations from numerous groups have demonstrated that substitution of a neutral asparagine (N598) in the ion channel pore of the NR1 subunit (and also at an equivalent position of NR2) with glutamine or a positively charged arginine markedly reduces or abolishes voltage-dependent  $Mg^{2+}$  block,  $Ca^{2+}$  permeation and inhibition by open channel blockers such as MK-801 in the resultant mutant receptors (Sakurada et al., 1993; Burnashev et al., 1992; Dingledine et al., 1999; McBain and Mayer, 1994). This asparagine forms the narrow constriction of the receptor channel, where  $Mg^{2+}$  and MK-801 are assumed to bind (1.3.2). Introduction of a positively charged arginine at the narrow constriction (i.e. at the N site) then leads to repulsion of divalent cations, such as  $Mg^{2+}$  and  $Ca^{2+}$ , and also MK-801.

Indeed, in both cases, in the monomeric NR1-1a(N598R) co-expressed with NR2A and the dimeric NR1-1a(N598R)-TG4L2-NR2A construct expressed alone, the N598R mutation in NR1-1a abolished the block by external 1.8 mM  $Mg^{2+}$  normally found below ca. - 20 mV (Fig. 27). For NR1-1a(N598R), the current amplitude was too low (lower than background currents in Fig. 12) to draw any conclusion (the same was the case for the  $Ca^{2+}$ -Ringer, APV- and MK-801-block experiments; n = 3 or 2 in all cases).

Also, in cells expressing NR1-1a(N598R)-NR2A receptors, the shape of the I/V relation was - contrary to a J-shaped I/V for receptors with wild type NR1-1a (Figs. 17 - 19) - insensitive to block by  $Mg^{2+}$  (Figs. 28, 29).

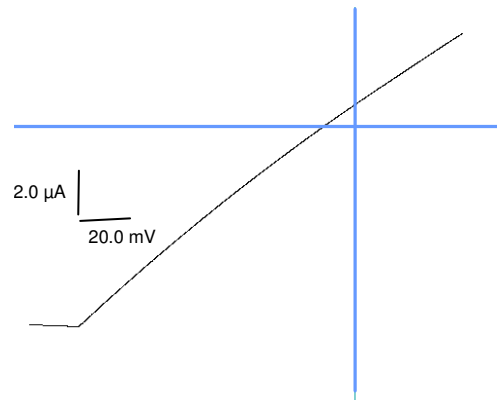
**NR1-1a(N598R) + NR2A (1:1) in Mg<sup>2+</sup>-Ringer**

Fig. 28 : I/V for NR1-1a(N598R) + NR2A in MgR during superfusion with 100 μM glutamate and 10 μM glycine. The N598R mutation rendered the receptor unblockable by Mg<sup>2+</sup>.

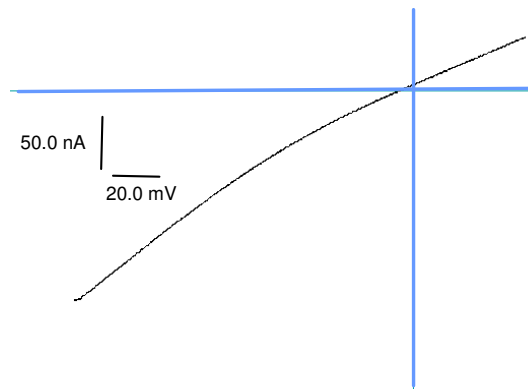
**NR1-1a(N598R)-TG4L2-NR2A in Mg<sup>2+</sup>-Ringer**

Fig. 29 : I/V for NR1-1a(N598R)-TG4L2-NR2A in MgR with 100 μM glutamate and 10 μM glycine. The linear (i.e. non-blocked) I/V indicates the presence of the 1<sup>st</sup>, not Mg<sup>2+</sup> blockable subunit of the dimer in the receptor.

At the same time, the linear (i.e. non-blocked) I/V for NR1-1a(N598R)-TG4L2-NR2A indicated the presence of the 1<sup>st</sup> (not Mg<sup>2+</sup> blockable) subunit in the concatemeric NMDA receptor.

### 3.2.2.1.2 Ca<sup>2+</sup> impermeability

#### NR1-1a(N598R)-TG4L2-NR2A currents in Ca<sup>2+</sup>-Ringer

	% NR1-1a + NR2A current (-70 mV)	SEM	n
sNR1-1a(N598R) + NR2A (1:1) in NFR	38.5	6.7	7
sNR1-1a(N598R) + NR2A in CaR	-2.2		3
NR1-1a(N598R)-TG4L2-NR2A in NFR	4.1	2.5	3
NR1-1a(N598R)-TG4L2-NR2A in CaR	0.0	0.0	3
sNR1-1a(N598R) in NFR	0.1	0.3	3
sNR1-1a(N598R) in CaR	0.0	0.0	3

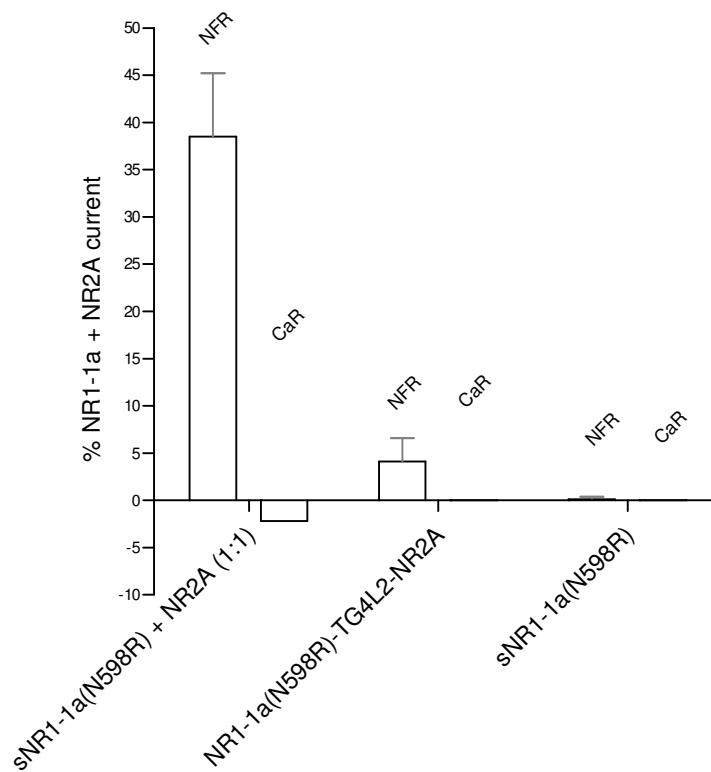


Fig. 30 : The N598R mutation caused the NMDA receptors formed from monomeric NR1-1a(N598R) + NR2A or the heterodimer NR1-1a(N598R)-TG4L2-NR2A to be impermeable to Ca<sup>2+</sup>.

Currents were recorded in the indicated Ringer with 100  $\mu$ M glutamate and 10  $\mu$ M glycine.

Ca<sup>2+</sup>-Ringer (CaR) contains 80 mM CaCl<sub>2</sub>.

According to expectations, the N598R mutation in NR1-1a caused channels built from co-expressed monomers NR1-1a(N598R) + NR2A or the dimer NR1-1a(N598R)-TG4L2-NR2A to exhibit no measurable  $\text{Ca}^{2+}$  permeability in 80 mM CaR (Fig. 30). The (negative) outward current (- 2.2 % of NR1-1a + NR2A) for the NR1-1a(N598R) + NR2A co-expression in  $\text{Na}^+$  and  $\text{K}^+$  free, high extracellular  $\text{Ca}^{2+}$  solution is characteristic for the low  $\text{Ca}^{2+}$  permeability of this mutant channel (Burnashev et al., 1992; Sakurada et al., 1993) : Under these conditions, a  $\text{Ca}^{2+}$  impermeable, but  $\text{Na}^+$  and  $\text{K}^+$  permeable channel can only allow an outward flux of intracellular  $\text{K}^+$  (ca. 115 mM intracellular; Weber, 1999).

### 3.2.2.2 Pharmacological properties

#### 3.2.2.2.1 Inhibition by APV and insensitivity to MK-801

##### a) APV

Since APV competes with NMDA and glutamate for the agonist binding site formed by the extracellular S1 and S2 domains of the receptor (cf. 3.2.1.2.1 and 1.2.2), the arginine substitution at amino acid 598 within the NR1-1a ion pore domain should not alter antagonist potency. Similar to receptors with wild type NR1-1a, the co-expressed monomeric NR1-1a(N598R) + NR2A and the dimer NR1-1a(N598R)-TG4L2-NR2A were both blocked by 100  $\mu\text{M}$  APV.

The slightly smaller block of NR1-1a(N598R)-TG4L2-NR2A by APV to only 45 % (and not ca. 20 % as for the other recordings; 3.2.1.2.1) is probably not significant because of the rather large standard error (SEM) of this measurement (Fig. 31).

### Block of NR1-1a(N598R)-TG4L2-NR2A currents by APV

	% NR1-1a + NR2A current (-70 mV)	SEM	n
sNR1-1a(N598R) + NR2A (1:1)	50.9	8.2	4
sNR1-1a(N598R) + NR2A + APV	12.2	4.0	4
NR1-1a(N598R)-TG4L2-NR2A	6.0	2.7	5
NR1-1a(N598R)-TG4L2-NR2A + APV	2.7	1.8	5
sNR1-1a(N598R)	0.1	0.4	2
sNR1-1a(N598R) + APV	0.1	0.3	2

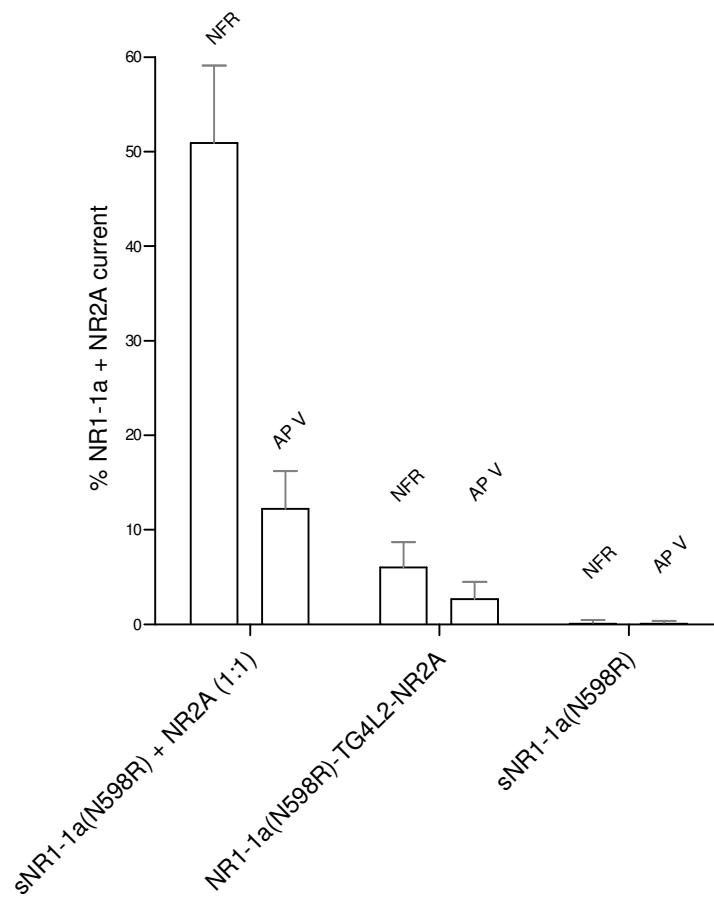


Fig. 31 : NR1-1a(N598R)-TG4L2-NR2A and the co-expressed monomeric NR1-1a(N598R) + NR2A current are both suppressed by 100  $\mu$ M APV, just like wild type constructs (Fig. 21).

Antagonist was co-applied with 100  $\mu$ M glutamate and 10  $\mu$ M glycine in NFR for 20 s.

## b) MK-801

**Insensitivity of NR1-1a(N598R)-TG4L2-NR2A currents to MK-801**

	% NR1-1a + NR2A current (-70 mV)	SEM	n
sNR1-1a(N598R) + NR2A (1:1)	50.9	8.2	4
sNR1-1a(N598R) + NR2A + (+)MK-801	33.1	6.6	4
sNR1-1a(N598R) + NR2A washout	29.7	6.3	4
NR1-1a(N598R)-TG4L2-NR2A	6.0	2.7	5
NR1-1a(N598R)-TG4L2-NR2A + (+)MK-801	4.2	2.3	5
NR1-1a(N598R)-TG4L2-NR2A washout	5.1	2.5	5
sNR1-1a(N598R)	0.1	0.4	2
sNR1-1a(N598R) + (+)MK-801	0.1	0.4	2
sNR1-1a(N598R) washout	0.2	0.6	2

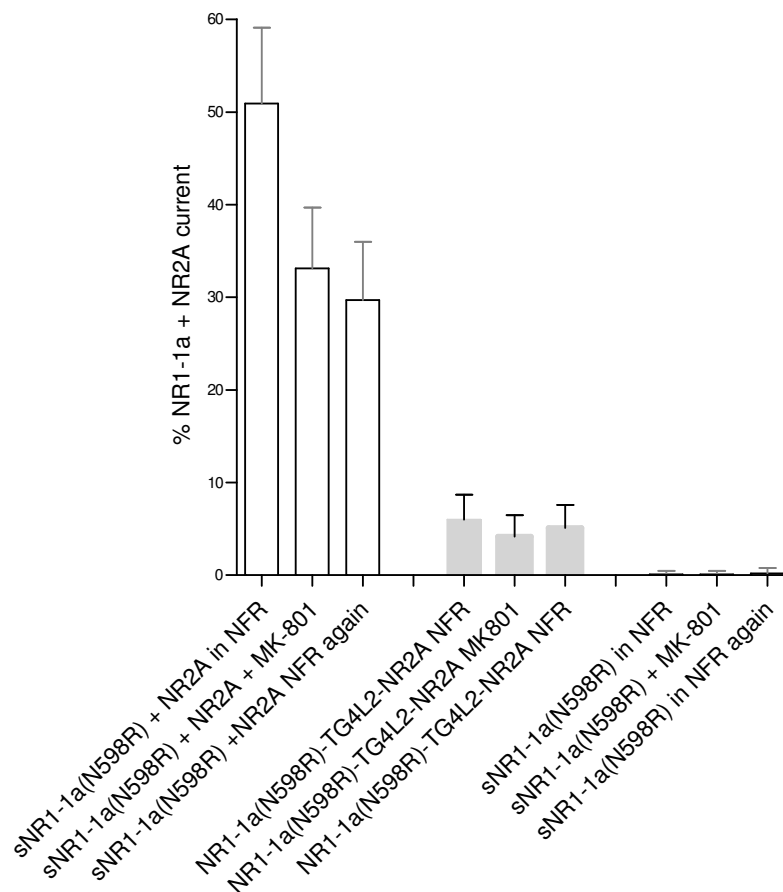


Fig. 32 : Unlike wild type constructs (Fig. 22), NR1-1a(N598R)-TG4L2-NR2A and the co-expressed monomeric NR1-1a(N598R) + NR2A are almost insensitive to 1  $\mu$ M MK-801 (application of antagonist in the presence of 100  $\mu$ M glutamate and 10  $\mu$ M glycine in NFR lasted 20 s).

In agreement with the results by Sakurada et al. (1993), 1  $\mu$ M MK-801 was ineffective in blocking the current response of any construct containing the N598R mutation (Fig. 32). These results prove the presence of the 1<sup>st</sup>, MK-801 insensitive subunit in the concatemeric NMDA receptor, supporting the  $Mg^{2+}$  block experiments (cf. 3.2.2.1.1).

### 3.3 Analysis of NR1-1a and NR2A homodimers

#### 3.3.1 The homodimers NR1-1a-TG4L2-NR1-1a and NR2A-TG4L2-NR2A are not functional alone but give currents together with monomeric NR2A and NR1-1a, respectively

As seen for single NR1-1a and NR2A (3.2.1.1), NR1-1a-TG4L2-NR1-1a individually elicited small currents in oocytes ( $0.1 \pm 0.4$  % of wild type NR1-1a + NR2A, which is at the level of background responses in Fig. 12), but not NR2A-TG4L2-NR2A (Fig. 33). Next, cRNA transcribed from NR1-1a-TG4L2-NR1-1a was expressed together with NR2A. The same was done for NR2A-TG4L2-NR2A in combination with NR1-1a.

For the co-expressions, currents could be measured which were larger than the ones recorded for NR1-1a-TG4L2-NR2A or NR1-1a(N598R)-TG4L2-NR2A (heterodimers alone) : > 20 % of wild type for NR2A-TG4L2-NR2A + NR1-1a and 60 % of wild type for NR1-1a-TG4L2-NR1-1a + NR2A (Fig. 33). This can be seen as a further evidence that the linker in the concatemer is responsible for the drastic decrease in current amplitude already seen in comparison to wild type NR1-1a + NR2A (3.2.1.1 and 3.5).

Furthermore, the clearly larger current amplitude for NR1-1a-TG4L2-NR1-1a + NR2A than for NR2A-TG4L2-NR2A + NR1-1a might indicate that monomeric NR2A facilitates receptor assembly (cf. 3.4.1).

### Homodimer currents in normal frog Ringer

	% NR1-1a + NR2A current (-70 mV)	SEM	n
NR1-1a-TG4L2-NR1-1a	0.1	0.4	6
NR1-1a-TG4L2-NR1-1a + NR2A (1:2)	59.8	8.3	8
NR2A-TG4L2-NR2A	0.0	0.0	6
NR2A-TG4L2-NR2A + NR1-1a (1:2)	21.7	5.1	6

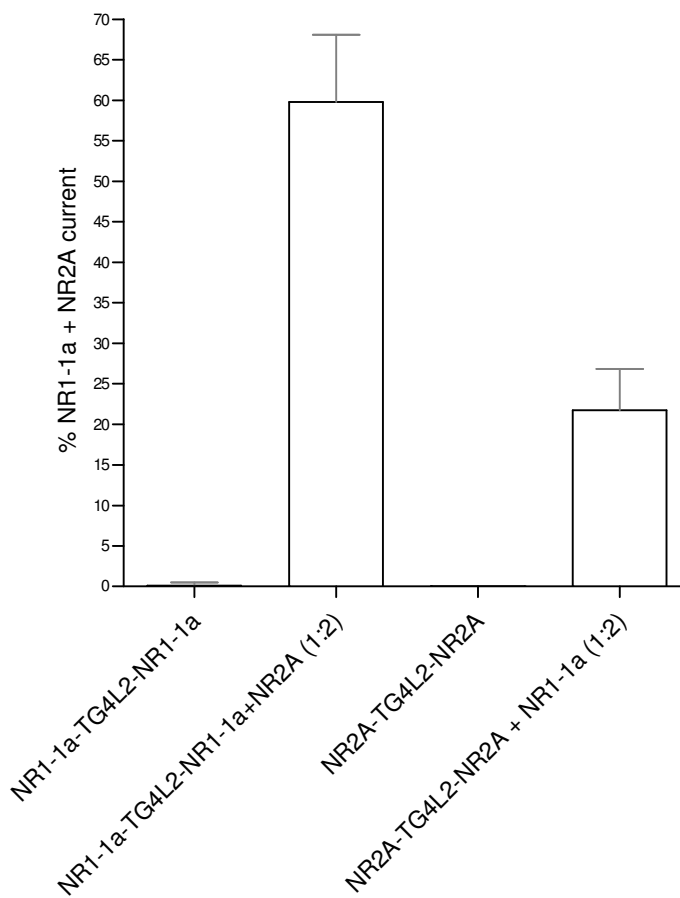


Fig. 33 : NR1-1a-TG4L2-NR1-1a and NR2A-TG4L2-NR2A elicited distinct currents with 100  $\mu$ M glutamate and 10  $\mu$ M glycine in NFR only upon co-expression with monomeric NR2A and NR1-1a, respectively. The clearly larger amplitude seen for NR1-1a-TG4L2-NR1-1a + NR2A as compared to NR2A-TG4L2-NR2A + NR1-1a might indicate that monomeric NR2A facilitates receptor assembly (cf. 3.4.1).

### 3.3.2 NR1-1a-TG4L2-NR1-1a(N598R) proves incorporation of the tail subunit in the receptor complex

To further support the notion that no degradation of the concatemer occurred, and that the tail subunit became integrated in the channel complex, NR1-1a-TG4L2-NR1-1a(N598R) was constructed, the cRNA transcript injected in combination with NR2A, and its rectifying properties examined in oocytes.

The observed linear I/V in MgR indicated the presence of the 2<sup>nd</sup>, not Mg<sup>2+</sup> blockable subunit in the NMDAR complex and also demonstrated the dominance of the N598R mutation with respect to Mg<sup>2+</sup> block (Fig. 34).

#### NR1-1a-TG4L2-NR1-1a(N598R) + NR2A in Mg<sup>2+</sup>-Ringer

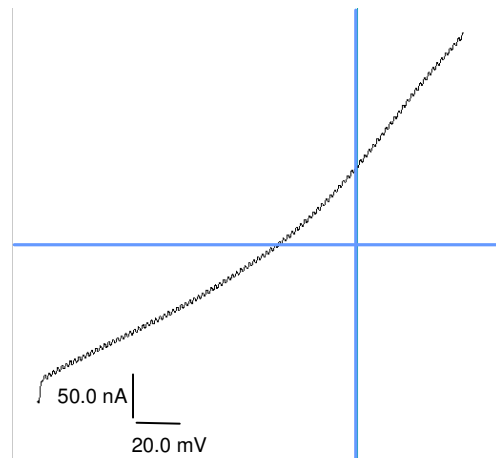


Fig. 34 : I/V for NR1-1a-TG4L2-NR1-1a(N598R) + NR2A in MgR with 100  $\mu$ M glutamate and 10  $\mu$ M glycine.

NR1-1a-TG4L2-NR1-1a(N598R) + NR2A was not blocked in the presence of Mg<sup>2+</sup>, proving the integration of the tail subunit of the dimer into the concatemeric channel.

Consistently, NR1-1a-TG4L2-NR1-1a together with NR2A showed Mg<sup>2+</sup> block below ca. -20 mV (Fig. 35).

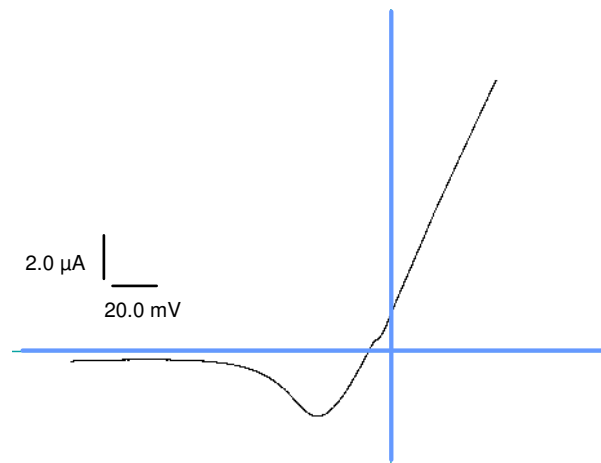
**NR1-1a-TG4L2-NR1-1a + NR2A in Mg<sup>2+</sup>-Ringer**

Fig. 35 : I/V for NR1-1a-TG4L2-NR1-1a + NR2A in MgR with 100  $\mu$ M glutamate and 10  $\mu$ M glycine. NR1-1a-TG4L2-NR1-1a + NR2A, however, showed voltage-dependent block by Mg<sup>2+</sup>.

Importantly, together with the data from the not Mg<sup>2+</sup> blockable dimer NR1-1a(N598R)-TG4L2-NR2A (cf. Fig. 29), this proves that both, head and tail, subunits of a dimer get incorporated in the concatemeric channel.

Thus, TG4L2 is a suitable linker for the construction of covalently linked dimers in the NMDAR subfamily (using dimeric NR1-1a + NR2A concatemers as an example).

As seen for the homodimers NR1-1a-TG4L2-NR1-1a and NR2A-TG4L2-NR2A (Fig. 33), NR1-1a-TG4L2-NR1-1a(N598R) could be boosted by the monomeric counterpart (NR2A) (see Fig. 38).

### 3.3.3 Combining NR1-1a-TG4L2-NR1-1a with NR2A-TG4L2-NR2A generates functional channels as well

#### Co-expression of NR1-1a-TG4L2-NR1-1a and NR2A-TG4L2-NR2A

	% NR1-1a + NR2A current (-70 mV)	SEM	n
NR1-1a-TG4L2-NR1-1a	0.1	0.4	6
NR1-1a-TG4L2-NR1-1a + NR2A (1:2)	59.8	8.3	8
NR2A-TG4L2-NR2A	0.0	0.0	6
NR2A-TG4L2-NR2A + NR1-1a (1:2)	21.7	5.1	6
NR1-1a-TG4L2-NR1-1a + NR2A-TG4L2-NR2A (1:1)	12.3	3.6	13

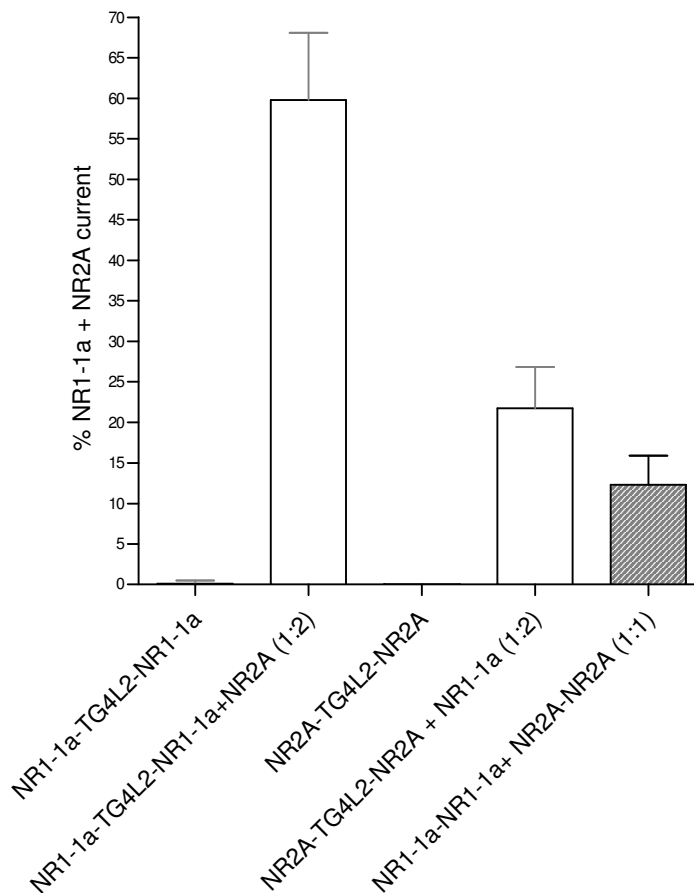


Fig. 36 : The combination of the two homodimers yielded currents ( $12.3 \pm 3.6$  % of wild type) comparable to those for the heterodimers NR1-1a-TG4L2-NR2A or NR1-1a(N598R)-TG4L2-NR2A where no monomeric subunits can contribute to the receptor either ( $12.1 \pm 3.7$  % and  $5.2 \pm 2.3$  % of wild type in Fig. 12 and Fig. 26). Agonists were 100  $\mu$ M glutamate and 10  $\mu$ M glycine in NFR.

NR1-1a-NR1-1a + NR2A-NR2A (1:1) : NR1-1a-TG4L2-NR1-1a + NR2A-TG4L2-NR2A (1:1).

The homodimers NR1-1a-TG4L2-NR1-1a and NR2A-TG4L2-NR2A - in addition to being expressed separately - were also co-injected in oocytes and functionally tested using two-electrode voltage clamping (Fig. 36). The combined dimers were functional as well with a clearly larger current amplitude ( $12.3 \pm 3.6$  % of wild type) than for NR1-1a-TG4L2-NR1-1a (or NR2A-TG4L2-NR2A) alone, but a distinctly smaller one than for NR1-1a-TG4L2-NR1-1a or NR2A-TG4L2-NR2A in complex with NR2A or NR1-1a, respectively (cf. Fig. 33). The functionality of the homodimer combination can be taken as proof that two different dimers can assemble in a functional channel (cf. 4.2.3). The smaller amplitude observed for the homodimer combination than for the individual dimers in co-expression with their monomeric counterparts again indicates that the presence of the linker in the concatemer decreases ion conductance (cf. 3.5).

### **3.4 Trafficking of NR1-1a + NR2A dimers**

#### **3.4.1 NR2A facilitates the assembly of NR1-1a-TG4L2-NR2A and NR1-1a-TG4L2-NR1-1a**

The functional analyses carried out earlier were extended to the question whether the addition of monomers to dimers would influence the current amplitude. In all experiments, molar ratios of dimer and monomer cRNAs were co-injected.

When monomers were co-expressed with the dimer NR1-1a-TG4L2-NR2A, NR2A produced apparently larger currents - but not NR1-1a : The currents for NR1-1a-TG4L2-NR2A co-expressed with NR2A ( $36.7 \pm 6.6$  % of NR1-1a + NR2A) were about three times larger than for the dimer by itself or upon co-expression with NR1-1a ( $12.1 \pm 3.7$  % or  $11.9 \pm 2.3$  % of wild type, respectively) (Fig. 37). Referring to 3.3.1, NR2A also caused larger currents with NR1-1a-TG4L2-NR1-1a (again, approximately three times larger) than NR1-1a did with NR2A-TG4L2-NR2A ( $59.8 \pm 8.3$  % compared to  $21.7 \pm 5.1$  %; Fig. 33). Both findings imply that NR2A - unlike NR1-1a - might be able to facilitate the assembly of NMDAR dimers.

### Trafficking of NR1-1a-TG4L2-NR2A

	% NR1-1a + NR2A current (- 70 mV)	SEM	n
NR1-1a-TG4L2-NR2A	12.1	3.7	9
NR1-1a-TG4L2-NR2A + NR2A (1:2)	36.7	6.6	6
NR1-1a-TG4L2-NR2A + NR1-1a (1:2)	11.9	2.3	6

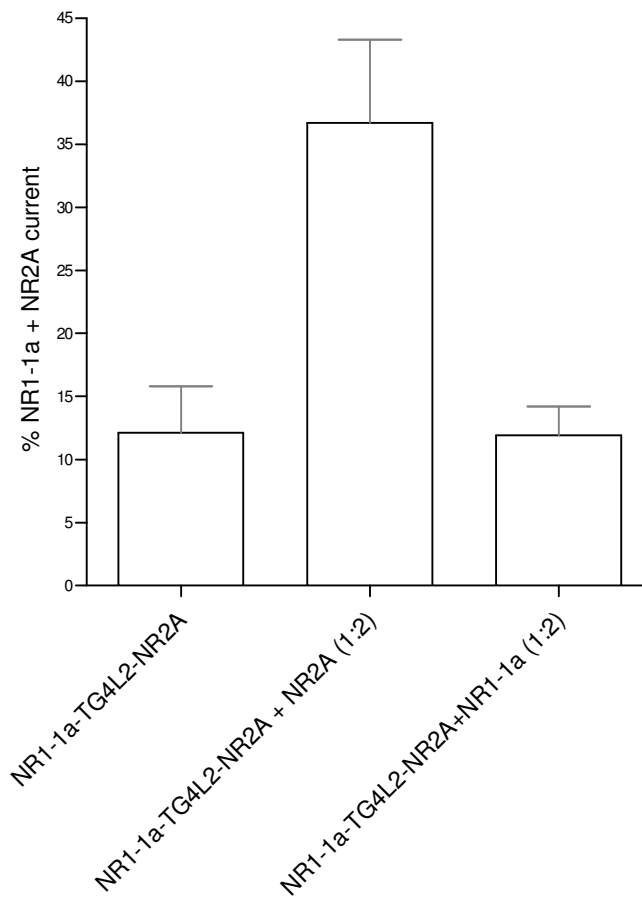


Fig. 37 : The clearly larger amplitude seen for NR1-1a-TG4L2-NR2A + NR2A than for NR1-1a-TG4L2-NR2A + NR1-1a or NR1-1a-TG4L2-NR2A alone might indicate that monomeric NR2A facilitates receptor assembly (as also seen in Fig. 33 for NR1-1a-TG4L2-NR1-1a + NR2A).

Agonists were 100  $\mu$ M glutamate and 10  $\mu$ M glycine in NFR.

In heterologous cells, the NR1 subunit is retained in the ER when expressed alone, but when expressed together with NR2, the assembled receptor can exit the ER and reach the cell surface (McIlhinney et al., 1996 and 1998).

In primary cerebellar granule cells, Prybylowski et al. (2002) saw that overexpression of either NR2A or NR2B, but not splice variants of NR1, by transfection caused an apparent increase in the total number of NMDA receptors expressed on the cell surface.

Based on these findings summarised in 1.3.3.2, one could speculate that a pool of NR1-1a-containing concatemers is retained in the ER which assembles with incoming NR2A monomers. These monomers would help mask the NR1 retention signal, leading to rapid ER export of the concatemeric NMDAR complex and its targeting to the oocyte membrane. The increased number of cell surface receptors would explain the observed increase in current amplitude as a consequence of NR2A overexpression.

### **3.4.2 NR1-1a(N598R)-TG4L2-NR2A cannot be boosted by NR2A**

When monomers were co-expressed with the dimer NR1-1a(N598R)-TG4L2-NR2A, NR2A was not able to boost the dimer current to such an extent as seen for dimers with wild type NR1-1a (3.4.1) : The current amplitudes for NR1-1a(N598R)-TG4L2-NR2A ( $5.2 \pm 2.3 \%$ ) and for NR1-1a(N598R)-TG4L2-NR2A in combined expression with NR2A ( $9.8 \pm 3.3 \%$ ) or NR1-1a ( $8.1 \pm 3.1 \%$ ) are not significantly different within the error limits (Fig. 38).

In agreement with this, the dimer NR1-1a-TG4L2-NR1-1a(N598R) was boosted by NR2A, but only to  $4.7 \pm 2.3 \%$  of wild type NR1-1a + NR2A current (Fig. 38). The homodimer NR1-1a-TG4L2-NR1-1a, however, was boosted by NR2A to  $59.8 \pm 8.3 \%$  of wild type current (Fig. 33). Replacement of the neutral asparagine with the positively charged arginine at the N site of NR1-1a usually causes an approximate 50 % reduction in ion conductance of the channel (3.2.2 and Sakurada et al., 1993). The drastically larger difference between the two dimers might be explained by the ability of NR2A to enhance the ER export and trafficking of NMDA receptors with wild type NR1-1a but not with NR1-1a mutated at the N site.

Thus, although reports about the role of the N site of NR1-1a in mediating NMDAR trafficking have not been published yet, the data of the current study presented in 3.4 might suggest a control of ER export exerted by arginine 598 in NR1-1a similar to arginine 586 in GluR2 (1.2.3).

### Retention of concatemers with mutated NR1-1a

	% NR1-1a + NR2A current (- 70 mV)	SEM	n
NR1-1a(N598R)-TG4L2-NR2A	5.2	2.3	16
NR1-1a(N598R)-TG4L2-NR2A + NR2A (1:2)	9.8	3.3	11
NR1-1a(N598R)-TG4L2-NR2A + NR1-1a (1:2)	8.1	3.1	7
NR1-1a-TG4L2-NR1-1a(N598R) + NR2A (1:2)	4.7	2.3	9
NR1-1a-TG4L2-NR1-1a(N598R)	0.0	0.3	3

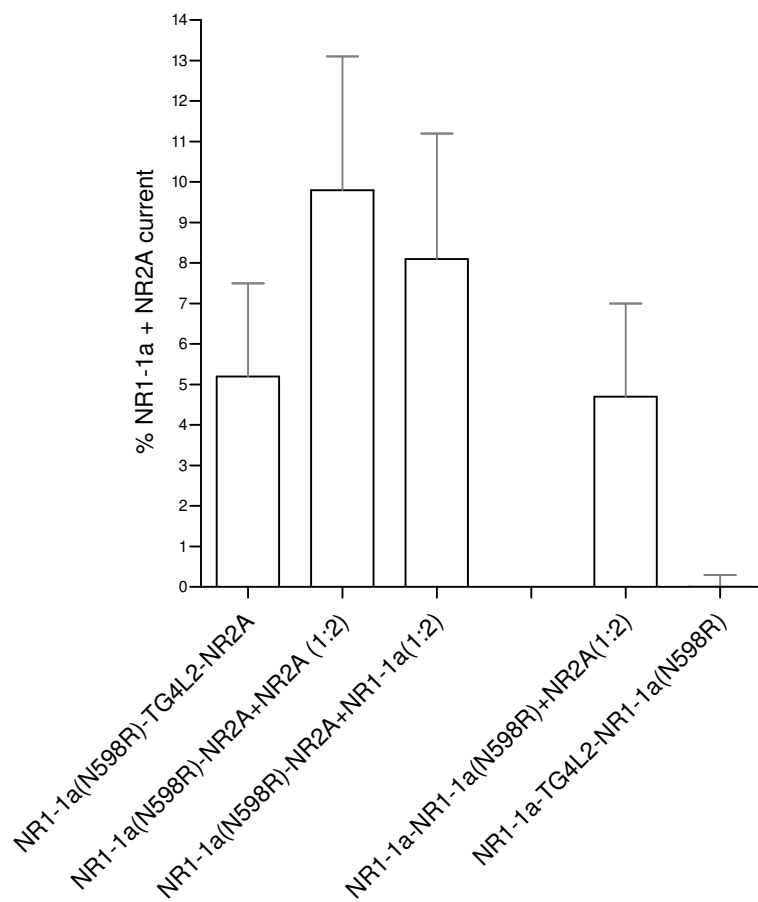


Fig. 38 : The assembly of hetero- and homodimeric NR1-1a(N598R)-containing concatemers does not seem to be boosted by single NR2A to a similar extent as the concatemers containing wild type NR1-1a (NR1-1a-TG4L2-NR2A and NR1-1a-TG4L2-NR1-1a) which are shown in Fig. 37 and Fig. 33.

Agonists were 100  $\mu$ M glutamate and 10  $\mu$ M glycine in NFR.

NR1-1a(N598R)-NR2A + NR2A (1:2) : NR1-1a(N598R)-TG4L2-NR2A + NR2A (1:2);

NR1-1a(N598R)-NR2A + NR1-1a (1:2) : NR1-1a(N598R)-TG4L2-NR2A + NR1-1a (1:2);

NR1-1a-NR1-1a(N598R) + NR2A (1:2) : NR1-1a-TG4L2-NR1-1a(N598R) + NR2A (1:2)

### 3.5 Effects of the linkage on dimer function

#### Influence of the linker on dimer currents

	% NR1-1a + NR2A current (-70 mV)	SEM	n
sNR1-1a(N598R) + NR2A (1:1)	45.7	7.0	15
NR1-1a-TG4L2-NR2A	12.1	3.7	9
NR1-1a(N598R)-TG4L2-NR2A	5.2	2.3	16
NR1-1a-TG4L2-NR1-1a + NR2A-TG4L2-NR2A (1:1)	12.3	3.6	13
NR2A-TG4L2-NR2A + NR1-1a (1:2)	21.7	5.1	6

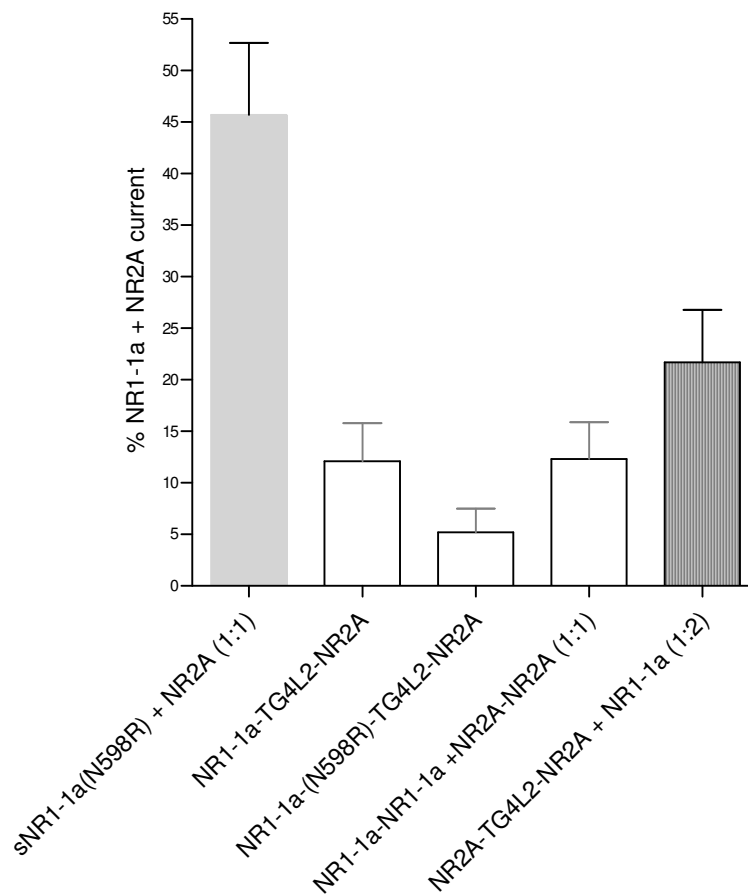


Fig. 39 : Comparison of different constructs suggests that the presence of one or two linkers (TG4L2) in the tetrameric receptor is responsible for a reduction in current amplitude compared to monomeric co-expressions (e.g. NR1-1a + NR2A).

Agonists were 100  $\mu$ M glutamate and 10  $\mu$ M glycine in NFR.

NR1-1a-NR1-1a + NR2A-NR2A (1:1) : NR1-1a-TG4L2-NR1-1a + NR2A-TG4L2-NR2A (1:1)

All dimers were characterised by a substantial reduction in current amplitude (70-95 % smaller than wild type). This was presumably caused by the covalent linkage of the two subunits. Comparison of different constructs supports this (Fig. 39) :

1) Single dimers (NR1-1a-TG4L2-NR2A and NR1-1a(N598R)-TG4L2-NR2A) - with two linker domains present in the final tetrameric receptor - evoked smaller currents than "linker-free" monomers (NR1-1a + NR2A and NR1-1a(N598R) + NR2A).

2) Co-expression of NR2A-TG4L2-NR2A with monomeric NR1-1a ( $21.7 \pm 5.1$  % of wild type) - with one linker present in the resulting tetrameric receptor - yielded larger currents than the co-expression of NR2A-TG4L2-NR2A and NR1-1a-TG4L2-NR1-1a ( $12.3 \pm 3.6$  % of wild type). Additionally, the current amplitude of the latter co-expression is equivalent to the one of the single dimer NR1-1a-TG4L2-NR2A alone ( $12.1 \pm 3.7$  % of wild type). In both cases, two linkers get incorporated in the resulting tetrameric receptor.

### 3.5.1 Glutamate affinity for NR1-1a-TG4L2-NR2A

Based on the assumption that the linker in the concatemer is responsible for the reduction in dimer currents, it was necessary to find out more precisely about the consequences of the linkage for dimer function : To examine whether the linker led to steric constraints in the receptor molecule which caused a reduced agonist affinity, dose-response curves were recorded for NR1-1a-TG4L2-NR2A and wild type at varying glutamate concentrations and a constant glycine concentration of 10  $\mu$ M. Both curves were almost identical (within the error limits; Fig. 40) : The  $EC_{50}$  values (efficient concentration at half maximal response) were calculated to be 4.8  $\mu$ M for NR1-1a-TG4L2-NR2A (from 4 different oocytes) and 5.0  $\mu$ M for wild type NR1-1a + NR2A (from 3 oocytes). The  $EC_{50}$  value measured for wild type confirms data from the literature, with 1.7  $\mu$ M measured by Kutsuwada et al. (1992) and  $4.4 \pm 0.2$   $\mu$ M by Hatton and Paoletti (2005). These results indicate that the affinity for the agonist and thus the structure of the glutamate binding site are not altered in the dimer.

### EC<sub>50</sub> curves of glutamate

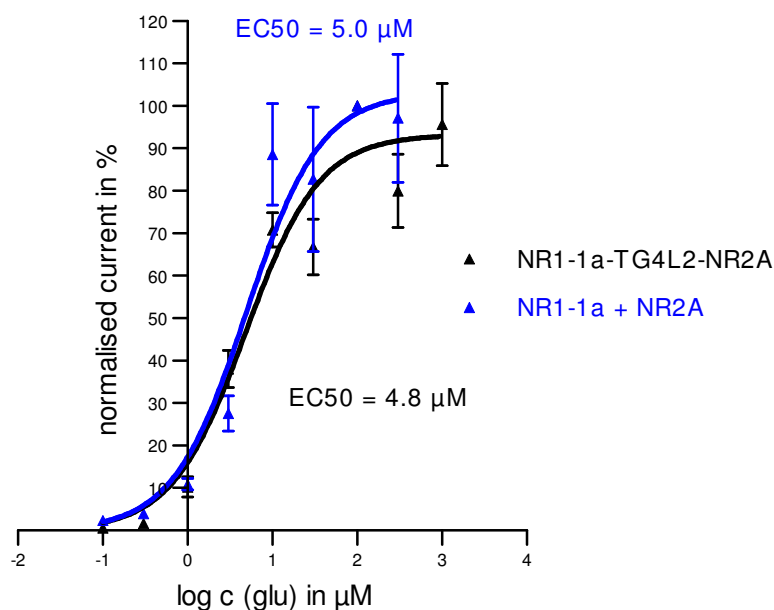


Fig. 40 : Dose-response curves of glutamate (at a constant glycine concentration of 10 μM) for NR1-1a-TG4L2-NR2A and wild type NR1-1a + NR2A. Steady-state currents were recorded at the indicated glutamate concentrations in NFR at -70 mV holding potential.

The responses to the application of 100 μM glutamate are expressed as 100 %.

Each curve was calculated from 4 (NR1-1a-TG4L2-NR2A) and 3 (NR1-1a + NR2A) different oocytes, respectively, using the programme GraphPad Prism, version 4.03 (GraphPad Software).

The high SEM values at high glutamate concentrations are possibly caused by large leakage currents at the end of the recording of the EC<sub>50</sub> curves.

NR1-1a-TG4L2-NR2A has an EC<sub>50</sub> value for glutamate identical to wild type.

### 3.5.2 Glycine affinity for NR1-1a-TG4L2-NR2A

To further investigate a possibly altered agonist affinity of the dimer, dose-response patterns for the co-agonist glycine were measured equivalently to the curves for glutamate in 3.5.1 : Currents were recorded for NR1-1a-TG4L2-NR2A and wild type at varying glycine concentrations and a constant glutamate concentration of 100 μM (Fig. 41). Again, both curves yielded almost identical EC<sub>50</sub> values which were estimated to be 1.9 μM for NR1-1a-TG4L2-NR2A (from 5 different oocytes) and 1.1 μM for wild type (from 4 oocytes). These data agree well with published data by Kutsuwada et al. (1992) who had determined the EC<sub>50</sub> value of wild type to be 2.1 μM glycine.

### EC<sub>50</sub> curves of glycine

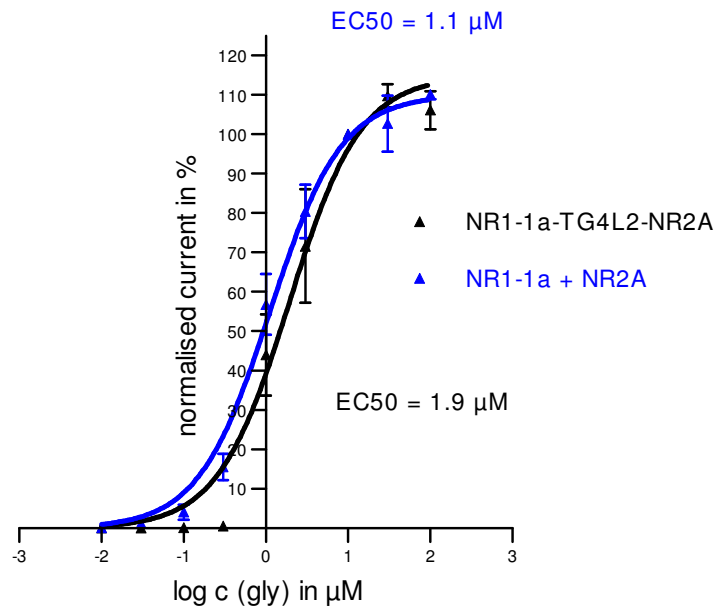


Fig. 41 : Dose-response curves of glycine (at a constant glutamate concentration of 100 μM) for NR1-1a-TG4L2-NR2A and wild type (NR1-1a + NR2A). Steady-state currents were recorded at the indicated glycine concentrations in NFR at -70 mV.

The responses to the application of 10 μM glycine are taken as 100 %.

Each curve was calculated from 5 (NR1-1a-TG4L2-NR2A) and 4 (NR1-1a + NR2A) different oocytes, respectively, using the programme GraphPad Prism (cf. Fig. 40).

The EC<sub>50</sub> value for glycine of NR1-1a-TG4L2-NR2A is also identical to wild type.

To conclude, despite the insertion of a long additional transmembrane domain between two full-length NMDAR subunits, the ligand binding sites for glutamate as well as glycine are unhampered in the dimer. Other factors influenced by the covalent linkage of the two receptor subunits must be the reason for the significant reduction in current amplitudes of dimers in comparison with the wild type receptor. These will be discussed in 4.1.3.2, 4.2.1 and 4.2.2.

## 4 Discussion

### 4.1 Interpretation of existing data

The two main conclusions from this work are (1) that a modified version of the 4<sup>th</sup> transmembrane domain of the  $\alpha_1$ -subunit of the bovine GABA<sub>A</sub> receptor allows to functionally link two full-length NMDAR subunits, thereby preserving the major electrophysiological qualities of a wild type NMDA receptor, and (2) that a specific subunit order within the dimers is presumably not required for the functionality of the resulting tetramer. One possible subunit order within the tetrameric receptor is a pairwise arrangement of two NR1 and two NR2 subunits.

In the past, concatemers have been used to study the stoichiometry of several types of ion channels, e.g. K<sup>+</sup> channels, P2X receptors, the nicotinic acetylcholine receptor, and NMDA receptors (1.4.1). For NMDA receptors, two reports exist - one meeting abstract (Prybylowski et al., Soc. Neurosci. Abstr., 1999), which remained unpublished as a full-length publication, and one original paper (Schorge and Colquhoun, 2003). In the following, the data obtained in the present study will be discussed by comparing them to the results of these two previous studies.

#### 4.1.1 Comparison to concatemer studies in general

Currents were seen for all NR1-1a + NR2A concatemers analysed in this thesis when superfused with agonists in *Xenopus* oocytes. However, concatemers had been found susceptible to cleavage, and subunits to behave independently in previous investigations (1.4.1). In this context, three intrinsic properties of the oocyte expression system had to be taken into account for NMDA receptors : On the one hand, the heterologous oocyte system offers the advantage that wild type as well as mutated or engineered receptors of interest can be expressed and studied in a single cell without being superimposed by "contaminating" native receptors. On the other hand, two complications for NMDA receptors exist only in oocytes compared to, e.g. fibroblasts as an expression system : Firstly, a high concentration of intracellular Ca<sup>2+</sup> ions is known to induce a fast Ca<sup>2+</sup>-activated Cl<sup>-</sup> conductance. These Cl<sup>-</sup> channel currents are superimposed onto the currents evoked by Na<sup>+</sup>, K<sup>+</sup> and Ca<sup>2+</sup> fluxes of NMDAR channels. Secondly, NR1 by itself appears to homodimerise to form functional receptors, which can produce small current responses. Thus, before starting the functional analysis of NMDAR dimers, it was essential to verify

that the currents investigated truly originated (1) from NMDA receptors, and not mainly from  $\text{Ca}^{2+}$ -activated  $\text{Cl}^-$  responses, and (2) from full-length NR1-1a + NR2A dimers, and not from the NR1-1a part of the dimer alone which might have been generated by disruption of the concatemer.

The following four experimental findings support this notion of intact, functional dimers :

(1) NR1-1a + NR2A dimers (in contrast to  $\text{Ca}^{2+}$ -impermeable NR1-1a(N598R) + NR2A dimers) very often elicited an inward current peak at the beginning of the agonist application, prior to the steady-state inward current typical of NMDA receptors. This peak most likely arose from  $\text{Ca}^{2+}$ -activated  $\text{Cl}^-$  channels, which activate when  $\text{Ca}^{2+}$  enters the oocyte through the opening of the NMDAR concatemer. The  $\text{Cl}^-$  channel contamination disappeared with pre-injection of 50 nL of 200 mM EGTA in the oocyte prior to the measurement. This injection achieves an intracellular concentration of ~ 10 mM EGTA (given the volume of an oocyte estimated to be ~ 1  $\mu\text{L}$ ), which ensures chelation of any incoming  $\text{Ca}^{2+}$  before endogenous  $\text{Cl}^-$  channels can open (M. Hollmann, personal communication). Thus, the steady-state current must have originated from the engineered NR1-1a + NR2A dimers.

(2) The current amplitudes for the heterodimers NR1-1a-TG4L2-NR2A and NR1-1a(N598R)-TG4L2-NR2A in a sufficient number of oocytes were clearly larger (about 5 to 10 times) than those for monomeric NR1-1a [or NR1-1a(N598R)]. This can only be the case if both head and tail subunits of the dimers are functionally incorporated.

(3) The dimers had rectifying properties typical of those known for NMDA receptors : NMDA receptors possess an N site, which is the equivalent of the Q/R editing site in AMPA and kainate receptors. A neutral glutamine (Q) at this site leads to block by cytoplasmic spermine and thus to inward rectification at positive membrane potentials, since the positively charged polyamines plug the ion channel pore from the inside. This prevents outflow of intracellular  $\text{K}^+$  that would occur at membrane potentials above 0 mV (Donevan and Rogawski, 1995; Williams, 1997).

The smaller asparagine (N) or a positively charged arginine (R) compared to the glutamine (Q) at this site both abolish inward rectification (Williams, 1997; 1.2.3; McBain and Mayer, 1994). Thus, for wild type (i.e. "N"-type) NMDA receptors (as for all "R"-type glutamate receptors), the I/V relationship is linear above 0 mV (Araneda et al., 1999; Hollmann and Heinemann, 1994).

In agreement with this, all I/V curves analysed were linear over the entire voltage range in  $Mg^{2+}$  free normal frog Ringer (data not shown). In the presence of 1.8 mM  $Mg^{2+}$ , all currents increased linearly at positive membrane potentials.

It is known that presence of an R at the N site in NR1-1a (among other things) abolishes  $Mg^{2+}$  block of NMDA receptors (1.2.3). The amino acid exchange N598R in NR1-1a could therefore be used as a dominant marker mutation : In  $Mg^{2+}$ -Ringer, all I/V curves of concatemers with wild type NR1-1a showed rectification with no significant ion flow below -20 mV. If NR1-1a featured the mutated amino acid at position 598 in the pore, all I/V curves were linear in  $Mg^{2+}$ -Ringer.

Hence, I/V curves electrophysiologically proved the integration of the head and, importantly, also the tail subunits of the concatemer into the receptor complex.

(4) Complementing I/V curve analysis, use of the drug ifenprodil allowed to distinguish between an NR1-NR2A-containing receptor and NR1 alone : NR1-1a-TG4L2-NR2A was insensitive to ifenprodil, while NR1-1a would have been distinctly blocked (3.2.1.2.1).

Thus, a premature stop of translation or a proteolytic cleavage of the full-length concatemer did not seem to occur for the dimers studied in this thesis, at least not to such an extent as seen for P2X receptors or the acetylcholine receptor (Nicke et al., 2003; Groot-Kormelink et al., 2004) (cf. 1.4.1).

#### **4.1.2 Comparison to Prybylowski et al.**

Prybylowski et al. (Soc. Neurosci. Abstr., 1999) generated two NMDAR "tandems" and tested them in HEK cells : NR1-TMD4-NR2A and NR2A-TMD4-NR1. Both tandems were not functional alone, but required the co-expression of monomers (NR2A and NR1, respectively) to produce functional channels. Initially, the authors interpreted the requirement for monomers as an indication for a pentameric structure of NMDA receptors. By Western blotting, they later found out that the requirement for monomers was caused by a disruption of their tandems in the linker region, i.e. by the fact that their tandems lacked their tail subunits. Prybylowski et al. used the same transmembrane domain as the intersubunit linker domain as was used in the current study (Fig. 6), but a short linker (termed TMD4) that contained just a single amino acid neighbouring the transmembrane domain (K. Prybylowski, personal communication).

In contrast to their results, the dimer NR1-1a-TG4L2-NR2A and all other dimeric constructs analysed in this thesis were shown to be functional with contributions of both of

the linked subunits in *Xenopus* oocytes. Thus, the problem of breakdown of the concatemers in the linker region, which was encountered by Prybylowski et al., could apparently be solved by the insertion of additional hydrophilic amino acids flanking the transmembrane linker ("TG4L2"). However, occurrence of degradation cannot be excluded using solely electrophysiological tests of receptor function (cf. 4.2.1 and 4.2.2).

### 4.1.3 Comparison to Schorge and Colquhoun

Schorge and Colquhoun (2003) generated four NMDAR "tandems" and tested them in HEK cells : the heterodimers NR1-1a(truncated)-NR2A and NR2A(truncated)-NR1-1a, and the homodimers NR1-1a(truncated)-NR1-1a and NR2A(truncated)-NR2A. None of their tandems was functional alone under conditions sufficient to activate control full-length receptors. Only with high agonist concentrations (1 mM glutamate and 1 mM glycine), NR2A(truncated)-NR1-1a produced currents, which, however, were unstable and rapidly ran down in amplitude after repeated stimulation with agonists. This was interpreted as an indication that subunits within the tetrameric complex behave independently, a common problem of concatemers (4.1.1).

The most striking difference between the results presented here and the results by Schorge and Colquhoun is therefore that NR1-1a-TG4L2-NR2A is functional. Their dimer NR1-1a(truncated)-NR2A failed to generate currents at all, probably due to the fact that it contained a C-terminally truncated head subunit. The functionality of NR1-1a-TG4L2-NR2A therefore sheds a new light on the conclusions that Schorge and Colquhoun drew from their work.

#### 4.1.3.1 Qualitative behaviour

After verifying the dimer currents electrophysiologically (4.1.1), the *Xenopus* oocyte expression system was used to functionally characterise the dimers.

Since no co-expression of monomers - as it is the case for individual homodimers - was required, the individual heterodimer NR1-1a-TG4L2-NR2A and its electrophysiologically "tagged" variant NR1-1a(N598R)-TG4L2-NR2A were chosen for characterisation. Additionally, the heterodimer NR1-1a-TG4L2-NR2A was of particular interest for functional analysis since it reflects the functional unit in NR1-NR2A receptors found by Furukawa et al. (2005).

To characterise the homodimer combination NR1-1a-TG4L2-NR1-1a + NR2A-TG4L2-NR2A and to compare it to the data of Schorge and Colquhoun would have also been useful and should be pursued in the future.

Five different key properties of native NMDA receptors were tested including (a) voltage-dependent block by external  $Mg^{2+}$ , (b)  $Ca^{2+}$  permeability, (c) block by the competitive antagonist APV, (d) block by MK-801 and its partial reversibility, and (e) differential sensitivity to ifenprodil, which depends on the type of NR2 subunit present. As controls, results were always compared to heteromeric co-expressions of wild type NR1-1a + NR2A or NR1-1a(N598R) + NR2A and to monomers [NR1-1a or NR1-1a(N598R)].

These five different tests concerned different sites within the channel molecule :

$Mg^{2+}$ ,  $Ca^{2+}$  and MK-801 all interact with a site at the narrowest part of the channel pore. An altered behaviour towards  $Ca^{2+}$  and the open channel blockers  $Mg^{2+}$  and MK-801 would thus have indicated corresponding changes in ion pore structure of the dimer.

Differences in APV block would have pointed to an altered sensitivity of the S1 and S2 domains in the NR2A subunits of the dimer to glutamate. Ifenprodil can serve as an indicator for the sensitivity of the receptor N termini to protons. Use of five different tests should assure reliability of results.

Common experimental problems required repetition of some experiments : A transcript was not expressing, although radio-labelled RNA could be detected after transcription and purification. The size of the transcript was as expected when analysed in an agarose gel. An explanation for the lack of expression was probably an unnoticed contamination with RNases at some point after finishing the *in vitro* transcription. Secondly, capping of the transcript could have been insufficient.

Additionally, the quality of the oocyte batches varied depending on the frog. This concerned the survival rate of oocytes and thus the number of oocytes on hand for electrophysiological analysis as well as the expression level of transcripts.

Furthermore, control results were contradictory to established data, i.e. on one day co-expression of NR1-1a(N598R) + NR2A generated larger currents than co-expression of NR1-1a + NR2A. Since technical problems could be excluded, this might be explained by the fact that the expression level and / or quality of individual transcripts in the particular oocyte batch inevitably varied (and that this could not be anticipated from agarose gel analysis of the cRNAs following the transcription reaction as described above).

For reliable conclusions, normally each clone should be tested at least three times in three independent oocyte batches. Time limitations and limitations in the availability of oocytes and frogs meant that this was not possible for all measurements.

Data for the monomeric control NR1-1a(N598R) are not interpretable because the current amplitudes were equal to or lower than (0.1 - 0.4 % of wild type corresponding to 1.5 - 5 nA as absolute response) compared to those of uninjected oocytes ( $0.4 \pm 0.7$  % of wild type corresponding to 2 - 3.5 nA ) for the number of oocytes tested (3.2.2 and 3.2.1.1). For the reason of consistency, these experiments should be repeated in an oocyte batch with a higher expression level for NR1-1a(N598R) in the future.

However, all other data are interpretable :

In all except one case, currents observed for both heterodimers were - qualitatively - identical to those of wild type heteromeric co-expressions (NR1-1a + NR2A and NR1-1a(N598R) + NR2A, respectively) for all five functional parameters tested. Wild type receptor data and currents for monomeric NR1-1a were in turn consistent with data from the literature. Only the block of NR1-1a by 100  $\mu$ M APV represents an exception : NR1-1a has commonly been thought to be significantly blocked by APV, identical to heteromeric receptors (3.2.1.2.1). Such a block was also observed for 4 oocytes in the present study. Strikingly, Green et al. (2002) did not observe a significant inhibitory effect of APV on NR1 alone. Their novel finding would mean that because NR1 alone obviously does not have a glutamate or APV binding site (which resides on the NR2 subunit of heteromeric receptors), a different glutamate binding site must be present in NR1, and for this other site APV obviously does not compete. This explanation would assume a uniformly homomeric NR1 receptor functional in *Xenopus* oocytes. However, if NR1 was indeed inhibited as it was the case in the present study, this would vote for the presence of an endogenous NR2-like subunit in *Xenopus* which assembles with injected NR1, providing a "common" glutamate binding site. It is still a matter of debate whether NR1 is able to form channels as a homomer or binds to a second subunit endogenous to *Xenopus laevis*, which might be similar to rat NR2 (Ishimaru et al., 1996; Green et al., 2002). Future experiments need to clarify the contradictions of these APV block experiments. In this context, the reason for the difference in sensitivity to MK-801 between NR1 and NR1-NR2 receptors is still unclear, too (3.2.1.2.1).

The N598R mutation introduced into NR1-1a changed the conductance and pharmacological properties of the respective receptors in a dominant manner, again in agreement with previous reports. For NR1-1a(N598R), the low current amplitude was not interpretable (see above), but NR1-1a(N598R) would have been expected to not be blocked by  $Mg^{2+}$  and MK-801, be  $Ca^{2+}$  impermeable (unlike NR1-1a), and be blockable by APV (i.e. to behave like the heteromeric mutant receptor as NR1-1a behaves like NR1-1a + NR2A in these cases). Reports studying NR1-1a(N598R) as homomer do not exist yet.

To summarise, NR1-1a-TG4L2-NR2A was blocked by 1.8 mM  $Mg^{2+}$  at oocyte membrane potentials below - 20 mV, while  $Mg^{2+}$  block was undetectable in NR1-1a (N598R)-TG4L2-NR2A.

$Ca^{2+}$  permeability was high for NR1-1a-TG4L2-NR2A, but not measurable for NR1-1a(N598R)-TG4L2-NR2A.

Both heterodimers were blocked by APV, suggesting that glutamate binding was not impaired by the covalent linker in the concatemers.

NR1-1a-TG4L2-NR2A, in contrast to the NR1-1a + NR2B control, was insensitive to ifenprodil.

In addition, it would have been interesting to test low concentrations of  $Zn^{2+}$  on NR1-1a-TG4L2-NR2A. Although many antagonists act on heteromeric NMDA receptors like on monomeric NR1-1a (3.2.1.1.2),  $Zn^{2+}$  allows to differentiate between both : Whereas 1  $\mu M$   $Zn^{2+}$  potentiated NR1-1a, it inhibited heteromeric (e.g. NR1-1a/NR2A) receptors and would have been expected to do so also for NR1-1a-TG4L2-NR2A (Hollmann et al., 1993). This would allow to confirm the ifenprodil studies.

In addition to the functional characterisation of heterodimers, homodimers were initially tested : NR1-1a-TG4L2-NR1-1a showed small currents in oocytes (yet in the range of background current) like monomeric NR1-1a that were strongly enhanced by NR2A. The same was observed for NR1-1a-TG4L2-NR1-1a(N598R). Both dimers differed in their  $Mg^{2+}$  block properties : NR1-1a-TG4L2-NR1-1a, but not NR1-1a-TG4L2-NR1-1a(N598R), was blocked by 1.8 mM  $Mg^{2+}$  at a holding potential below - 20 mV in all I/V curves.

Also, it would have been interesting to investigate whether NR1-1a-TG4L2-NR1-1a showed the same behaviour as monomeric NR1-1a in terms of block by  $Mg^{2+}$ , sensitivity to APV, MK-801 and ifenprodil, and permeability of  $Ca^{2+}$ .

Like NR2A, NR2A-TG4L2-NR2A was non-functional in oocytes, but was boosted with NR1-1a.

Therefore, the five dimers (two heterodimers and three homodimers) did not seem to exhibit remarkable functional and thus structural changes in comparison to the wild type NMDA receptor.

Only in one case, when NR1-1a-TG4L2-NR2A was treated with MK-801, the dimer currents differed from wild type behaviour : The blocker did not get trapped tightly within the channel pore and could be easily washed out (3.2.1.2.1). This was the only observation from the qualitative tests indicating that structural alterations in the concatemer might have occurred, apparently at the site in the ion pore where MK801 binds to the concatemer.

By comparison, Schorge and Colquhoun used three paradigms to examine the homodimer combination NR1-1a(truncated)-NR1-1a plus NR2A(truncated)-NR2A (only this tandem mixture produced sustained currents).

The tandem combination behaved, qualitatively, like control channels as well, in the sense that currents were blocked by 1 mM  $Mg^{2+}$ , 100  $\mu$ M APV, and 100  $\mu$ M kynurenic acid (a competitive antagonist for the glycine binding site on the NMDAR complex; Birch et al., 1988; Kemp et al., 1988) (data not shown in the publication).

#### **4.1.3.2 Quantitative behaviour**

Despite their qualitative wild type-like behaviour, the currents resulting from all of the dimers analysed here differed quantitatively from those resulting from control (NR1-1a + NR2A) : Dimer currents were substantially smaller (70 - 95 % smaller) than those seen after monomeric co-injections. This reduction could be explained by the presence of the linker in the receptor complex (3.5). One might think of at least two main disadvantages of the insertion of a transmembrane linker, which could affect the ability of the concatemeric receptor to permit ions and which will be discussed below. These are 1) steric constraints owing to the covalent linkage, and 2) a reduced expression level owing to the large size of the concatemeric protein.

More precisely, steric constraints due to the covalent linkage could be the reason for a (a) reduced agonist affinity, or (b) reduced single-channel conductivity. The single-channel

conductivity itself is made up by three receptor qualities. These are single-channel conductance, open time and open probability.

As  $EC_{50}$  values for glutamate and glycine for NR1-1a-TG4L2-NR2A were virtually identical to those for the co-expression of single wild type subunits, the covalent linkage of the two subunits apparently does not influence the structure of the S1 and S2 domains in the dimer. Consistently, inhibition by APV was not reduced for the dimer. It would have been useful to investigate inhibition by kynurenic acid to gain additional information about the glycine binding site in NR1-1a-TG4L2-NR2A.

Thus, a reduced agonist affinity cannot explain the observed reduction in current amplitude of the dimer.

This is again contrary to the data from Schorge and Colquhoun : For the co-expression of NR1-1a(truncated)-NR1-1a with NR2A(truncated)-NR2A,  $EC_{50}$  values of glutamate and glycine were radically different from controls. The  $EC_{50}$  value of glutamate was decreased to  $< 10$  nM, and the one of glycine increased to  $153 \pm 16$   $\mu$ M, compared to  $2.05 \pm 0.60$   $\mu$ M for controls. This was presumably caused by a disruption of the ligand binding sites for glutamate and glycine owing to the truncation of the head subunit in their tandems. However, this damage was evidently not severe enough to prevent binding and inhibition by APV and by kynurenic acid in the qualitative tests. The truncation of the head subunit most likely was also responsible for a near-complete abolishment of desensitisation in their tandem constructs.

Obviously, truncation of the head subunit led to functional impairments.

However, two wild type (i.e. full-length) NMDAR subunits could be linked to each other without apparent functional impairment, using the concatemer approach chosen for the present work.

To conclude, the results shown here indicate that this strategy allows the construction of concatemers which produce receptors with more wild type-like qualities than the strategy followed by Schorge and Colquhoun.

#### 4.1.3.3 Subunit arrangement within the NR1-1a + NR2A dimer

In their attempt to determine stoichiometry and relative arrangement of NMDAR subunits, Schorge and Colquhoun made the following observations :

(A) NR1-1a(truncated)-NR2A was non-functional alone in HEK cells. (B) NR2A (truncated)-NR1-1a produced currents similar in amplitude to control currents. Tandem currents were, however, characterised by a high rundown rate. (C) NR1-1a(truncated)-NR2A produced currents in co-expression with NR2A(truncated)-NR1-1a. Current amplitudes were in the range of controls with a rundown rate between that of controls and NR2A(truncated)-NR1-1a alone. (D) NR1-1a(truncated)-NR1-1a was functional in co-expression with NR2A(truncated)-NR2A. Currents were sustained that were almost as large as the controls.

Briefly, their data were interpreted to be suggestive of a 1-1-2-2 arrangement of the subunits within the receptor, i.e. an organisation of the two types of subunits (two NR1 and two NR2) into two pairs : Only a dimeric pair of like subunits was able to give stable currents. Such dimeric pairs were formed from combining NR1-1a(truncated)-NR1-1a with NR2A(truncated)-NR2A (D) or NR1-1a(truncated)-NR2A with NR2A(truncated)-NR1-1a (C). The unstable currents elicited from NR2A(truncated)-NR1-1a (B) were explained by the fact that the dimer flipped or folded around in the membrane to force such an arrangement (Fig. 42). Additionally, the intermediate rundown rate observed for the co-expression of NR1-1a(truncated)-NR2A with NR2A(truncated)-NR1-1a (C) was explained by a "contamination" with these highly unstable currents coming from the tandem alone.

## Subunit arrangement in NMDAR tetramers by Schorge and Colquhoun

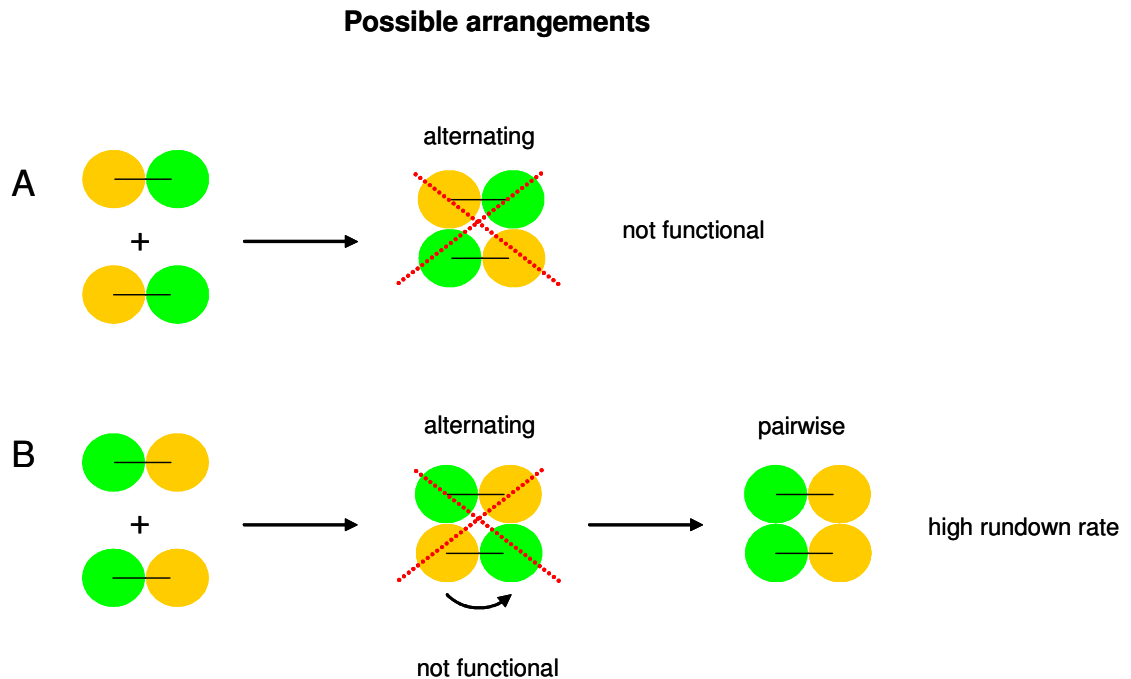


Fig. 42 : From their electrophysiological experiments, Schorge and Colquhoun (2003) deduced that NMDAR subunits need to arrange as a pair of two NR1 and two NR2 subunits to be functional.

The **NR1 subunit** is sketched as **orange** circle, the **NR2A subunit** as **green** circle. To facilitate understanding, symbols and colour code are the same in this and all following figures (except Fig. 43). Note that for reasons of simplicity, the distinguishing property of the tandems by Schorge and Colquhoun, i.e. the truncation of the tandem head subunit and the co-expression of the missing C tail, are not drawn in this figure.

A: Expression of **NR1-1a(truncated)-NR2A**, perhaps resulting in an alternating arrangement of two NR1 and two NR2 subunits as this tandem was not functional.

B: Expression of **NR2A(truncated)-NR1-1a**, with a probably alternating arrangement of two NR1 and two NR2 subunits; flipping around of one of the tandem molecules (indicated by the bent arrow) might produce a pairwise arrangement, as indicated by unstable currents. Why this "flipping around" was not seen for the tandem in A was not explained by Schorge and Colquhoun.

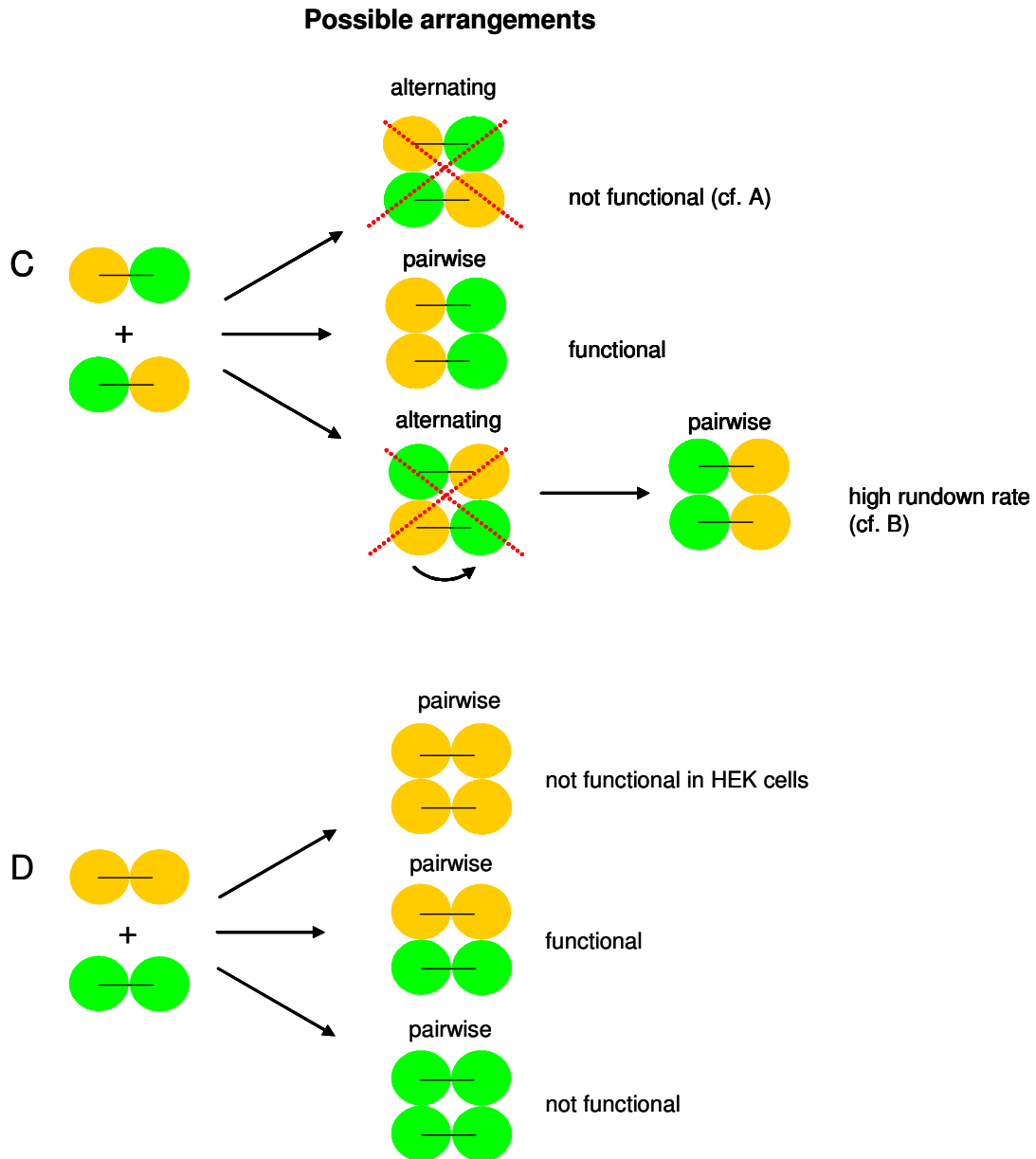


Fig. 42 continued :

C: Co-expression of **NR1-1a(truncated)-NR2A** and **NR2A(truncated)-NR1-1a**, which produces a mixture of three sorts of channels. The co-expression of both tandems likely resulted in a pairwise arrangement as it was functional (tetramer in the middle). Secondly, if **NR2A(truncated)-NR1-1a** was capable of flipping around, it might be able to generate a pairwise arrangement alone, but probably with unstable currents (cf. B). The third sort of channel would be the same as in A.

D: Co-expression of **NR1-1a(truncated)-NR1-1a** and **NR2A(truncated)-NR2A**, which also produces three sorts of channels. Only the combination of the two different tandem molecules (tetramer in the middle) can be responsible for the function seen in HEK cells. It reflects a pairwise arrangement of like NMDAR subunits.

For further explanations compare the text above.

The current amplitude of the tandems, which was not compromised in comparison to the steady-state current of controls (this is another difference to the current study), might be a further indication for independent behaviour of the tandem subunits of Schorge and Colquhoun.

The two-pair orientation was proposed to have dramatic effects on the mechanism of channel gating and binding.

Using the alternative concatemer approach described in the present study, two wild type GluR subunits have been covalently tied to each other, apparently without influencing functionality by imposing too much steric hindrance. As examples, two dimers were shown to have wild type-like qualities, and one dimer to have wild type-like agonist potencies. Consequently, our approach seems to offer a better way to determine the subunit stoichiometry of an NMDA receptor.

At the same time, the results gained from the experiments here raise doubts whether the results by Schorge and Colquhoun are reliable and whether their conclusions drawn are correct. The appearance of unstable currents for NR2A(truncated)-NR1-1a and also the complete loss of function for NR1-1a(truncated)-NR2A made by Schorge and Colquhoun is likely caused by functional impairments due to the truncation of the head subunit, and thus should not be used to make predictions about NMDAR stoichiometry.

Schorge and Colquhoun concluded from their experiments that there is a distinct subunit order within the dimer required for functionality. The electrophysiological analyses of the currently available constructs, however, point to the conclusion that the subunit order within the dimer may be irrelevant for the functionality of the tetrameric receptor, because all the dimers reported here produced currents independently of the type or order of the individual subunit in the dimer. NR1-1a-TG4L2-NR2A in itself reflects the heterodimeric substructure within a tetramer, which was suggested by Furukawa et al. (2005) (Fig. 43).

**Subunit arrangement in NMDAR dimers by Furukawa et al.**

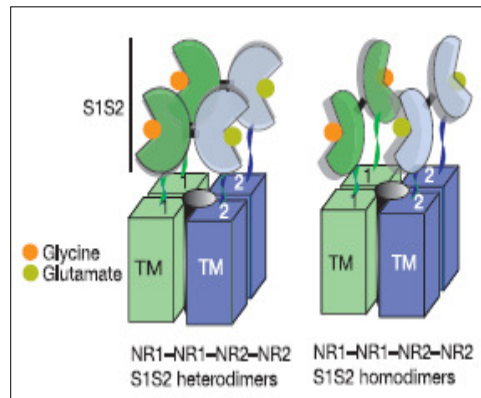


Fig. 43 : Subunit arrangement in NMDAR tetramers as deduced from crystallisation of the NR1 and NR2A ligand binding domains by Furukawa et al. (2005). S1S2 heterodimers were found to be the functional unit of the crystal. In the publication, S1S2 heterodimers (left image) as well as the obviously non-existing homodimers (right image) were drawn in an overall pairwise arrangement which refers to the findings by Schorge and Colquhoun (2003).

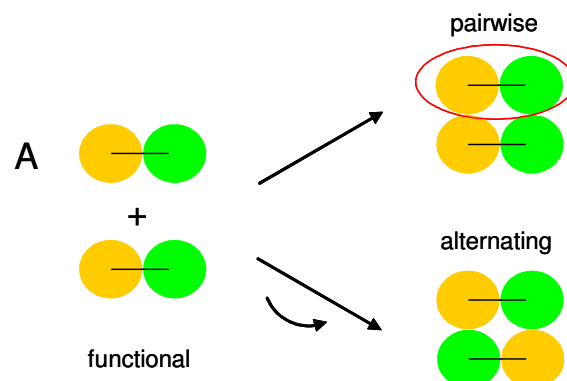
1: NR1 subunit; 2: NR2A subunit; S1S2: ligand binding domains; TM: transmembrane domains of each receptor subunit.

Figure reprinted by written permission from Macmillan Publishers Ltd : Nature, (c) 2005, "[www.nature.com](http://www.nature.com)".

Apparently, two molecules of the heterodimer NR1-1a-TG4L2-NR2A can arrange and combine such that a functional NMDA receptor can form (Fig. 44A). However, the exact arrangement of the four subunits of two NR1-1a-TG4L2-NR2A molecules in the tetrameric receptor is unknown.

**Possible subunit arrangement in NMDAR dimers based on the results of the present study**

**Possible arrangements**



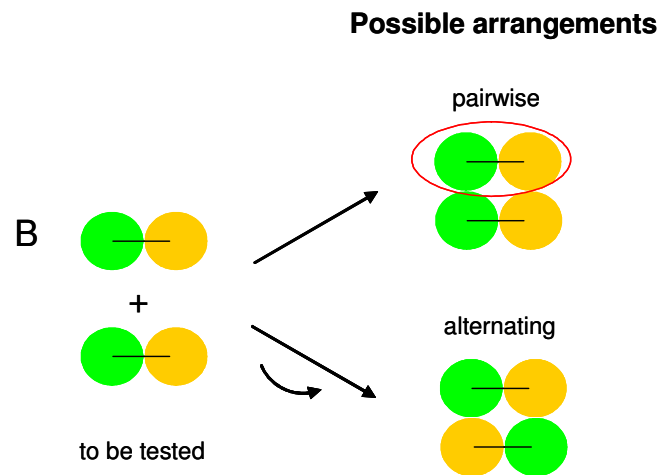


Fig. 44 : Model for the arrangement of NMDAR subunits based on the results of the present study, and according to Furukawa et al. (2005), implying a heterodimeric substructure within an overall pairwise arrangement in the tetrameric receptor. All dimers made in the present study were functional and allow such an arrangement to be formed (A and C).

**NR1-1a-TG4L2-NR1-1a** can only form a pairwise arrangement with **NR2A-TG4L2-NR2A** (C). The question remains whether this is the only possible subunit arrangement, i.e. whether also an alternating arrangement is functional. For this reason, the heterodimer **NR2A-TG4L2-NR1-1a** needs to be constructed and tested.

The **NR1 subunits** are drawn as **orange** circles, the **NR2A subunits** as **green** circles. The **red** ellipses designate the **heterodimeric substructure** within a pairwise arrangement of NR1 and NR2 subunits. This heterodimeric substructure is supported by X-ray crystallography (Furukawa et al., 2005).

A: Expression of **NR1-1a-TG4L2-NR2A**. The resulting subunit order is unknown, i.e., it could be pairwise (upper image) or alternating (lower image).

B: Expression of **NR2A-TG4L2-NR1-1a**. This dimer still needs to be tested, because construction of it has remained unsuccessful until now, for unknown reasons (4.1.3.3).

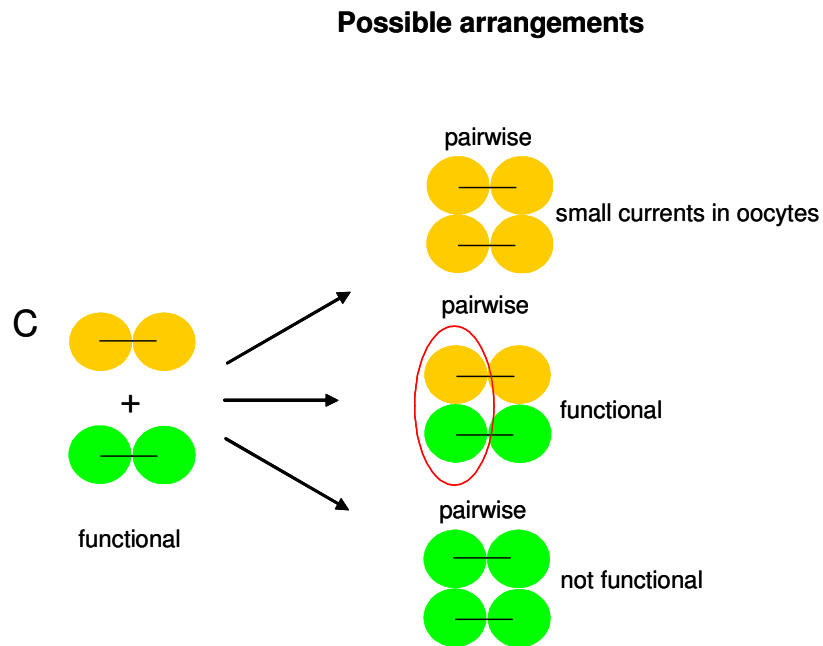


Fig. 44 continued :

C: Co-expression of **NR1-1a**-TG4L2-**NR1-1a** and **NR2A**-TG4L2-**NR2A**, which produces a mixture of three sorts of channels. The co-expression of both tandems can only produce a pairwise arrangement. The tetramer in the middle must be responsible for the function observed in *Xenopus laevis* voltage clamp experiments, as in control experiments **NR1-1a**-TG4L2-**NR1-1a** elicited only very small currents, and **NR2A**-TG4L2-**NR2A** was non-functional.

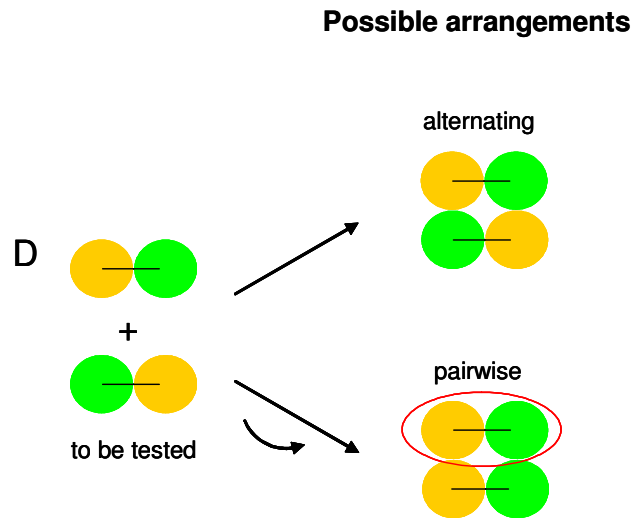


Fig. 44 continued :

D: Co-expression of **NR1-1a-TG4L2-NR2A** and **NR2A-TG4L2-NR1-1a**. Both heterodimers could combine in two different ways, arranging in an alternating or a pairwise fashion. For a pairwise order (lower image), one of the dimer molecules obviously needs to turn around.

This co-expression still needs to be tested since construction of NR2A-TG4L2-NR1-1a could not be completed during the current work, for unknown reasons (4.1.3.3).

Additionally, both heterodimers could form functional channels on their own (A and B). To overcome this problem, see 4.2.3.

For further explanations see the text below.

NR1-1a-TG4L2-NR1-1a combined with NR2A-TG4L2-NR2A elicited currents of the same amplitude as NR1-1a-TG4L2-NR2A. Contrary to the heterodimer, both homodimers can only form one kind of receptor : A tetramer with a pairwise arrangement of two NR1-1a and two NR2A subunits (Fig. 44C).

The preliminary results described here are therefore more consistent with a heterodimeric NR1-1a + NR2A substructure as proposed from the crystallisation studies by Furukawa et al. (2005) (Fig. 43), probably under preservation of a pairwise arrangement of two NR1-1a and two NR2A subunits. All three dimers generated in the present study would allow such an arrangement to be formed (Fig. 44A + C). The only question remains whether this is the only possible arrangement that can confer functionality to a tetrameric NMDA receptor (s. below).

Since the reverse heterodimer NR2A-TG4L2-NR1-1a [and also NR2A-TG4L2-NR1-1a(N598R)] is still missing, no final conclusion can be drawn from the measurements shown here regarding the subunit stoichiometry of an NMDA receptor. Despite multiple cloning experiments using different restriction enzymes, different insert-to-vector ratios and several bacterial strains, cloning of these dimers has failed so far. After transformation, agar plates either contained false colonies or were blank. Three cloning attempts carried out on the same day using the same solutions yielded the construct NR2A-TG4L2-NR2A, but not NR2A-TG4L2-NR1-1a or NR2A-TG4L2-NR1-1a(N598R). Cloning of these latter constructs has remained unsuccessful since then.

NR2A-TG4L2-NR1-1a and NR2A-TG4L2-NR1-1a(N598R) are expected to be functional alone (Fig. 44B) as were NR1-1a-TG4L2-NR2A and NR1-1a(N598R)-TG4L2-NR2A (Fig. 44A). If NR2A-TG4L2-NR1-1a and NR2A-TG4L2-NR1-1a(N598R) were functional and were able to give stable currents with their reverse counterpart [NR1-1a-TG4L2-NR2A or NR1-1a(N598R)-TG4L2-NR2A], this would confirm the suspected independence of subunit order within a dimer. Apparently, either NR2A-TG4L2-NR1-1a or NR1-1a-TG4L2-NR2A then would need to "fold around" to generate a pair of NR1-1a and a pair of NR2A subunits in co-expression with each other (Fig. 44D, lower complex). Alternatively, more than one arrangement of the four subunits, i.e. also an "alternating" pattern, could be functional (Fig. 44D, upper complex). In both cases, a heterodimeric substructure of one NR1-1a and one NR2A molecule would exist, as found by Furukawa et al. (2005) (Fig. 43).

The existence of different stoichiometries is, however, not known from other receptor types, where a precise stoichiometry is required for functionality (as, e.g., for the nicotinic acetylcholine receptor, the GABA<sub>A</sub> receptor, and the glycine receptor channels (Kandel et al., 2000)).

If NR2A-TG4L2-NR1-1a was not functional in combination with NR1-1a-TG4L2-NR2A, this would indicate that a subunit arrangement is not arbitrary, but somehow restricted within the dimer to generate an overall functional receptor complex. Only a certain dimer combination could then assemble to be functional. As determined by the NR1-1a-TG4L2-NR1-1a + NR2A-TG4L2-NR2A combination, this might be a pairwise arrangement of like subunits (Fig. 44C).

In any case, it is not known how NR1-1a-TG4L2-NR2A really "dimerises" (Fig. 44A) and how NR2A-TG4L2-NR1-1a might assemble with NR1-1a-TG4L2-NR2A (Fig. 44D). Therefore, dimers cannot be used to reliably determine a specific stoichiometry of NMDA

receptors, i.e. whether it is necessarily pairwise, or whether an alternating pattern is also possible.

Tetramers will be useful - if functional - to determine whether one (and only one) defined subunit order exists in NMDA receptors formed from NR1-1a and NR2A (cf. 4.2.4).

#### **4.1.3.4 Trafficking of NR1-1a + NR2A dimers**

A major advantage of the concatemer approach is that it allows to constrain the subunit ratio within the resulting receptor complex, and therefore permits a "more precise" overexpression of monomers in terms of stoichiometry.

Schorge and Colquhoun also expressed full-length monomers with individual tandems to test whether tetrameric receptors could form, which presumably would contain one tandem and two control subunits. Each of the tandems NR1-1a(truncated)-NR2A and NR2A(truncated)-NR1-1a was co-expressed with either full-length NR1-1a or NR2A. For none of the four combinations significant currents were observed, i.e. current amplitudes of tandems were not influenced by monomers. The explanation given by the authors was that 1:3 combinations of NR1-1a and NR2A subunits could not form or were not functional.

By contrast, when monomers were injected with dimers constructed during this thesis work, the overexpression of monomers had an effect on dimer currents. NR1-1a or NR2A were co-expressed with NR1-1a-TG4L2-NR2A and NR1-1a(N598R)-TG4L2-NR2A, and also with the homodimers NR1-1a-TG4L2-NR1-1a or NR2A-TG4L2-NR2A. This influence depended on the type of monomer subunit and also on the type of amino acid at the N site in NR1-1a. NR2A, but not NR1-1a, was able to markedly increase the current amplitude and thus facilitate receptor trafficking, as reported previously (1.3.3.2). Additionally, this was only the case for dimers containing wild type NR1-1a.

It is known that the Q/R site is a critical position in AMPA and kainate receptors (e.g. GluR2) which controls  $\text{Ca}^{2+}$  permeability, channel conductance, and rectification properties (1.2.3). As an ER retention motif, it is a major trafficking determinant in GluR2. Similarly, in the present study the N site in NR1-1a controlled NMDAR conductance properties and was also able to exert ER retention. The latter finding is novel but should be repeated with a larger number of oocytes and complemented by additional methods, e.g. co-immunoprecipitation and sedimentation analyses. In summary, the concatemer approach was also suitable to study the overexpression of monomers on the trafficking of concatemers.

## 4.2 Outlook

### 4.2.1 Protein biochemistry

During the course of the present study, engineered NMDAR dimers were functionally characterised in *Xenopus* oocytes using solely electrophysiological assays. Importantly, dimers elicited distinct currents (on average 600 nA or 5 - 10 % of NR1-1a + NR2A controls) and were functional in both head and tail subunits. However, voltage clamp experiments cannot provide information about the actual quality and amount of concatemeric protein synthesised in the oocyte. Thus, it cannot be excluded that a certain portion of the dimers undergoes proteolytic cleavage or degradation. For this reason, it would have been useful to isolate dimeric proteins from total membrane homogenate from oocytes. However, the putative presence of degradation products should not qualitatively influence the current responses presented in this thesis.

Membrane preparations from whole oocytes were performed and the lysates subjected to Western blotting using a standard homogenisation method (M. Hollmann, personal communication). This protocol employs 1 % Triton X-100 for solubilisation contained in the homogenisation buffer (200  $\mu$ L per clone / consisting of 100 mM NaCl, 20 mM Tris-Cl pH 7.4, and protease inhibitors in addition to Triton X-100). Oocytes were smashed with a drill or douncer. Due to bad quality of the oocytes, only 6-10 oocytes (instead of 20 as recommended) could be pooled for each clone, which each had been injected with 20 ng of cRNA (in total) before. Dimers containing wild type and mutant NR1-1a, as well as heteromeric [NR1-1a + NR2A and NR1-1a(N598R) + NR2A] and homomeric [NR1-1a and NR1-1a(N598R)] controls were injected. The bad quality of the oocytes also led to the disadvantage that oocytes could not be tested for RNA expression in voltage clamp experiments prior to homogenisation.

After homogenisation, the protein equivalent of approximately one oocyte per lane was loaded in 6 - 7.5 % polyacrylamide gels. Westerns blots were performed with 3 % milk, 0.1 % Tween-20 in 1x PBS (phosphate buffered saline) as blocking reagent, and blocking lasted 30 mins at room temperature or over night at 4°C.

The primary antibody was a polyclonal rabbit anti-NR1 (against N-terminal peptide) from Upstate (AB1516; 1 : 1000 dilution), incubated in block for 1 hr at room temperature or over night at 4 °C.

The secondary antibody used was a goat anti-rabbit IgG from Sigma (A 6154, coupled to horseradish peroxidase; 1 : 1000 dilution) for 1 hr at room temperature.

Although the homogenisation time was increased from 30 minutes until up to 2 hrs, no NR1-1a protein could be detected on the X-ray films in five experiments. Since all X-ray films were blank, the data are not shown in the present study.

However, as a positive control, HeLa cell lysates (gift from R. Trippe) from cells transfected with myc-tagged NR1-1a were recognised on Western blots under the same conditions (data not shown).

Thus, in principal, NR1-1a protein could be detected by Western blotting using the antibody available, but not NR1-1a from oocyte membranes. Reasons for this might be that the concentration of the oocyte proteins on the blots was too low or that the NR1-1a solubilisation out of the oocyte membrane was insufficient. The fact that NR1-1a from HeLa cell lysate was detectable indicates that the efficiency of solubilisation may be membrane-dependent. Additionally, NMDA receptors require urea for membrane extraction, being obviously more difficult to extract from the membrane than AMPA or kainate receptors (M. Hollmann, personal communication).

The assumption that the protein concentration in a whole cell homogenate from oocytes might be too low for detection by Western blotting is supported by previous studies : Firstly, Strutz-Seebohm et al. (2003) labelled glycosylated surface proteins from oocytes with biotinylated concanavalin A (ConA), solubilised the biotinyl-ConA protein complexes and precipitated them with streptavidin-sepharose. Protein (in this case the *C. elegans* GLR1 subunit) could only be detected in the pellet fraction containing the streptavidin-sepharose beads (18 oocytes / lane). However, the total homogenate (1 oocyte / lane) was empty (upper and middle image in Fig. 45). Oocytes had been injected with 10 ng of cRNA in that experiment.

### Failed attempt to detect oocyte protein from total homogenate

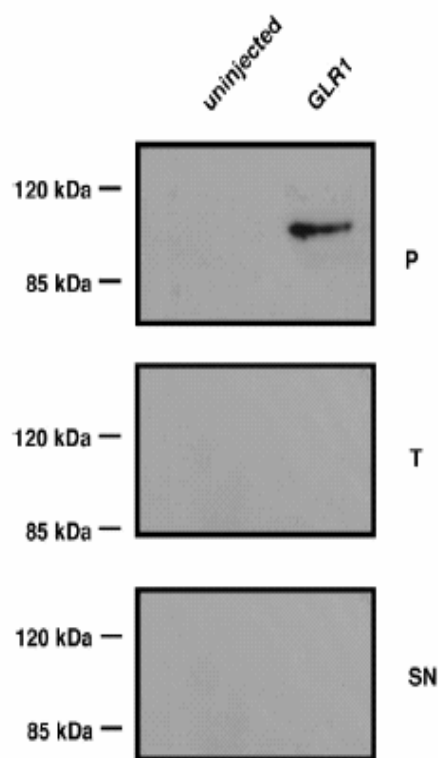


Fig. 45 : Western blot showing expression of the *C. elegans* GLR1 receptor subunit (~ 108 kDa) in the *Xenopus* plasma membrane by Strutz-Seebohm et al. (2003). Surface protein was bound to biotinyl-ConA and pelleted using streptavidin-sepharose. Concentration of protein was only sufficient in the pellet fraction, but not in the total homogenate. The protein concentration in the total homogenate is similar to the one in the unsuccessful attempts to detect concatemeric proteins isolated from oocytes in this thesis.

P: pellet fraction (18 oocytes / lane); T: total homogenate (1 oocyte / lane); SN: supernatant of pellet fraction (1 oocyte / lane); uninjected: uninjected oocytes underwent the same procedure as GLR1-injected oocytes and served as negative control.

Image reprinted with permission from the Journal of Biological Chemistry, (c) 2003 by the American Society for Biochemistry and Molecular Biology, "[www.jbc.org](http://www.jbc.org)".

Thus, it would be worth using the same method to detect the insertion of NR1-1a + NR2A dimers in the oocyte plasma membrane. Apparently, this leads to an increase in concentration of glycosylated proteins (e.g. glutamate receptors).

Furthermore, in an NR3A study, Sucher et al. (1995) attempted to detect NR1 in *Xenopus* oocytes. Oocytes were injected with 30 ng of cRNA / subunit. This was done as double injections with NR1 and NR2B or as triple injections with NR1, NR2B and NR3A. After solubilisation using a method similar to the one described in this thesis, NR1-1a was isolated by immunoprecipitation using an anti-NR1 antibody. Although protein of 40 oocytes was loaded in the polyacrylamide gel per lane, i.e. 40 times more than in the present work, NR1 levels were low. Thus, for NR1 even solubilisation of receptor protein followed by immunoprecipitation and an initially larger amount of oocyte protein were not successful to concentrate NR1 protein to sufficient levels. Consequently, the investigators switched to a different expression system : In HEK cells, the amount of isolated protein was considerably increased (Fig. 46).

#### Difficulties in detecting NR1 protein in membranes prepared from oocytes

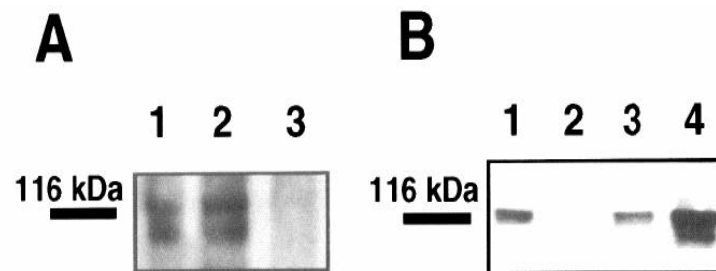


Fig. 46 :

A : Western blot showing expression of NR1 (~ 116 kDa) in the *Xenopus* plasma membrane by Sucher et al. (1995). NR1 protein was solubilised using a method similar to the one in this work, followed by immunoprecipitation; lane 1: oocytes (n = 40) injected with cRNA (~ 30 ng / subunit) to NR1, NR2B and NR3A; lane 2: 40 oocytes injected with cRNA (~ 30 ng / subunit) to NR1 and NR2B; lane 3: 40 native oocytes.

B: Western blot of NR1 in HEK cells. HEK 293 membrane proteins (1 mg) were subjected to immunoprecipitation; lane 1: HEK cells transfected with cDNAs encoding NR1, NR2B and NR3A; lane 2: cells transfected with cDNAs for NR2B and NR3A; lane 3: cells transfected with cDNAs for NR1 and NR2B; lane 4: cells after transfection with cDNA (~ 20 µg) encoding NR1.

In all other lanes, ~ 10 µg / subunit were used in all transfections.

Obviously, protein levels for NR1 were only sufficiently high in HEK cells, but not in *Xenopus* oocytes, for unknown reasons.

Images reprinted, with written permission, from the Journal of Neuroscience, (c) 1995 by the Society for Neuroscience, "[www.jneurosci.org](http://www.jneurosci.org)".

Thus, membrane protein preparations from HEK cells would be another possibility worth trying to detect NMDAR dimers in the plasma membrane. The HEK cell system would be useful for patch clamping experiments as well (see below). However, if concatemeric protein could be isolated in sufficient quantities only from HEK cells, the electrophysiological analyses of the dimers would have to be repeated in this expression system.

It is still unknown what caused the substantial reduction in current amplitude observed for all dimers compared to wild type receptors. As one possibility, one might think of a reduced expression level of the concatemeric molecule (4.1.3.2). The large size of the protein could render translation inefficient, or the insertion of the protein into the membrane of the transport vesicle could be impaired. Determining the expression level of dimers in oocytes would be another reason to emphasise the necessity for protein biochemistry.

Alternatively, confocal microscopy of cells would allow to visualise the concatemer inserted in the plasma membrane. HEK cells are used for these experiments. Contrary to protein biochemistry, confocal microscopy is not able to differentiate between a full-length concatemer and degradation products, which arise due to degradation somewhere after the fluorescent dye-labelled N terminus of the concatemer. However, more precisely than protein biochemistry, it would show the localisation of the concatemer in the cell, i.e. distinguish between ER, plasma membrane and cytosolic localisation.

Furthermore, confocal microscopy would allow to verify the ER retention experiments made for the N598R mutants. NR1-1a(N598R)-TG4L2-NR2A should be detected in the ER, while NR1-1a-TG4L2-NR2A should reach the plasma membrane, which should be enhanced by the addition of NR2A.

Biotinyl-ConA membrane protein preparations from oocytes combined with high speed sedimentation centrifugation allows to separate membrane fractions from the ER and the oocyte plasma membrane and could be used for the same ER retention experiments. This would also show whether putative degradation products of dimers are localised to the ER or even reach the oocyte membrane.

#### 4.2.2 Patch clamping

If a reduced expression level of the concatemer was not the reason for the reduced macroscopic currents of dimers, the second possibility would be reduced single-channel currents, which could be caused by reductions in single-channel conductance, open time, or open probability (4.1.3.2). A reduced single-channel conductivity could be determined using patch clamp recordings from HEK cells or single-channel recordings from *Xenopus laevis* oocyte macropatches.

The whole cell two-electrode voltage clamp experiments might give a first hint in this direction :

The easy and fast removal of MK-801 from its binding site inside the ion pore of NR1-1a-TG4L2-NR2A might point to an altered ion pore structure in the dimer ( $n = 6$ ). The blocker does not seem to be caught in the dimeric pore as efficiently as in the wild type pore (3.2.1.2.1).

Changes in ion pore structure might lead to a reduced single-channel conductance, explaining a reduction in steady-state current.

Alternatively, the open probability or open time of the channel formed from NR1-1a-TG4L2-NR2A could be lowered. However, the data from the same MK-801 block experiments suggest that this did not occur (3.2.1.2.1) : MK-801 can only bind to the channel in its open state (1.3.2). NR1-1a-TG4L2-NR2A was blocked by MK-801 down to ca. 10 % as was NR1-1a + NR2A, suggesting that the dimer did not possess an open probability and / or open time different from wild type.

These two hypotheses need to be verified in future patch clamp experiments.

Patch-clamp experiments would also be useful to complement the two-electrode voltage clamp experiments in the sense that they would prove the generation of complete, uncleaved dimeric concatemers. As the NR1 subunit does not form functional channels in HEK cells (Monyer et al., 1992), NR1-1a-TG4L2-NR2A and NR1-1a(N598R)-TG4L2-NR2A could only produce currents if both subunits of the dimer were incorporated into the receptor complex. Three expression constructs have already been generated for this purpose, the two heterodimers NR1-1a-TG4L2-NR2A-pcDNA3.1(+) and NR1-1a(N598R)-TG4L2-NR2A-pcDNA3.1(+), and one homodimer NR1-1a-TG4L2-NR1-1a-pcDNA3.1(+).

The monomeric controls, NR1-1a / pcDNAI/Amp, sNR1-1a(N598R) / pcDNAI/Amp and NR2A repaired / pcDNAI/Amp, are already ready for use, too.

To conclude, the reduced current amplitude could be explained by one of the three hypotheses discussed above or by a combination of them. Thus, it could be in part due to degradation of the concatemer, a reduced gene expression or / and a decreased single-channel conductivity.

#### **4.2.3 Construction of the 4<sup>th</sup> dimer to investigate the anticipated arbitrary subunit order within NMDAR dimers**

As described above, construction of the 4<sup>th</sup> dimeric concatemer NR2A-TG4L2-NR1-1a, which is necessary to investigate the subunit arrangement within a dimer, could not be completed during the present study. After constructing it, NR2A-TG4L2-NR1-1a should be tested for functionality alone, and together with its reverse construct NR1-1a-TG4L2-NR2A. Three experiments would be necessary to be carried out in the same oocyte batch :

Firstly, NR2A-TG4L2-NR1-1a should be injected in oocytes and tested for functionality alone. Since NR1-1a-TG4L2-NR2A is functional, it is expected to see the same for NR2A-TG4L2-NR1-1a, which differs from its reverse counterpart only in the order (but not in the symmetry) of subunits (cf. Figs. 44A, B).

Secondly, the same should be done for NR1-1a-TG4L2-NR2A. Both tests would assure that both cRNAs are indeed functional, i.e. are principally capable to form functional channels with each other. That two dimers are capable to form functional channels with each other has already been shown for the combination of NR1-1a-TG4L2-NR1-1a and NR2A-TG4L2-NR2A (3.3.3).

If transcripts for NR1-1a-TG4L2-NR2A and NR2A-TG4L2-NR1-1a were functional on their own, the co-expression of both dimers should be tested. If no currents were seen for the co-expression, this would indicate that the two dimers cannot assemble into functional channels, apparently because the subunit arrangement in the NMDA receptor is not free, but rather limited in a certain fashion (4.1.3.3).

If the co-expression of both heterodimers produced currents, no conclusion could be drawn from this experiment because the currents seen could also arise from the dimers alone (Figs. 47, 44D; cf. 44A, B).

### Combining NR1-1a-TG4L2-NR2A with NR2A-TG4L2-NR1-1a

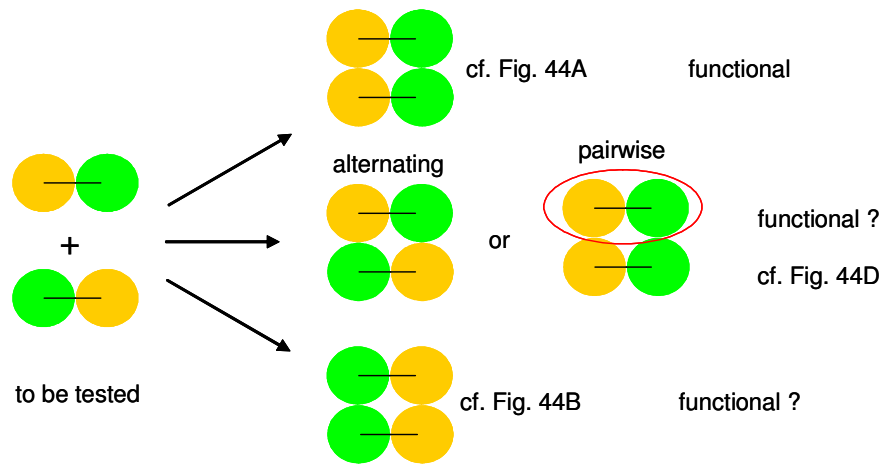


Fig. 47 : Co-expression of **NR1-1a-TG4L2-NR2A** with **NR2A-TG4L2-NR1-1a** could yield three sorts of channels. Since **NR1-1a-TG4L2-NR2A** is functional and possibly also **NR2A-TG4L2-NR1-1a** (this still needs to be tested), currents for the double injection could solely arise from one of the heterodimers alone (top and bottom tetramers). This experiment is therefore not sufficient to prove the formation of functional NMDA receptors incorporating not only **NR1-1a-TG4L2-NR2A** but also **NR2A-TG4L2-NR1-1a**.

The **NR1 subunits** are drawn as **orange** circles, the **NR2A subunits** as **green** circles.

The **red** ellipse designates the **heterodimeric substructure** within a pairwise arrangement of NR1 and NR2 subunits [proposed by Furukawa et al. (2005)].

The assumption that the currents possibly seen indeed arise from channels incorporating both and not only one of the dimers can, more precisely, be shown by using the dominant N598R mutation in NR1-1a and by introducing a recessive glutamate affinity mutation, the amino acid exchange T690I, in NR2A (Hatton and Paoletti, 2005). The construct NR2A(T690I)-TG4L2-NR1-1a(N598R) should be constructed and co-expressed with NR1-1a-TG4L2-NR2A. It would be expected that oocytes, expressing a combination of both dimers, could produce three sorts of channels : (A) NR1-1a-TG4L2-NR2A alone, which should be inducible by standard agonist concentrations, and is  $Mg^{2+}$  blockable and highly  $Ca^{2+}$  permeable, (B) receptors with one NR1-1a-TG4L2-NR2A and one NR2A(T690I)-TG4L2-NR1-1a(N598R) molecule, which should respond to standard agonist concentrations, but are insensitive to  $Mg^{2+}$  and impermeable to  $Ca^{2+}$ , and (C) NR2A(T690I)-TG4L2-NR1-1a(N598R) alone, which would be suppressed under usual agonist concentrations, e.g. 10  $\mu$ M glutamate and 10  $\mu$ M glycine (Fig. 48).

**Functional isolation of a receptor combined from  
NR1-1a-TG4L2-NR2A and NR2A(T690I)-TG4L2-NR1-1a(N598R)**

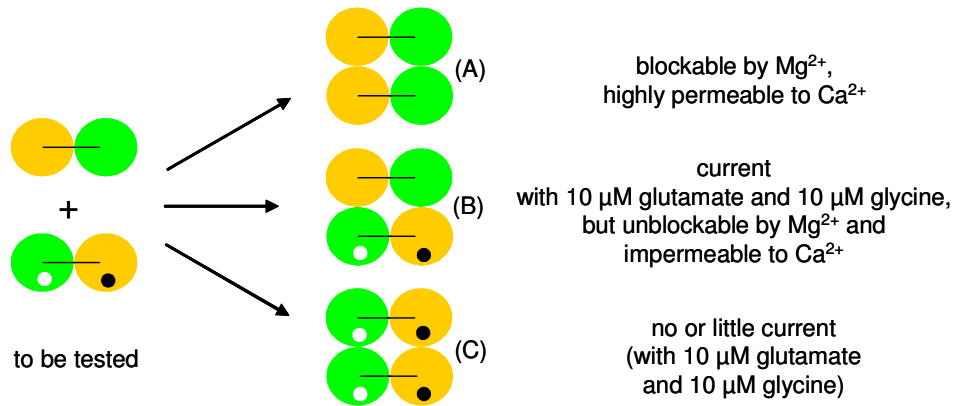


Fig. 48 : Tagging **NR2A(T690I)**-TG4L2-**NR1-1a(N598R)** with one dominant (N598R) and one recessive (T690I) marker mutation, would allow to isolate the receptor composed of two different heterodimers - if functional. This experiment could be used to derive a reliable conclusion about the possibly arbitrary subunit arrangement in NMDAR dimers.

The **NR1 subunit** is coloured in **orange**, the **NR2A subunit** in **green**. The **black dot** specifies the **dominant N598R mutation**, the **white dot** the **recessive T690I mutation**.

Therefore, receptors composed of the two different concatemers (B) could be distinguished from single concatemers, (C) and (A), by their unchanged glutamate affinity and their activity even under 1 mM extracellular  $Mg^{2+}$ . Thus, in  $Mg^{2+}$ -Ringer with 10  $\mu$ M glutamate and 10  $\mu$ M glycine, currents can only stem from a combination of both dimers, which would indicate that the subunit order within a dimer is irrelevant for functionality of the overall receptor. Under these conditions, "contaminating" complexes consisting of only one of the heterodimers would be suppressed.

The interpretations that can be derived from the results of these experiments have already been discussed in 4.1.3.3. As discussed above, the 4<sup>th</sup> and still missing heterodimer will likely confirm the anticipated lack of importance of subunit order within a dimer, but cannot be used to unambiguously elucidate the stoichiometry of NMDA receptors.

#### 4.2.4 Cloning of four tetramers to determine the stoichiometry of NMDA receptors

Contrary to dimers, functional tetramers could serve to determine the oligomeric state of full-length NMDA receptors. They could serve as an alternative to crystallography or electron microscopy [used, e.g., for the acetylcholine receptor by Miyazawa et al. (2003)], which have not succeeded in elucidating the stoichiometry of native glutamate receptors so far (1.2.4).

Two tetramers need to be made (Fig. 49) :

- (1) **NR1-1a**-TG4L2-**NR1-1a(N598R)**-TG4L2-**NR2A**-TG4L2-**NR2A** (this would allow a pairwise stoichiometry)
- (2) **NR1-1a**-TG4L2-**NR2A**-TG4L2-**NR1-1a(N598R)**-TG4L2-**NR2A** (alternating stoichiometry)

#### Tetramers permitting to determine NMDAR stoichiometry

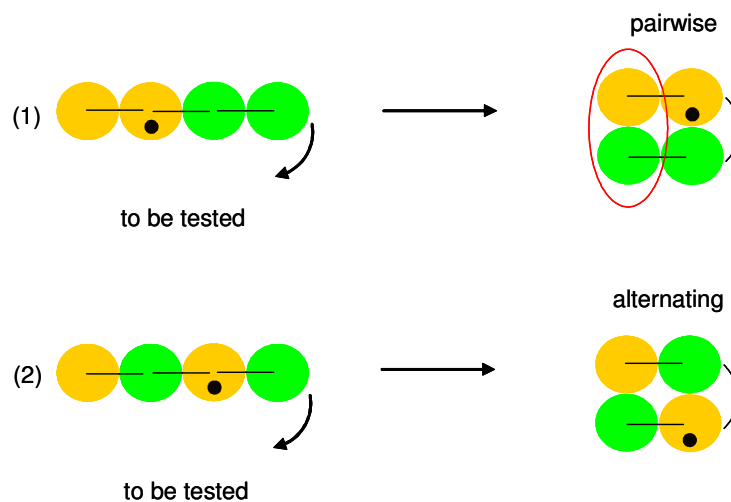


Fig. 49 : The functional tetramers **NR1-1a**-TG4L2-**NR1-1a(N598R)**-TG4L2-**NR2A**-TG4L2-**NR2A** and **NR1-1a**-TG4L2-**NR2A**-TG4L2-**NR1-1a(N598R)**-TG4L2-**NR2A** directly reflect two alternative subunit stoichiometries of NMDA receptors.

The **NR1 subunits** are drawn as **orange** circles, the **NR2A subunits** as **green** circles. The **black** dot designates the **dominant N598R mutation**. The **red** ellipse designates the **heterodimeric substructure** within a pairwise arrangement of NR1 and NR2 subunits [proposed by Furukawa et al. (2005)].

If one or more of these tetramers were functional, this would immediately tell which subunit order exists in the NMDAR complex, provided that functional tetramers would not be missed during the screening of the constructs because breakdown of the large tetramers occurred. The N598R amino acid exchange in NR1-1a would again serve as an electrophysiological marker mutation to prove incorporation of this subunit (and the following subunit or subunits) in the receptor complex. Protein biochemistry would again be necessary to indicate the presence of any degradation products.

#### **4.2.5 Role of the NR3 subunit for NMDAR stoichiometry**

While dimers could not be used to determine the stoichiometry of NMDA receptors, they could still be used to determine the role of the elusive NR3 subunits for NMDAR stoichiometry. Tetrameric constructs are not required for this approach.

Most importantly, the 4<sup>th</sup>, still missing dimer, NR2A-TG4L2-NR1-1a, is not necessary for this study. A distinct subunit order in the dimer is not required because there are only two possibilities for the integration of the NR3 subunit in an NMDAR complex : Either one NR1 or one NR2 subunit is replaced by one NR3 subunit within a tetramer, or the NR3 subunit is integrated into the tetramer, which then becomes a pentamer.

These two possibilities can easily be tested using the already existing NR1-1a + NR2A dimers generated in the present study :

First, one new dimer needs to be made : NR1-1a-TG4L2-NR3A can be generated by replacing the NR2A tail subunit in NR1-1a-TG4L2-NR2A by NR3A [cDNA from N. Sucher (1.2.1) is already available in the lab].

The following co-expressions should then be tested (Fig. 50) :

(1) **NR1-1a-TG4L2-NR2A** + **NR1-1a-TG4L2-NR3A**

### NMDA receptors incorporating the NR3A subunit may be tetramers

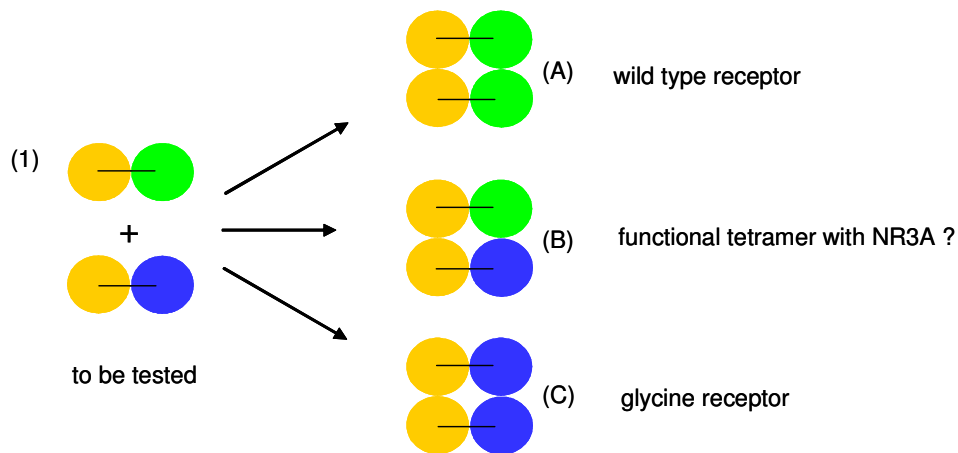


Fig. 50 : If co-expression of **NR1-1a-TG4L2-NR2A** and **NR1-1a-TG4L2-NR3A** produced functional receptors, this would indicate that one NR3 subunit is able to replace one NR2 subunit within the tetramer.

The **NR1 subunits** are drawn as **orange** circles, the **NR2A subunit** as **green** circles, and the **NR3A subunit** is **blue**.

The double expression should give rise to three sorts of channels : (A) NR1-1a-TG4L2-NR2A alone, which should have wild type-like qualities, (B) the NR3-containing tetramer with one NR1-1a-TG4L2-NR2A and one NR1-1a-TG4L2-NR3A molecule, and (C) NR1-1a-TG4L2-NR3A alone, the so-called glycine receptor (Chatterton et al., 2002; 1.3.2).

The glycine receptor formed from NR1-1a-TG4L2-NR3A alone (C) could be distinguished from (A) and (B) by its reduced block by external  $Mg^{2+}$  (Chatterton et al., 2002; Sucher et al., 1995). The presence of one NR3A subunit in the channel complex (B) could be recognised by a distinctly reduced current amplitude (down to at least 20 %) and a drastically lowered  $Ca^{2+}$  permeability, as compared to NR1-1a-TG4L2-NR2A alone (A) (Ciabarra et al., 1995; Sucher et al., 1995; Perez-Otano et al., 2001). All currents should of course always be compared to the heteromeric control of NR1-1a + NR2A.

The functionality of this heterodimer combination would confirm the theory by Atlason and McIlhinney (1.2.4), who proposed the assembly of NR1-NR2 and NR1-NR3 heterodimers in HEK cells exclusively based on biochemical and expression studies.

Since NR1 + NR3A are able to form a glycine receptor, it is likely that two NR1 copies are required for an NR3-containing tetramer. To additionally test NR1-1a-TG4L2-NR2A + NR3A-TG4L2-NR2A could thus serve as a negative control since the currents evoked should be wild type currents of NR1-1a-TG4L2-NR2A. NR3A-TG4L2-NR2A can be obtained by substituting the NR1-1a head subunit in NR1-1a-TG4L2-NR2A (or the NR2A head subunit in NR2A-TG4L2-NR2A) with NR3A.

NR2A-TG4L2-NR2A + NR1-1a-TG4L2-NR3A could serve as a test for the glycine receptor which is the only functional receptor potentially formed from this co-expression.

(2) If co-expression (1) does not produce functional channels, this might mean that NR3-containing NMDA receptors are obviously not tetramers, but pentamers. To test for the formation of pentamers, **NR1-1a**-TG4L2-**NR1-1a** + **NR2A**-TG4L2-**NR2A** + **NR3A** should be triple-injected (Fig. 51).

### NMDA receptors incorporating the NR3A subunit may be pentamers

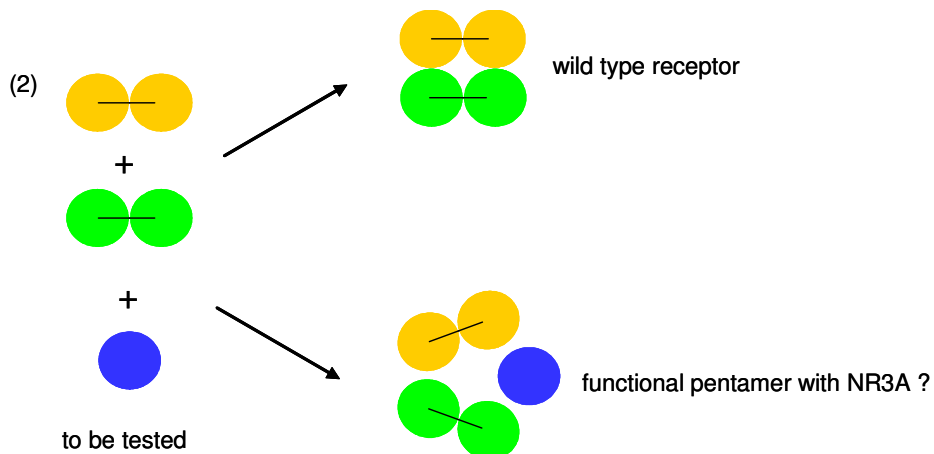


Fig. 51 : If NR3-containing NMDA receptors turned out not to be tetramers (Fig. 50), triple injection of **NR1-1a**-TG4L2-**NR1-1a** with **NR2A**-TG4L2-**NR2A** and **NR3A** would be expected to give rise to functional pentamers. Incorporation of the NR3A subunit could be recognised by the unique electrophysiological properties that this subunit conveys to the receptor channel.

The integration of the NR3A subunit into the channel complex could be indicated by the same characteristics as mentioned above (for tetramer B in Fig. 50), which differ from only NR1-1a + NR2A-containing receptors.

In conclusion, cloning of one dimer composed of NR1-1a and one NR3 subunit will be the next step to understand the stoichiometry of NR3-containing NMDA receptors.

Investigating the degree of degradation and finding the reason(s) for the current reduction of concatemeric dimers will also be necessary to complete the functional studies on NMDAR concatemers in *Xenopus laevis* presented in this thesis. It will be important to compare insights into the stoichiometry obtained in *Xenopus* oocytes to the expression and assembly of individual NMDAR subunits in neurons with their polarised structure and postsynaptic densities. Additional mechanisms and interacting partners may be involved in the assembly, localisation and stabilisation of the receptors at specific synaptic sites, which are not present in a heterologous expression system.

## 5 Summary

Usually, monomeric glutamate receptor subunits are co-expressed in heterologous cell systems, and electrophysiological recordings of those cells are used to study receptor function.

However, a drawback of this approach is a resulting heterogenous population of receptors with a varying ratio of different subunits that give a functional response.

With the concatemer strategy, i.e. two (or more) intact subunits connected by a covalent linker, it is possible to define the ratio, order and stoichiometry of subunits within the concatemer and around the pore.

NR1-1a + NR2A dimers were generated using the 4<sup>th</sup> TMD of the  $\alpha_1$ -subunit of the GABA<sub>A</sub> receptor flanked by hydrophilic amino acids as a linker (TG4L2) and their electrophysiological properties analysed in *Xenopus laevis* oocytes.

The main conclusions are as follows :

- 1) NR1-1a + NR2A dimers using TG4L2 are functional. The dominant N598R mutation in the NR1-1a subunit could be used to prove that both (especially the tail) subunits were integrated in the receptor.
- 2) Qualitatively, the dimers behaved like wild type channels. Quantitatively, however, the covalent linkage led to a drastic reduction in current amplitude. This reduction is not due to reduced agonist affinity, since glutamate and glycine EC<sub>50</sub> values for NR1-1a-linker-NR2A were unaltered compared to monomeric NR1-1a + NR2A. This is contrary to the dimers reported by Schorge and Colquhoun (2003) which displayed drastically altered agonist potencies.
- 3) Monomeric NR2A facilitated the assembly of the dimers confirming previous studies. Consistently, dimers containing the N598R mutation in NR1-1a did not underlie forward trafficking by NR2A.
- 4) Based on the electrophysiological analyses of currently available constructs, the order of NR1-1a and NR2A subunits within the dimer might be irrelevant for functionality. This is again contrary to the results by Schorge and Colquhoun who predicted from their data that there is a distinct subunit order within a dimer required for functionality.

Tetramers will be useful - if functional - to determine whether a defined subunit order exists in NMDA receptors formed from NR1-1a and NR2A.

- 5) The results shown here indicate that the strategy used in the present study perhaps represents a more favourable way for concatemer construction of NMDA receptors than the strategy followed by Schorge and Colquhoun, who constructed dimers with a C-terminally truncated head subunit.

In contrast to that other group, two full-length subunits were connected via an additional transmembrane domain. Dimers could be constructed that are functional and - qualitatively - behave like wild type NMDA receptors, including wild type-like agonist potencies. Thus, the constructs generated in this thesis appear to be a better tool to determine the stoichiometry of an NMDA receptor and can be used for future studies making use of the advantages of the concatemer strategy, particularly concerning the role of the NR3 subunits.

## 6 References

### Books :

- Sambrook, J. and Russell, D. W. (2001). *Molecular Cloning : A laboratory manual*. Cold Spring Harbor Laboratory Press, Cold Spring Harbor; pp 1.32 - 1.34.
- Kandel, E. R., Schwartz, J. H. and Jessell, T. M. (2000). *Principles of Neural Science*. 4<sup>th</sup> edition, McGraw-Hill; pp. 165 + p. 220.

### Reviews :

- Behe, P., Colquhoun, D., Wyllie, D. J. (1999). "Activation of single AMPA- and NMDA-type glutamate-receptor channels". *Ionotropic Glutamate Receptors in the CNS*. Edited by Jonas P, Monyer H. Berlin: Springer; 175-218.
- Bliss, T. V. and Collingridge, G. L. (1993). "A synaptic model of memory: long-term potentiation in the hippocampus." *Nature* 361(6407): 31-9.
- Cull-Candy, S., Brickley, S. and Farrant, M. (2001). "NMDA receptor subunits: diversity, development and disease." *Curr Opin Neurobiol* 11(3): 327-35.
- Dingledine, R., Borges, K., Bowie, D. and Traynelis, S. F. (1999). "The glutamate receptor ion channels." *Pharmacol Rev* 51(1): 7-61.
- Hollmann, M. and Heinemann, S. (1994). "Cloned glutamate receptors." *Annu Rev Neurosci* 17: 31-108.
- Hollmann, M. (1999). "Structure of ionotropic glutamate receptors". *Ionotropic Glutamate Receptors in the CNS*. Edited by Jonas P., Monyer H. Berlin: Springer; 1-98.
- McBain, C. J. and Mayer, M. L. (1994). "N-methyl-D-aspartic acid receptor structure and function." *Physiol Rev* 74(3): 723-60.
- Palmer, C. L., Cotton, L. and Henley, J. M. (2005). "The molecular pharmacology and cell biology of alpha-amino-3-hydroxy-5-methyl-4-isoxazolepropionic acid receptors." *Pharmacol Rev* 57(2): 253-77.
- Prybylowski, K. and Wenthold, R. J. (2004). "N-Methyl-D-aspartate receptors: subunit assembly and trafficking to the synapse." *J Biol Chem* 279(11): 9673-6.
- Stuehmer, W. (1992). "Electrophysiological Recording from *Xenopus* Oocytes (in *Methods in Enzymology*, Vol. 207: Ion Channels. Edited by Rudy, B. and Iverson, L. E. Academic Press; 319-339.

- Weber, W. (1999). "Ion currents of *Xenopus laevis* oocytes: state of the art." Biochim Biophys Acta 1421(2): 213-33.
- Wenthold, R. J., Sans, N., Standley, S., Prybylowski, K. and Petralia, R. S. (2003). "Early events in the trafficking of N-methyl-D-aspartate (NMDA) receptors." Biochem Soc Trans 31(Pt 4): 885-8.
- Original papers :
- Aarts, M., Iihara, K., Wei, W. L., Xiong, Z. G., Arundine, M., Cerwinski, W., MacDonald, J. F. and Tymianski, M. (2003). "A key role for TRPM7 channels in anoxic neuronal death." Cell 115(7): 863-77.
- Anson, L. C., Chen, P. E., Wyllie, D. J., Colquhoun, D. and Schoepfer, R. (1998). "Identification of amino acid residues of the NR2A subunit that control glutamate potency in recombinant NR1/NR2A NMDA receptors." J Neurosci 18(2): 581-9.
- Araneda, R. C., Lan, J. Y., Zheng, X., Zukin, R. S. and Bennett, M. V. (1999). "Spermine and arcaine block and permeate N-methyl-D-aspartate receptor channels." Biophys J 76(6): 2899-911.
- Armstrong, N., Sun, Y., Chen, G. Q. and Gouaux, E. (1998). "Structure of a glutamate-receptor ligand-binding core in complex with kainate." Nature 395(6705): 913-7.
- Atlason, P. T. and McIlhinney, R. A. J. (2006). "Folding and assembly of NMDA receptor subunits." FENS Abstr., vol. 3, A081.1, 2006.
- Barish, M. E. (1983). "A transient calcium-dependent chloride current in the immature *Xenopus* oocyte." J Physiol 342: 309-25.
- Barria, A. and Malinow, R. (2005). "NMDA receptor subunit composition controls synaptic plasticity by regulating binding to CaMKII." Neuron 48(2): 289-301.
- Beck, C., Wollmuth, L. P., Seeburg, P. H., Sakmann, B. and Kuner, T. (1999). "NMDAR channel segments forming the extracellular vestibule inferred from the accessibility of substituted cysteines." Neuron 22(3): 559-70.
- Behe, P., Stern, P., Wyllie, D. J., Nassar, M., Schoepfer, R. and Colquhoun, D. (1995). "Determination of NMDA NR1 subunit copy number in recombinant NMDA receptors." Proc Biol Sci 262(1364): 205-13.
- Birch, P. J., Grossman, C. J. and Hayes, A. G. (1988). "Kynurenic acid antagonises responses to NMDA via an action at the strychnine-insensitive glycine receptor." Eur J Pharmacol 154(1): 85-7.

- Birnboim, H. C. and J. Doly (1979). "A rapid alkaline extraction procedure for screening recombinant plasmid DNA." *Nucleic Acids Res* 7(6): 1513-23.
- Bliss, T. V. and Lomo, T. (1973). "Long-lasting potentiation of synaptic transmission in the dentate area of the anaesthetized rabbit following stimulation of the perforant path." *J Physiol* 232(2): 331-56.
- Boulter, J., Hollmann, M., O'Shea-Greenfield, A., Hartley, M., Deneris, E., Maron, C. and Heinemann, S. (1990). "Molecular cloning and functional expression of glutamate receptor subunit genes." *Science* 249(4972): 1033-7.
- Boulter, J. (1997). Nucleotide sequence of rat NMDA receptor gene NMDAR2A. GenBank entry AF001423.1; gi:2155309.
- Burnashev, N., Schoepfer, R., Monyer, H., Ruppersberg, J. P., Gunther, W., Seeburg, P. H. and Sakmann, B. (1992). "Control by asparagine residues of calcium permeability and magnesium blockade in the NMDA receptor." *Science* 257(5075): 1415-9.
- Chatterton, J. E., Awobuluyi, M., Premkumar, L. S., Takahashi, H., Talantova, M., Shin, Y., Cui, J., Tu, S., Sevarino, K. A., Nakanishi, N., Tong, G., Lipton, S. A. and Zhang, D. (2002). "Excitatory glycine receptors containing the NR3 family of NMDA receptor subunits." *Nature* 415(6873): 793-8.
- Chen, L., Chetkovich, D. M., Petralia, R. S., Sweeney, N. T., Kawasaki, Y., Wenthold, R. J., Brecht, D. S. and Nicoll, R. A. (2000). "Stargazin regulates synaptic targeting of AMPA receptors by two distinct mechanisms." *Nature* 408(6815): 936-43.
- Ciabarra, A. M., Sullivan, J. M., Gahn, L. G., Pecht, G., Heinemann, S. and Sevarino, K. A. (1995). "Cloning and characterization of chi-1: a developmentally regulated member of a novel class of the ionotropic glutamate receptor family." *J Neurosci* 15(10): 6498-508.
- Das, S., Sasaki, Y. F., Rothe, T., Premkumar, L. S., Takasu, M., Crandall, J. E., Dikkes, P., Conner, D. A., Rayudu, P. V., Cheung, W., Chen, H. S., Lipton, S. A. and Nakanishi, N. (1998). "Increased NMDA current and spine density in mice lacking the NMDA receptor subunit NR3A." *Nature* 393(6683): 377-81.
- Donevan, S. D. and Rogawski, M. A. (1995). "Intracellular polyamines mediate inward rectification of Ca(2+)-permeable alpha-amino-3-hydroxy-5-methyl-4-isoxazolepropionic acid receptors." *Proc Natl Acad Sci U S A* 92(20): 9298-302.
- Furukawa, H., Singh, S. K., Mancusso, R. and Gouaux, E. (2005). "Subunit arrangement and function in NMDA receptors." *Nature* 438(7065): 185-92.
- Gotti, B., Duverger, D., Bertin, J., Carter, C., Dupont, R., Frost, J., Gaudilliere, B., MacKenzie, E. T., Rousseau, J., Scatton, B. and et al. (1988). "Ifenprodil and SL

- 82.0715 as cerebral anti-ischemic agents. I. Evidence for efficacy in models of focal cerebral ischemia." J Pharmacol Exp Ther 247(3): 1211-21.
- Green, T., Rogers, C. A., Contractor, A. and Heinemann, S. F. (2002). "NMDA receptors formed by NR1 in *Xenopus laevis* oocytes do not contain the endogenous subunit XenU1." Mol Pharmacol 61(2): 326-33.
- Greger, I. H., Khatri, L. and Ziff, E. B. (2002). "RNA editing at arg607 controls AMPA receptor exit from the endoplasmic reticulum." Neuron 34(5): 759-72.
- Greger, I. H., Khatri, L., Kong, X. and Ziff, E. B. (2003). "AMPA receptor tetramerization is mediated by Q/R editing." Neuron 40(4): 763-74.
- Groot-Kormelink, P. J., Broadbent, S. D., Boorman, J. P. and Sivilotti, L. G. (2004). "Incomplete incorporation of tandem subunits in recombinant neuronal nicotinic receptors." J Gen Physiol 123(6): 697-708.
- Hatton, C. J. and Paoletti, P. (2005). "Modulation of triheteromeric NMDA receptors by N-terminal domain ligands." Neuron 46(2): 261-74.
- Hawkins, L. M., Prybylowski, K., Chang, K., Moussan, C., Stephenson, F. A. and Wenthold, R. J. (2004). "Export from the endoplasmic reticulum of assembled N-methyl-D-aspartic acid receptors is controlled by a motif in the c terminus of the NR2 subunit." J Biol Chem 279(28): 28903-10.
- Hollmann, M., O'Shea-Greenfield, A., Rogers, S. W. and Heinemann, S. (1989). "Cloning by functional expression of a member of the glutamate receptor family." Nature 342(6250): 643-8.
- Hollmann, M., Boulter, J., Maron, C., Beasley, L., Sullivan, J., Pecht, G. and Heinemann, S. (1993). "Zinc potentiates agonist-induced currents at certain splice variants of the NMDA receptor." Neuron 10(5): 943-54.
- Hollmann, M., Maron, C. and Heinemann, S. (1994). "N-glycosylation site tagging suggests a three transmembrane domain topology for the glutamate receptor GluR1." Neuron 13(6): 1331-43.
- Ishii, T., Moriyoshi, K., Sugihara, H., Sakurada, K., Kadotani, H., Yokoi, M., Akazawa, C., Shigemoto, R., Mizuno, N., Masu, M. and et al. (1993). "Molecular characterization of the family of the N-methyl-D-aspartate receptor subunits." J Biol Chem 268(4): 2836-43.
- Ishimaru, H., Kamboj, R., Ambrosini, A., Henley, J. M., Soloviev, M. M., Sudan, H., Rossier, J., Abutidze, K., Rampersad, V., Usherwood, P. N., Bateson, A. N. and Barnard, E. A.

- (1996). "A unitary non-NMDA receptor short subunit from *Xenopus*: DNA cloning and expression." Receptors Channels 4(1): 31-49.
- Jonas, P. and Burnashev, N. (1995). "Molecular mechanisms controlling calcium entry through AMPA-type glutamate receptor channels." Neuron 15(5): 987-90.
- Kemp, J. A., Foster, A. C., Leeson, P. D., Priestley, T., Tridgett, R., Iversen, L. L. and Woodruff, G. N. (1988). "7-Chlorokynurenic acid is a selective antagonist at the glycine modulatory site of the N-methyl-D-aspartate receptor complex." Proc Natl Acad Sci U S A 85(17): 6547-50.
- Kim, E., Cho, K. O., Rothschild, A. and Sheng, M. (1996). "Heteromultimerization and NMDA receptor-clustering activity of Chapsyn-110, a member of the PSD-95 family of proteins." Neuron 17(1): 103-13.
- Kornau, H. C., Schenker, L. T., Kennedy, M. B. and Seeburg, P. H. (1995). "Domain interaction between NMDA receptor subunits and the postsynaptic density protein PSD-95." Science 269(5231): 1737-40.
- Krieg, P. A. and Melton, D. A. (1984). "Functional messenger RNAs are produced by SP6 in vitro transcription of cloned cDNAs." Nucleic Acids Res 12(18): 7057-70.
- Kuner, T. and Schoepfer, R. (1996). "Multiple structural elements determine subunit specificity of Mg<sup>2+</sup> block in NMDA receptor channels." J Neurosci 16(11): 3549-58.
- Kuner, T., Wollmuth, L. P., Karlin, A., Seeburg, P. H. and Sakmann, B. (1996). "Structure of the NMDA receptor channel M2 segment inferred from the accessibility of substituted cysteines." Neuron 17(2): 343-52.
- Kutsuwada, T., Kashiwabuchi, N., Mori, H., Sakimura, K., Kushiya, E., Araki, K., Meguro, H., Masaki, H., Kumanishi, T., Arakawa, M. and et al. (1992). "Molecular diversity of the NMDA receptor channel." Nature 358(6381): 36-41.
- Laurie, D. J. and Seeburg, P. H. (1994). "Ligand affinities at recombinant N-methyl-D-aspartate receptors depend on subunit composition." Eur J Pharmacol 268(3): 335-45.
- Leonard, J. P. and Kelso, S. R. (1990). "Apparent desensitization of NMDA responses in *Xenopus* oocytes involves calcium-dependent chloride current." Neuron 4(1): 53-60.
- Leuschner, W. D. and Hoch, W. (1999). "Subtype-specific assembly of alpha-amino-3-hydroxy-5-methyl-4-isoxazole propionic acid receptor subunits is mediated by their N-terminal domains." J Biol Chem 274(24): 16907-16.
- Liman, E. R., Tytgat, J. and Hess, P. (1992). "Subunit stoichiometry of a mammalian K<sup>+</sup> channel determined by construction of multimeric cDNAs." Neuron 9(5): 861-71.

- Liu, S. Q. and Cull-Candy, S. G. (2000). "Synaptic activity at calcium-permeable AMPA receptors induces a switch in receptor subtype." *Nature* 405(6785): 454-8.
- MacDonald, J. F. and Nowak, L. M. (1990). "Mechanisms of blockade of excitatory amino acid receptor channels." *Trends Pharmacol Sci* 11(4): 167-72.
- Macdonald, R. L. and Olsen, R. W. (1994). "GABAA receptor channels." *Annu Rev Neurosci* 17: 569-602.
- Masuko, T., Kashiwagi, K., Kuno, T., Nguyen, N. D., Pahk, A. J., Fukuchi, J., Igarashi, K. and Williams, K. (1999). "A regulatory domain (R1-R2) in the amino terminus of the N-methyl-D-aspartate receptor: effects of spermine, protons, and ifenprodil, and structural similarity to bacterial leucine/isoleucine/valine binding protein." *Mol Pharmacol* 55(6): 957-69.
- Mayer, M. L. (2005). "Crystal structures of the GluR5 and GluR6 ligand binding cores: molecular mechanisms underlying kainate receptor selectivity." *Neuron* 45(4): 539-52.
- McIlhinney, R. A., Molnar, E., Atack, J. R. and Whiting, P. J. (1996). "Cell surface expression of the human N-methyl-D-aspartate receptor subunit 1a requires the co-expression of the NR2A subunit in transfected cells." *Neuroscience* 70(4): 989-97.
- McIlhinney, R. A., Le Bourdelles, B., Molnar, E., Tricaud, N., Streit, P. and Whiting, P. J. (1998). "Assembly intracellular targeting and cell surface expression of the human N-methyl-D-aspartate receptor subunits NR1a and NR2A in transfected cells." *Neuropharmacology* 37(10-11): 1355-67.
- Meguro, H., Mori, H., Araki, K., Kushiya, E., Kutsuwada, T., Yamazaki, M., Kumanishi, T., Arakawa, M., Sakimura, K. and Mishina, M. (1992). "Functional characterization of a heteromeric NMDA receptor channel expressed from cloned cDNAs." *Nature* 357(6373): 70-4.
- Miyazawa, A., Fujiyoshi, Y. and Unwin, N. (2003). "Structure and gating mechanism of the acetylcholine receptor pore." *Nature* 423(6943): 949-55.
- Monaghan, D. T. and Larsen, H. (1997). "NR1 and NR2 subunit contributions to N-methyl-D-aspartate receptor channel blocker pharmacology." *J Pharmacol Exp Ther* 280(2): 614-20.
- Monyer, H., Sprengel, R., Schoepfer, R., Herb, A., Higuchi, M., Lomeli, H., Burnashev, N., Sakmann, B. and Seeburg, P. H. (1992). "Heteromeric NMDA receptors: molecular and functional distinction of subtypes." *Science* 256(5060): 1217-21.

- Monyer, H., Burnashev, N., Laurie, D. J., Sakmann, B. and Seeburg, P. H. (1994). "Developmental and regional expression in the rat brain and functional properties of four NMDA receptors." Neuron 12(3): 529-40.
- Moriyoshi, K., Masu, M., Ishii, T., Shigemoto, R., Mizuno, N. and Nakanishi, S. (1991). "Molecular cloning and characterization of the rat NMDA receptor." Nature 354(6348): 31-7.
- Nanao, M. H., Green, T., Stern-Bach, Y., Heinemann, S. F. and Choe, S. (2005). "Structure of the kainate receptor subunit GluR6 agonist-binding domain complexed with domoic acid." Proc Natl Acad Sci U S A 102(5): 1708-13.
- Naundorf, B., Wolf, F. and Volgushev, M. (2006). "Unique features of action potential initiation in cortical neurons." Nature 440(7087): 1060-3.
- Naur, P., Vestergaard, B., Skov, L. K., Egebjerg, J., Gajhede, M. and Kastrup, J. S. (2005). "Crystal structure of the kainate receptor GluR5 ligand-binding core in complex with (S)-glutamate." FEBS Lett 579(5): 1154-60.
- Nicke, A., Rettinger, J. and Schmalzing, G. (2003). "Monomeric and dimeric byproducts are the principal functional elements of higher order P2X1 concatamers." Mol Pharmacol 63(1): 243-52.
- Nishi, M., Hinds, H., Lu, H. P., Kawata, M. and Hayashi, Y. (2001). "Motoneuron-specific expression of NR3B, a novel NMDA-type glutamate receptor subunit that works in a dominant-negative manner." J Neurosci 21(23): RC185.
- Perez-Otano, I., Schulteis, C. T., Contractor, A., Lipton, S. A., Trimmer, J. S., Sucher, N. J. and Heinemann, S. F. (2001). "Assembly with the NR1 subunit is required for surface expression of NR3A-containing NMDA receptors." J Neurosci 21(4): 1228-37.
- Premkumar, L. S. and Auerbach, A. (1997). "Stoichiometry of recombinant N-methyl-D-aspartate receptor channels inferred from single-channel current patterns." J Gen Physiol 110(5): 485-502.
- Prybylowski, K., Vicini, S., Wang, J., Kirkness, E. and Wolfe, B. (1999). "Tandem proteins to study NMDA receptor stoichiometry." Soc f NSc Abstr 25(1): 1487.
- Prybylowski, K., Fu, Z., Losi, G., Hawkins, L. M., Luo, J., Chang, K., Wenthold, R. J. and Vicini, S. (2002). "Relationship between availability of NMDA receptor subunits and their expression at the synapse." J Neurosci 22(20): 8902-10.
- Rodriguez-Paz, J. M., Anantharam, V. and Treistman, S. N. (1995). "Block of the N-methyl-D-aspartate receptor by phencyclidine-like drugs is influenced by alternative splicing." Neurosci Lett 190(3): 147-50.

- Rosenmund, C., Stern-Bach, Y. and Stevens, C. F. (1998). "The tetrameric structure of a glutamate receptor channel." Science 280(5369): 1596-9.
- Sakurada, K., Masu, M. and Nakanishi, S. (1993). "Alteration of Ca<sup>2+</sup> permeability and sensitivity to Mg<sup>2+</sup> and channel blockers by a single amino acid substitution in the N-methyl-D-aspartate receptor." J Biol Chem 268(1): 410-5.
- Schorge, S. and Colquhoun, D. (2003). "Studies of NMDA receptor function and stoichiometry with truncated and tandem subunits." J Neurosci 23(4): 1151-8.
- Soloviev, M. M., Brierley, M. J., Shao, Z. Y., Mellor, I. R., Volkova, T. M., Kamboj, R., Ishimaru, H., Sudan, H., Harris, J., Foldes, R. L., Grishin, E. V., Usherwood, P. N. and Barnard, E. A. (1996). "Functional expression of a recombinant unitary glutamate receptor from *Xenopus*, which contains N-methyl-D-aspartate (NMDA) and non-NMDA receptor subunits." J Biol Chem 271(51): 32572-9.
- Stocker, M., Hellwig, M. and Kerschensteiner, D. (1999). "Subunit assembly and domain analysis of electrically silent K<sup>+</sup> channel alpha-subunits of the rat Kv9 subfamily." J Neurochem 72(4): 1725-34.
- Strutz-Seebohm, N., Werner, M., Madsen, D. M., Seebohm, G., Zheng, Y., Walker, C. S., Maricq, A. V. and Hollmann, M. (2003). "Functional analysis of *Caenorhabditis elegans* glutamate receptor subunits by domain transplantation." J Biol Chem 278(45): 44691-701.
- Sucher, N. J., Akbarian, S., Chi, C. L., Leclerc, C. L., Awobuluyi, M., Deitcher, D. L., Wu, M. K., Yuan, J. P., Jones, E. G. and Lipton, S. A. (1995). "Developmental and regional expression pattern of a novel NMDA receptor-like subunit (NMDAR-L) in the rodent brain." J Neurosci 15(10): 6509-20.
- Sullivan, J. M., Traynelis, S. F., Chen, H. S., Escobar, W., Heinemann, S. F. and Lipton, S. A. (1994). "Identification of two cysteine residues that are required for redox modulation of the NMDA subtype of glutamate receptor." Neuron 13(4): 929-36.
- Sun, Y., Olson, R., Horning, M., Armstrong, N., Mayer, M. and Gouaux, E. (2002). "Mechanism of glutamate receptor desensitization." Nature 417(6886): 245-53.
- Traynelis, S. F., Hartley, M. and Heinemann, S. F. (1995). "Control of proton sensitivity of the NMDA receptor by RNA splicing and polyamines." Science 268(5212): 873-6.
- Verdoorn, T. A., Kleckner, N. W. and Dingledine, R. (1989). "N-methyl-D-aspartate/glycine and quisqualate/kainate receptors expressed in *Xenopus* oocytes: antagonist pharmacology." Mol Pharmacol 35(3): 360-8.

- Vissel, B., Krupp, J. J., Heinemann, S. F. and Westbrook, G. L. (2001). "A use-dependent tyrosine dephosphorylation of NMDA receptors is independent of ion flux." Nat Neurosci 4(6): 587-96.
- Vogelstein, B. and D. Gillespie (1979). "Preparative and analytical purification of DNA from agarose." Proc Natl Acad Sci U S A 76(2): 615-9.
- Wentholt, R. J., Yokotani, N., Doi, K. and Wada, K. (1992). "Immunochemical characterization of the non-NMDA glutamate receptor using subunit-specific antibodies. Evidence for a hetero-oligomeric structure in rat brain." J Biol Chem 267(1): 501-7.
- Williams, K. (1993). "Ifenprodil discriminates subtypes of the N-methyl-D-aspartate receptor: selectivity and mechanisms at recombinant heteromeric receptors." Mol Pharmacol 44(4): 851-9.
- Williams, K. (1997). "Interactions of polyamines with ion channels." Biochem J 325 ( Pt 2): 289-97.
- Williams, K. (2001). "Ifenprodil, a novel NMDA receptor antagonist: site and mechanism of action." Curr Drug Targets 2(3): 285-98.
- Xia, H., Hornby, Z. D. and Malenka, R. C. (2001). "An ER retention signal explains differences in surface expression of NMDA and AMPA receptor subunits." Neuropharmacology 41(6): 714-23.
- Xiong, Z. G., Zhu, X. M., Chu, X. P., Minami, M., Hey, J., Wei, W. L., MacDonald, J. F., Wemmie, J. A., Price, M. P., Welsh, M. J. and Simon, R. P. (2004). "Neuroprotection in ischemia: blocking calcium-permeable acid-sensing ion channels." Cell 118(6): 687-98.
- Zamanillo, D., Sprengel, R., Hvalby, O., Jensen, V., Burnashev, N., Rozov, A., Kaiser, K. M., Koster, H. J., Borchardt, T., Worley, P., Lubke, J., Frotscher, M., Kelly, P. H., Sommer, B., Andersen, P., Seeburg, P. H. and Sakmann, B. (1999). "Importance of AMPA receptors for hippocampal synaptic plasticity but not for spatial learning." Science 284(5421): 1805-11.
- Zerangue, N., Schwappach, B., Jan, Y. N. and Jan, L. Y. (1999). "A new ER trafficking signal regulates the subunit stoichiometry of plasma membrane K(ATP) channels." Neuron 22(3): 537-48.
- Zheng, X., Zhang, L., Wang, A. P., Bennett, M. V. and Zukin, R. S. (1999). "Protein kinase C potentiation of N-methyl-D-aspartate receptor activity is not mediated by phosphorylation of N-methyl-D-aspartate receptor subunits." Proc Natl Acad Sci U S A 96(26): 15262-7.

## **Acknowledgements**

I would like to thank Prof. Dr. Michael Hollmann for the opportunity to pursue this project and PD Dr. Dietzel-Meyer for being the co-advisor.

Many thanks to everybody who showed interest in my work, provided invaluable experimental and technical support, and took part in helpful discussions.

Finally, I am especially indebted to my family for the compensation and for their endless support and care.

# Curriculum vitae

## Personal information

Name : Monika Jeromin

Date of birth : 13<sup>th</sup> January 1977

Place of birth : Hannover, Germany

## Education

- Feb. 2004 - Present : Ph.D. student in the lab of Prof. Dr. M. Hollmann, Department of Biochemistry I - Receptor Biochemistry, Ruhr-University Bochum, Germany (Graduate School of Chemistry and Biochemistry, GSCB)
- Sept. 2006 : Oral examination in the subsidiary subject ("Advanced Analytical Chemistry", mark : 1.3)
- July 2003 - Dec. 2003 : Research assistant of Dr. M. Kessels / Dr. B. Qualmann, Department of Neurochemistry / Molecular Biology, IfN Magdeburg, Germany
- May 2003 - June 2003 : Research student in the lab of Prof. Dr. A. Kispert, Department of Molecular Biology, Medical School of Hannover, Germany
- Nov. 2002 : Diploma in Biochemistry (mark : 1.3)
- Dec. 2001 - Sept. 2002 : Diploma thesis in the lab of Dr. I. Robinson, Department of Genetics, University of Cambridge, Cambridge (UK) ("The C2B and C2C domain of Dunc-13 bind syntaxin in a Ca<sup>2+</sup>-independent manner *in vitro*", mark : 1.7)
- Nov. 2001 : Oral examinations in Biochemistry, Biophysical Chemistry and Immunology

Sept. 1998 - Nov. 2002 : Undergraduate (diploma) studies of Biochemistry at the University of Hannover, Germany

Oct. 1996 - Sept. 1998 : Pre-diploma studies of Biochemistry at the University of Hannover, Germany (oral examinations, mark : 1.7)

May 1996: "Abitur" (mark : 1.3)

1989 - 1996 : High school education, Ganztagsgymnasium Barsinghausen, Germany

#### Poster presentations

Hoffmann, J., Werner, M., Schmaltz, D., Jeromin, M., Morth, T. and Hollmann, M. "Covalently linked AMPA receptor heterodimers are functional and potentiated by stargazin." FENS Abstr., vol. 3, A184.4, Vienna, 8<sup>th</sup> - 12<sup>th</sup> July 2006.

Jeromin, M., Schmaltz, D. and Hollmann, M.

"Engineered NMDA receptor hetero- and homodimers are functional in *Xenopus laevis* oocytes." Horizons in Molecular Biology, 3<sup>rd</sup> International Ph.D. Student Symposium, Göttingen, Germany, 14<sup>th</sup> - 16<sup>th</sup> September 2006.

#### Publication

Qualmann, B., Boeckers, T. M., Jeromin, M., Gundelfinger, E. D., Kessels, M. M. (2004). "Linkage of the actin cytoskeleton to the postsynaptic density via direct interactions of Abp1 with the ProSAP/Shank family." J Neurosci 24(10): 2481-95.